

2001

## Application of the genetic algorithm to an ecological simulation

William J. Seufzer

*College of William and Mary - Virginia Institute of Marine Science*

Follow this and additional works at: <https://scholarworks.wm.edu/etd>



Part of the [Computer Sciences Commons](#), [Ecology and Evolutionary Biology Commons](#), and the [Plant Sciences Commons](#)

---

### Recommended Citation

Seufzer, William J., "Application of the genetic algorithm to an ecological simulation" (2001).  
*Dissertations, Theses, and Masters Projects*. Paper 1539616851.  
<https://dx.doi.org/doi:10.25773/v5-sv9a-rj53>

This Dissertation is brought to you for free and open access by the Theses, Dissertations, & Master Projects at W&M ScholarWorks. It has been accepted for inclusion in Dissertations, Theses, and Masters Projects by an authorized administrator of W&M ScholarWorks. For more information, please contact [scholarworks@wm.edu](mailto:scholarworks@wm.edu).



APPLICATION OF THE GENETIC ALGORITHM  
TO AN ECOLOGICAL SIMULATION

---

A Dissertation

Presented To

The Faculty of the School of Marine Science  
The College of William and Mary in Virginia

In Partial Fulfillment

Of the Requirements for the Degree of  
Doctor of Philosophy

---

By

William James Seufzer

2001

UMI Number: 3012652

Copyright 2001 by  
Seufzer, William James

All rights reserved.

UMI<sup>®</sup>

---

UMI Microform 3012652

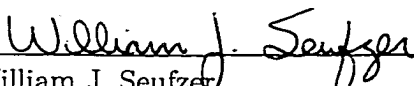
Copyright 2001 by Bell & Howell Information and Learning Company.  
All rights reserved. This microform edition is protected against  
unauthorized copying under Title 17, United States Code.

---

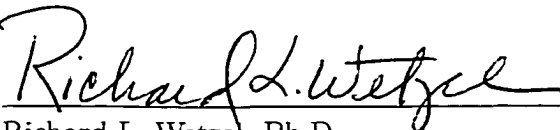
Bell & Howell Information and Learning Company  
300 North Zeeb Road  
P.O. Box 1346  
Ann Arbor, MI 48106-1346

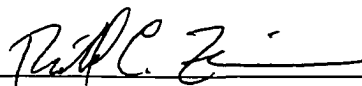
# APPROVAL SHEET

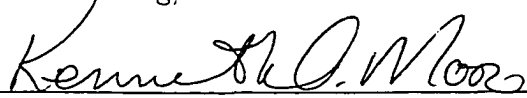
This Dissertation is submitted in partial fulfillment of  
the requirements for the degree of  
Doctor of Philosophy


  
\_\_\_\_\_  
William J. Seufzer

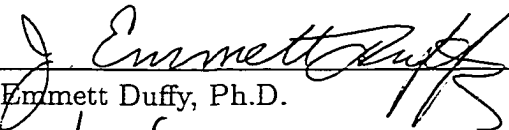
Approved, July 2001

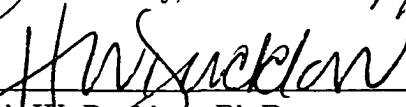
  
\_\_\_\_\_  
Richard L. Wetzel, Ph.D.  
Committee Chairman/Adviser

  
\_\_\_\_\_  
Richard C. Zimmerman, Ph.D.  
Moss Landing Marine Laboratories  
Moss Landing, California

  
\_\_\_\_\_  
Kenneth A. Moore, Ph.D.

  
\_\_\_\_\_  
Mark R. Patterson, Ph.D.

  
\_\_\_\_\_  
J. Emmett Duffy, Ph.D.

  
\_\_\_\_\_  
Hugh W. Ducklow, Ph.D.

# Contents

<b>1</b>	<b>Computational Plant Physiology</b>	<b>1</b>
1.1	Introduction . . . . .	1
1.2	Chapter Summaries . . . . .	4
1.3	Literature Cited . . . . .	8
<b>2</b>	<b>The Vgrass Model</b>	<b>9</b>
2.1	Introduction . . . . .	10
2.2	Model Summary . . . . .	12
2.3	Model Equations . . . . .	16
2.3.1	The environment . . . . .	16
2.3.2	Controlling Parameters . . . . .	22
2.3.3	Photosynthesis . . . . .	25
2.3.4	Respiration . . . . .	28
2.3.5	Allocation . . . . .	29
2.4	Vgrass Validation . . . . .	30
2.5	Vgrass Calibration . . . . .	31

<i>CONTENTS</i>	iv
2.6 Sensitivity Analysis . . . . .	37
2.7 Model Application . . . . .	40
2.8 Discussion . . . . .	44
2.9 Literature Cited . . . . .	51
<b>3 Vgrass With The Genetic Algorithm</b>	<b>54</b>
3.1 Introduction . . . . .	55
3.2 The Simple GA . . . . .	60
3.2.1 Vgrass-GA Interface . . . . .	63
3.2.2 GA Demonstration . . . . .	65
3.2.3 Goal Sensitivity . . . . .	72
3.3 Discussion . . . . .	78
3.4 Literature Cited . . . . .	84
<b>4 Testing Plant Growth Strategies</b>	<b>86</b>
4.1 Introduction . . . . .	87
4.2 Vgrass/GA . . . . .	89
4.3 Maximizing Relative Growth Rate (RGR) . . . . .	92
4.3.1 Strategy One: RGR-Plant . . . . .	92
4.3.2 Strategy Two: RGR-Population . . . . .	100
4.3.3 RGR-Plant vs. RGR-Population . . . . .	107
4.4 Maximizing Biomass (BIO) . . . . .	109
4.4.1 Strategy Three: BIO-Plant . . . . .	109

4.4.2	Strategy Four: BIO-Population . . . . .	117
4.4.3	BIO-Plant vs. BIO-Population . . . . .	123
4.5	Maximizing Net Primary Production (NPP) . . . . .	125
4.5.1	Strategy Five: NPP-Plant . . . . .	125
4.5.2	Strategy Six: NPP-Population . . . . .	129
4.5.3	NPP-Plant vs. NPP-Population . . . . .	138
4.6	Maximizing Longevity (LONG) . . . . .	139
4.6.1	Strategy Seven: LONG-Population . . . . .	139
4.7	Discussion . . . . .	155
4.7.1	The strategies . . . . .	155
4.7.2	Allocation . . . . .	158
4.7.3	The GA in ecological simulations . . . . .	162
4.7.4	Suggestions for further research . . . . .	164
4.8	Literature Cited . . . . .	166
<b>5</b>	<b>Concluding Remarks</b>	<b>169</b>
5.1	Literature Cited . . . . .	173



## ACKNOWLEDGMENTS

I have more people to thank than space will allow. Everyone around me has helped me in some direct or indirect manner.

A big thanks to my committee, Dick, Dick, Ken, Emmett, Mark, and Hugh. I still believe that some of the best moments of my life happened in our meetings. All of you challenged my thinking far more than it has ever been challenged... and I have to admit that I absolutely enjoyed it.

To my wife Mary, your support through this has been nothing less than amazing. I look forward to sharing more challenges with you. :)

To Olivia... thanks for the *magic!*

To the next one... I'm not sure how much more cuteness I can tolerate, but I'm willing to find out. Go for it!

I was blessed to grow up in a family with a dad, a mom, and four siblings who truly love each other. The wealth in my family cannot be measured in monetary units. Instead our wealth is based on an investment my parents made when we were very young. Somehow, day by day, spanking after spanking, they taught us how to think for ourselves, respect others around us, recover from mistakes, etc., etc. Their daily investments lead to all five children earning bachelor's degrees; three have masters; one Ph.D. Two of the sons have served as officers in the U.S. Air Force; one of them has gone from Airman Basic to Lieutenant Colonel, and will likely become a Colonel. The third son is an accomplished computer programmer who has a knack for solving *impossible* problems. One of their daughters is a

teacher who truly sets the standard in caring for and challenging very active young minds. Their other daughter is a biker chick who is trusted with managing financial information at a national credit union.

My parents are an example of the axiom: *it's not a matter of how much you got, it's what you do with it.* They grew up on farms and never had the opportunity of a college education, yet they managed to educate us. They went week to week on what would now be considered a meager income; we didn't get everything we wanted, but somehow we had everything we needed. I could write a long list of all the people who helped me along the way, but none were as important as my parents! Thank you Mom and Dad!

# List of Tables

2.1	Model Parameters . . . . .	17
2.2	Self shading array ordinates . . . . .	21
2.3	Nominal Configuration of Controlling Parameters . . . . .	23
2.4	Nominal configuration metrics . . . . .	32
2.5	Parameter Sensitivity . . . . .	37
2.6	Controlling Parameter Sensitivity . . . . .	39
2.7	Vgrass Compared To Published Data . . . . .	40
2.8	High-Shoot-Density Configuration Metrics . . . . .	41
3.1	Controlling Parameter Limits . . . . .	64
3.2	GA-Selected Configuration Metrics . . . . .	70
4.1	RGR Configurations of Controlling Parameters . . . . .	93
4.2	RGR-Plant Configuration Metrics . . . . .	95
4.3	RGR-Population Configuration Metrics . . . . .	102
4.4	BIO Configurations of Controlling Parameters . . . . .	110
4.5	BIO-Plant Configuration Metrics . . . . .	111

*LIST OF TABLES*

ix

4.6	BIO-Population Configuration Metrics . . . . .	119
4.7	NPP Configurations of Controlling Parameters . . . . .	126
4.8	NPP-Plant Configuration Metrics . . . . .	128
4.9	NPP-Population Configuration Metrics . . . . .	134
4.10	LONG Configurations of Controlling Parameters . . . . .	149
4.11	LONG Configuration Metrics . . . . .	151

# List of Figures

2.1	Model Diagrams . . . . .	13
2.2	3-D Self Shading Model . . . . .	19
2.3	$\Gamma$ Variable Plot . . . . .	22
2.4	Model Gross Production vs. Irradiance . . . . .	28
2.5	Nominal Plant and Areal Biomass . . . . .	33
2.6	Nominal Plant 5 Year Biomass . . . . .	34
2.7	Nominal Plant Leaf Growth . . . . .	35
2.8	Nominal Plant Production vs. Irradiance . . . . .	36
2.9	High-Shoot-Density Plant and Areal Biomass . . . . .	42
2.10	High-Shoot-Density Plant Leaf Growth . . . . .	43
2.11	Self Shade and Leaf Area Index . . . . .	45
3.1	Population Fitness . . . . .	67
3.2	GA selected Plant and Areal Biomass . . . . .	69
3.3	GA-Selected Plant 5 Year Biomass . . . . .	70
3.4	GA-Selected Plant Leaf Growth . . . . .	71

*LIST OF FIGURES*

3.5	GA-Selected Plant Production vs. Irradiance . . . . .	73
3.6	Controlling Parameter Histograms . . . . .	74
3.7	Top Performers Average Plant and Areal Biomass . . . . .	77
4.1	RGR-Plant Individual and Areal Biomass . . . . .	94
4.2	RGR-Plant 5 Year Biomass . . . . .	95
4.3	RGR-Plant Leaf Growth . . . . .	97
4.4	RGR-Plant $\Gamma$ Variables . . . . .	98
4.5	RGR-Plant Production vs. Irradiance . . . . .	99
4.6	RGR-Population Individual and Areal Biomass . . . . .	101
4.7	RGR-Population 5 Year Biomass . . . . .	102
4.8	RGR-Population Leaf Growth . . . . .	104
4.9	RGR-Population Production vs. Irradiance . . . . .	105
4.10	RGR-Population $\Gamma$ Variables . . . . .	106
4.11	BIO-Plant Individual and Areal Biomass . . . . .	112
4.12	BIO-Plant 5 Year Biomass . . . . .	113
4.13	BIO-Plant Leaf Growth . . . . .	114
4.14	BIO-Plant Production vs. Irradiance . . . . .	115
4.15	BIO-Plant $\Gamma$ Variables . . . . .	116
4.16	BIO-Population Individual and Areal Biomass . . . . .	118
4.17	BIO-Population 5 Year Biomass . . . . .	119
4.18	BIO-Population Leaf Growth . . . . .	120
4.19	BIO-Population Production vs. Irradiance . . . . .	121

*LIST OF FIGURES*

4.20 BIO-Population $\Gamma$ Variables . . . . .	122
4.21 NPP-Plant Individual and Areal Biomass . . . . .	127
4.22 NPP-Plant 5 Year Biomass . . . . .	128
4.23 NPP-Plant Leaf Growth . . . . .	130
4.24 NPP-Plant Production vs. Irradiance . . . . .	131
4.25 NPP-Plant $\Gamma$ Variables . . . . .	132
4.26 NPP-Population Individual and Areal Biomass . . . . .	133
4.27 NPP-Population 5 Year Biomass . . . . .	134
4.28 NPP-Population Leaf Growth . . . . .	135
4.29 NPP-Population Production vs. Irradiance . . . . .	136
4.30 NPP-Population $\Gamma$ Variables . . . . .	137
4.31 Degree-days Histograms . . . . .	140
4.32 Shoot Density Histograms . . . . .	141
4.33 Leaf Width Histograms . . . . .	142
4.34 PSU Density Histograms . . . . .	143
4.35 PSU Antenna Chl Histograms . . . . .	144
4.36 Stop Leaf P:R Ratio Histograms . . . . .	145
4.37 Abscise Leaf P:R Ratio Histograms . . . . .	146
4.38 Shoot To Root Ratio Histograms . . . . .	147
4.39 LONG Individual and Areal Biomass . . . . .	150
4.40 LONG 5 Year Biomass . . . . .	151
4.41 LONG Leaf Growth . . . . .	152

*LIST OF FIGURES*

xiii

4.42 LONG Production vs. Irradiance . . . . .	153
4.43 LONG $\Gamma$ Variables . . . . .	154



## ABSTRACT

A computational framework is built and demonstrated which is capable of testing plant growth strategies. The framework consists of Vgrass, a carbon based simulation model of a single *Zostera marina* plant, and the genetic algorithm (GA). Vgrass is based on published seagrass models, published photosynthetic data, and general plant physiology information. The model grows individual leaves whose initiation times are based on degree-day intervals. Leaf size is computed and combined with shoot density to compute population self shading. Leaf length is an emergent property since leaf growth is limited by light attenuation caused by population self shading. The model is able to show the relationship between leaf size and shoot density in response to light availability. Degree-days is also shown to be an effective method in modeling the emergence of *Zostera marina* leaves. The GA and Vgrass are combined to demonstrate the GA as an optimization method and to demonstrate a secondary sensitivity analysis. In an optimization exercise, the RMS error between Vgrass biomass and that of another published model is minimized. Solutions with fitness ranking within 10% of the smallest RMS error are compared in a secondary sensitivity analysis. The analysis can be used to indicate parameter sensitivity in regards to the models ability to attain the optimization goal. Plant growth strategies are tested by searching for configurations of Vgrass parameters best able to: maximize relative growth rate, maximize biomass, and maximize net primary production. Configurations found by the GA lead to plant growth patterns that are not biologically realistic; plant growth strategies based on maximizing "growth" lead to unrealistic plant growth. The plant growth patterns from each of the tests are discussed in relation to ecological and economic principles. Configurations found by the GA search are unique to the optimization goal and the resulting plant growth patterns are shown to support the given goal. Therefore, the computational framework is shown to be successful in testing plant growth strategies. Further, this study shows that care must be taken when defining the fitness function and that the GA is an effective tool at finding "holes" in a model.

APPLICATION OF THE GENETIC ALGORITHM  
TO AN ECOLOGICAL SIMULATION

# Chapter 1

## Computational Plant Physiology

### 1.1 Introduction

Plant physiological processes span a wide range of time scales and resources must be allocated between growth, storage, disease resistance, discouraging predators, reproduction, etc. The mechanisms driving allocation are still largely unknown (Thornley, 1998) and there is open debate regarding any specific goal to allocation (Givnish, 1983). Allocation between plant growth and reproduction, when viewed in an economic sense of costs and benefits of the alternative allocations, has been shown to be optimal at the evolutionary scale (Sakai, 1993). While the result is optimal in the sense of a cost-benefit analysis, was there a plant growth strategy that lead to this balance? Taking a hierarchical view, plant processes, including allocation, must be organized so that the species is persistent. Going to deeper levels in the hierarchy, to shorter time frames, how are the processes organized in order to meet the long-term objective of species persistence while simultaneously responding to

short-term environmental stresses? *Is there a strategy to plant growth?*

If there is a growth strategy, it appears to be impossible to determine experimentally. Meanwhile, computational science has evolved to a point where this question can be approached through a combination of simulation and artificial intelligence. The computational approach does not measure a plant growth strategy, but instead *searches* for plant growth patterns that would result from a given strategy.

This study shows the construction and demonstration of a computational framework to assist the study of plant allocation and growth strategies. The framework consists of two main components. The first component is a carbon based model of the eelgrass *Zostera marina* that models the allocation and growth of an individual plant. The model is controlled by 25 parameters which, when given values, are collectively referred to as a *configuration*. The second component is a search method from the field of artificial intelligence called the Genetic Algorithm (GA)<sup>1</sup>. The GA searches for configurations of controlling parameters that meet a prescribed plant growth goal or strategy. The combination of GA and simulation allows a researcher to address the question: *What configuration of controlling parameters is best able to describe a plant that is, for instance, maximizing biomass?*

The computational framework is shown to be effective at testing plant growth strategies. The framework is able to show that different plant growth goals lead to different parameter configurations and therefore plant growth patterns. Analysis of the resulting configurations and their behaviors reveals that they are achieving the given goal. In relation to the plant growth strategies, this study shows that strategies based on maximizing three

---

<sup>1</sup>The word genetic in *genetic algorithm* does not imply any connection to biological genetics. The GA is a search method based on natural selection; genetic is used here as a metaphor.

different growth measurements lead to unrealistic plant behaviors. Meanwhile a fourth goal, longevity, leads to plant configurations and behaviors that are more normal. Additionally, the computational framework is shown to be an effective tool for finding *mathematical holes* in models. Also, when combining a GA with an ecological simulation care must be taken when formulating the GA's fitness function.

## 1.2 Chapter Summaries

The primary objective of this study is to build and demonstrate a computational framework to test plant growth strategies. The intent is not to discern underlying mechanisms required for plant growth strategies, but to predict how a plant might behave if a given growth strategy were present. To meet this objective a plant simulation is coupled with a GA. This project is sub-divided into the following 3 chapters: 2) to show the design and performance of the plant simulation, Vgrass<sup>2</sup>, 3) to explain the GA, its interface to Vgrass, and demonstrate the combination (framework) of Vgrass with the GA, and 4) to apply the framework to three plant growth strategies.

Chapter 2 describes the model's construction, validation, calibration, sensitivity analysis, and performance. Vgrass was constructed mainly from the published *Zostera marina* models of Wetzel and Neckles (1986) and Verhagen and Nienhuis (1983), photosynthetic data from Dennison and Alberte (1986), and plant physiological data from Nobel (1991). *Zostera marina* was chosen since it has been studied extensively and is an ecologically important species (Dennison et al., 1993). The model includes the fundamental plant physiological processes (photosynthesis, respiration, and allocation), plant phenology (timing of new leaf initiation and abscission), and environmental factors (light, temperature, and self shading). Vgrass does not take the classical approach of limiting above-ground biomass with an internal parameter. Since Vgrass is based on an individual plant, and grows individual leaves, it uses leaf geometry to compute a self shading factor so that above-ground growth is limited by its own shade.

---

<sup>2</sup>The completed model will hereafter be referred to as Vgrass; the *V* is for *virtual*.

Vgrass validation was simplified by relying on its ancestral underpinnings and by showing that it can replicate *Zostera marina* biomass curves of a third published model, Buzzelli, et al. (1999).

Sensitivity analysis of Vgrass was similar to that of its ancestors; Vgrass showed sensitivity to light and temperature. Additionally Vgrass showed sensitivity to the timing of leaf initiation and abscission, both of which are indirectly related to light and temperature.

To demonstrate the self shading feature of the Vgrass model it was run at two different shoot densities based on Orth and Moore (1986). Vgrass was able to qualitatively show growth behavior similar to Orth and Moore (1986) and in agreement with Jacobs (1979). The results show that leaf length and shoot density are related to insolation; the possible influence of nitrogen is not needed to explain the relationship as suggested by Short (1983).

Chapter 3 describes the GA method and how the GA interfaces to Vgrass. The GA is used to calibrate Vgrass' 25 controlling parameters and results from the GA search are used to discuss the the model's flexibility in reaching a given search goal. Vgrass has 25 parameters that control plant allocation and leaf phenology, these parameters and a fitness function form the link between Vgrass and the GA. Briefly, the GA manipulates sets of the parameters and passes one set at a time to a fitness function. The fitness function passes the parameters to Vgrass and evaluates Vgrass' performance against a given criterion. Here the criterion is to minimize the RMS error between the biomass curve of Vgrass and the biomass curve of Buzzelli et al. (1999). For each set of parameters the fitness function returns a metric describing that configuration's ability to meet the criteria. The GA searches for a configuration of parameters best capable of meeting the criteria. The results demonstrate

Vgrass validation was simplified by relying on its ancestral underpinnings and by showing that it can replicate *Zostera marina* biomass curves of a third published model, Buzzelli, et al. (1999).

Sensitivity analysis of Vgrass was similar to that of its ancestors; Vgrass showed sensitivity to light and temperature. Additionally Vgrass showed sensitivity to the timing of leaf initiation and abscission, both of which are indirectly related to light and temperature.

To demonstrate the self shading feature of the Vgrass model it was run at two different shoot densities based on Orth and Moore (1986). Vgrass was able to qualitatively show growth behavior similar to Orth and Moore (1986) and in agreement with Jacobs (1979). The results show that leaf length and shoot density are related to insolation; the possible influence of nitrogen is not needed to explain the relationship as suggested by Short (1983).

Chapter 3 describes the GA method and how the GA interfaces to Vgrass. The GA is used to calibrate Vgrass' 25 controlling parameters and results from the GA search are used to discuss the the model's flexibility in reaching a given search goal. Vgrass has 25 parameters that control plant allocation and leaf phenology, these parameters and a fitness function form the link between Vgrass and the GA. Briefly, the GA manipulates sets of the parameters and passes one set at a time to a fitness function. The fitness function passes the parameters to Vgrass and evaluates Vgrass' performance against a given criterion. Here the criterion is to minimize the RMS error between the biomass curve of Vgrass and the biomass curve of Buzzelli et al. (1999). For each set of parameters the fitness function returns a metric describing that configuration's ability to meet the criteria. The GA searches for a configuration of parameters best capable of meeting the criteria. The results demonstrate



the ability of the GA to calibrate model parameters given a measurable criteria.

In addition, a *secondary* sensitivity analysis was done. Configurations were taken from the pool of trials used by the GA during its search for the optimum configuration. A group of configurations whose fitness values were within 10% of the best individual were culled and histograms of parameter values were made for each parameter. The purpose was to evaluate the *sensitivity* of each parameter in terms of Vgrass' ability to reach the search goal. The analysis showed that some controlling parameters could vary within a very narrow range, some displayed a bi-modal behavior, and some showed a wide range of values. This demonstrated a feature of the GA that standard optimization methods cannot replicate. When viewed as terrain, standard search methods rely on a reasonably well defined peak (*singular*) for convergence. The GA is able to reveal cases where the best solutions (*plural*) may exist on a mountain range. In the study of complex non-linear natural systems, the latter seems to be the more likely case.

During model runs interesting model behaviors were noted that required parts of the Vgrass model to be reconstructed. The discussion of chapter 3 describes how model design can affect the outcome of a GA search. The results show that when a model is to be used with a GA, the model builder must carefully evaluate the cost-benefit of the various possible model configurations.

Chapter 4 shows the results of applying the computational framework in testing plant growth strategies. The strategies were maximization of relative growth rate, maximization of biomass, and maximization of net primary production. As an example of a non-strategy, longevity (the ability to survive 20 simulated years) was also tested.

The test for maximizing relative growth rate (RGR) lead to a pattern of plant growth that was more related to how plant growth was measured. RGR was measured on a two week cycle and leaf emergence and abscission followed this two-week pattern. The results illustrate the care that must be taken when formulating a fitness function for the GA.

The test for maximizing biomass lead to huge plants. Leaf emergence for all of the season's leaves occurred early in the season and leaves were not abscised until P:R ratios were less than one. The results indicate that the goal of maximizing biomass leads to plant growth that totally ignores any economy to plant growth.

The test for maximizing net primary production (NPP) leads to large plants but also considers some economy in the plant growth. Maximizing NPP is a balance between maximizing production while minimizing respiration losses. The results show a pattern of leaf emergence and abscission that can be attributed to a strategy that optimizes carbon gain.

A test for longevity (surviving 20 years of simulated growth) revealed 88,479 of 90,000 solutions capable of achieving the goal. All of the 88,479 solutions were pooled and used to generate one representative of the test. Results from analysing that individual reveals plant growth patterns that were more *reasonable* when compared to the optimization tests.

Chapter 5 is a summary of the studies findings and relates them to research done in the field of artificial-life.

### 1.3 Literature Cited

- Buzzelli, C. P., Wetzel, R. L., and Meyers, M. B., 1999. A linked physical and biological framework to assess biogeochemical dynamics in a shallow estuarine ecosystem. *Estuarine, Coastal and Shelf Science*, 49, 829-851.
- Dennison, W. C., Orth, R. J., Moore, K. A., Stevenson, J. C., Carter, V., Kollar, S., Bergstrom, P. W., and Batiuk, R. A., 1993. Assessing water quality with submersed aquatic vegetation: Habitat requirements as barometers of Chesapeake Bay health. *Bioscience*, 43(2), 86-94.
- Givnish, T. J., 1983. *On the economy of plant form and function*. Cambridge University Press, New York, 717 pp.
- Jacobs, R. P. W. M., 1979. Distribution and aspects of the production and biomass of eelgrass, *Zostera marina*, at Roscoff, France. *Aquat. Bot.*, 7, 151-172.
- Nobel, P. S., 1991. *Physicochemical and Environmental Plant Physiology*. Academic Press, London, 635 pp.
- Orth, R. J., and Moore, K. A., 1986. Seasonal and year-to-year variations in the growth of *Zostera marina* L. (eelgrass) in the lower Chesapeake Bay. *Aquat. Bot.* 24, 335-341.
- Sakai, S., 1993. Allocation to attractive structures in animal-pollinated flowers. *Evolution*, 47(6), 1711-1720.
- Short, F. T., 1983. The response of interstitial ammonium in eelgrass (*Zostera marina* L.) beds to environmental perturbations. *J. Exp. Mar. Biol. Ecol.*, 68, 195-208.
- Thornley, J. H. M., 1998. Modelling shoot:root relations: the only way forward? *Ann. Bot.* 81, 165-171.
- Verhagen, J. H. G., and Nienhuis, P. H. 1983. A simulation model of production, seasonal changes in biomass and distribution of eelgrass (*Zostera marina*) in Lake Grevelingen. *Mar. Ecol. Prog. Ser.*, 10(2), 195-197.
- Wetzel, R. L., and Neckles, H. A., 1986. A model of *Zostera marina* L. photosynthesis and growth: simulated effects of selected physical-chemical variables and biological interactions. *Aquat. Bot.*, 26, 307-323.

## Chapter 2

# The Vgrass Model

### ABSTRACT

Published observations showing a relationship between leaf length and shoot density motivated the construction of an individual-based *Zostera marina* model. The model simulates one plant as a shoot with multiple leaves and simple meristem and root components. Leaf geometry is computed and combined with shoot density so that population self shading limits light availability and therefore above ground biomass. The model does not have a parameter that limits leaf growth; leaf growth is an emergent property of light availability. The individual based model also simulates the emergence and growth of individual leaves with the timing of emergence based on the integration of degree-days. Model output is compared to published observations and shows a relationship between leaf length, shoot density, and irradiance without the complicating factor of nitrogen availability. Degree-days is shown to be an effective method to simulate the timing of leaf initiation.

## 2.1 Introduction

Seagrass models have augmented the study of the relationship between environmental processes and the distribution and abundance of *Zostera marina*. Short (1980) provides a model of *Zostera marina* and demonstrates the role of light, temperature, and current velocity on the seasonal variation in seagrass production. Simulation results of production rates were correlated with independent observations made in neighboring seagrass communities. Verhagen and Nienhuis (1983) describe a model that includes the effects of aging on the production rates of leaves. Their model correlates with vertical and horizontal distributions of seagrass in Lake Grevelingen, The Netherlands. The model of Wetzel and Neckles (1986) includes epiphyte-grazer relationships and also indicates temperature and depth limits to seagrass growth in the lower Chesapeake Bay. Simulation results correlate well with independently obtained results of depth limits of seagrass growth (Wetzel and Neckles (1986) simulation, 1.0 – 2.0 meters; Orth and Moore (1983), 1.2 – 1.6 meters).

The above models are based on the average behavior of a population of plants. In the Wetzel and Neckles (1986) model, for example, one variable is used to represent the above ground biomass of plants contained within 1 m<sup>2</sup>. Likewise, all other model variables and parameters are spatially averaged to 1 m<sup>2</sup>. In the model there is a parameter that sets an upper limit on above-ground biomass. As above-ground biomass approaches this value photosynthesis is limited to slow down growth. Ultimately, photosynthesis is shut down when biomass equals this upper limit. This empirical approach simulates spatial limits to plant growth and, indirectly, the effect of plant self shading.

Meanwhile there are published observations that show a relationship between leaf length

and shoot density (Jacobs, 1979). Orth and Moore (1986) show the recovery of an eelgrass bed after periods of high temperatures likely caused a die off. In the year after the die-off shoot length is shorter, plant biomass is lower, but shoot density is higher. In the second year after the recovery these metrics more closely resembled those observed before the die off (Moore, personal conversation). Leaf length and shoot density may be related to nitrogen availability. Orth (1977) shows increases in leaf length and biomass due to an increase in nitrogen, while Short (1983) shows leaf length and shoot density variation across an ammonium and depth gradient. Jacobs (1979) shows a correlation between leaf length and shoot density and asserts that insolation controls shoot density.

These published observations motivated the design of an individual based seagrass model with the following objectives: 1) the model would use plant geometry and shoot density as a feedback mechanism to limit light through self shading. With these mechanisms in place shoot biomass becomes an emergent property since self shading negates the need for a parameter that limits shoot biomass; 2) to study the relationship between leaf length and shoot density as shown in Orth and Moore (1986).

This paper shows the construction, validation, calibration, sensitivity analysis, and performance of the Vgrass model. The model is run at two shoot densities based on Orth and Moore (1986) and shows a relationship between leaf length and shoot density that is a function of self shading.

## 2.2 Model Summary

The Vgrass model uses carbon as its currency and is based on a carbon fraction of 38% of tissue dry weight (Short 1987). An individual plant is modeled with simple root and meristem components and zero to several individual leaves. Natural root systems can have multiple shoots but for model simplicity one root component supports one shoot with multiple leaves. For the Vgrass model, plant and shoot are synonymous.

Vgrass has four state variables; leaf mobile carbon, leaf structural carbon, meristem carbon, and root/rhizome carbon (Figure 2.1b). Each active leaf is modeled individually (as opposed to lumping all leaves into one state variable) so that the total number of state variables actually changes as new leaves start and old leaves are abscised. Leaf mobile carbon can move between the leaf and the meristem and from there be allocated to leaf growth or root/rhizome storage. Leaf structural carbon is the result of leaf growth and, once allocated, cannot return to the meristem. This model also makes a distinction between leaves that are growing and those which have stopped growing (mature leaves). At the point where a leaf becomes *mature*, allocation to structural carbon is stopped. The mobile carbon pool is still free to exchange with the meristem. When a leaf is abscised, any mobile carbon within the leaf and the structural carbon are lost. The meristem state variable, while labeled as meristem, is mainly a mathematical construct to simplify the interactions between leaf state variables and the root/rhizome variable. The root/rhizome state variable represents both root and rhizome biomass and can exchange carbon bidirectionally with the meristem.

To describe Vgrass further a comparison is made with the Wetzel and Neckles (1986) model; both are shown in Figure 2.1. For brevity the Wetzel and Neckles (1986) model will

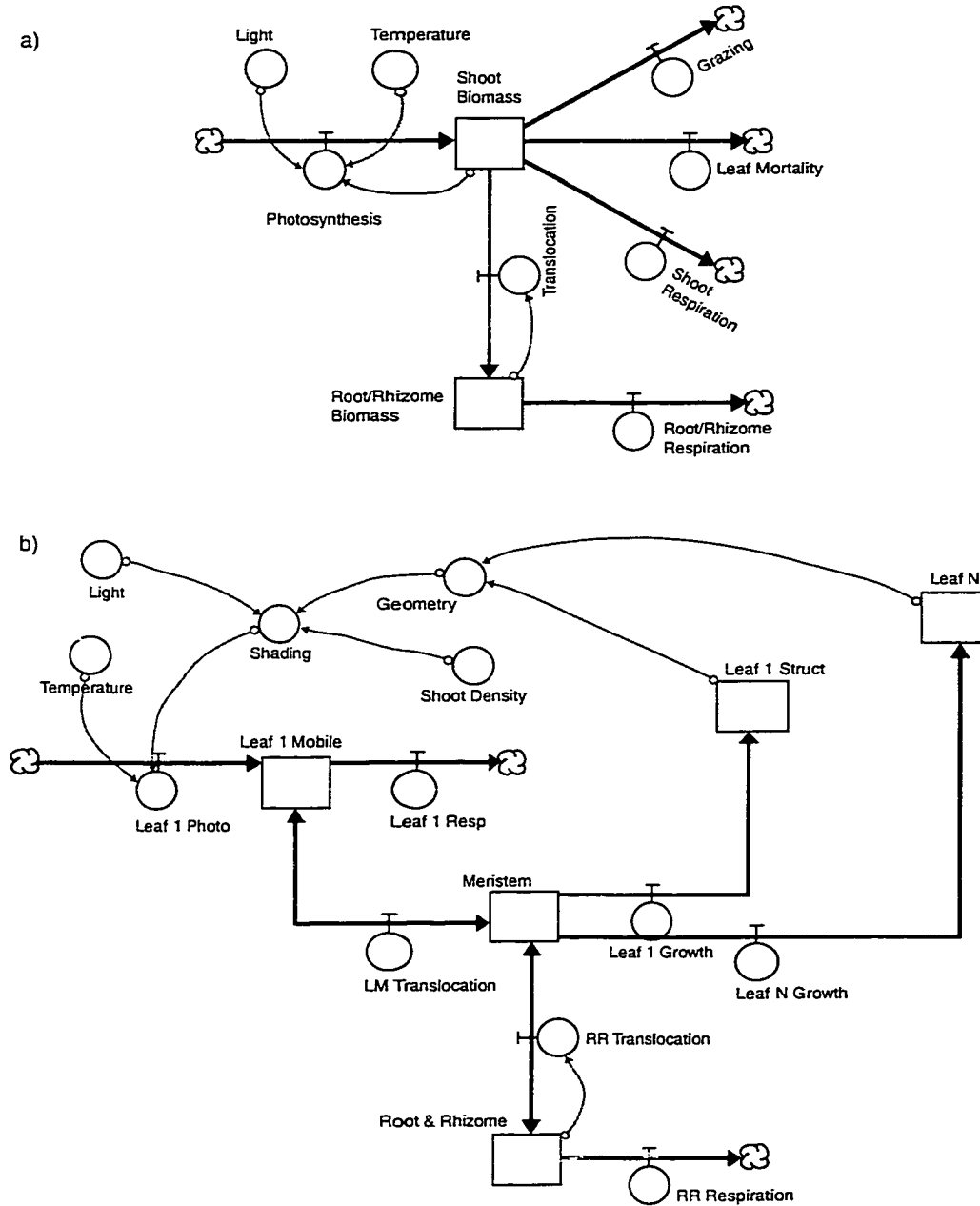


Figure 2.1: Simplified Forrester based diagrams of a) the Wetzel and Neckles (1986) model (WN86) and b) Vgrass. The diagrams show the primary differences between the models while not showing each model in its entirety. In the WN86 model biomass directly limits photosynthesis while in Vgrass photosynthesis is limited by leaf geometry and shoot density.



hereafter be referred to as WN86.

WN86 models the average behavior of a population of plants spread over a given area. Vgrass models an individual plant but is, basically, a scaled down version of a spatially averaged model. WN86 and Vgrass include the effects of light and temperature on photosynthesis but are different in how photosynthesis is limited by shoot biomass. Shoot biomass in WN86 is limited by a parameter set to an observed upper-limit on above ground biomass for *Zostera marina* ( $150 \text{ g C m}^{-2}$ ). As shoot biomass approaches  $150 \text{ g C m}^{-2}$ , photosynthesis is limited through a feedback equation. If shoot biomass reaches, or becomes greater than  $150 \text{ g C m}^{-2}$ , photosynthesis is stopped. In contrast, the Vgrass model grows individual leaves and the biomass of each leaf is used to compute leaf geometry. Leaf length does not decrease optical depth. Leaf lengths and shoot density are combined with Julian day, leaf width, and latitude to compute a shading factor. The computed shading factor is used to reduce the light available for photosynthesis. Biomass ultimately limits photosynthesis but through geometry and not a model parameter. Since there is no parameter that directly limits leaf growth, leaf growth becomes an emergent property (Cowan et al., 1994). The emergent nature of leaf growth should be the result of the interaction between leaf geometry and self shading. This behavior is assumed to be of critical importance in order to observe changes in leaf length, and thereby biomass, based on changes in the surrounding environment.

Another difference between WN86 and Vgrass is that Vgrass splits leaf carbon into a mobile carbon variable and a structural carbon variable (Figure 2.1). Leaf photosynthesis contributes to the leaf mobile carbon pool which is used for leaf respiration and which can

be translocated to the meristem. Carbon allocated to leaf structure, from the meristem, cannot be brought back into the mobile carbon pool and is lost when the leaf is abscised. Leaf carbon in WN86 can be translocated to root/rhizome but the flow is unidirectional. Leaf carbon is also lost to grazers, leaf respiration, and leaf mortality. Leaf carbon in Vgrass is zero when no leaves are attached. A leaf is started by translocating meristem carbon into structural leaf carbon.

Translocation from above-ground tissue to the root/rhizome is limited by root/rhizome biomass identically in each model; there is a parameter, based on spatial limitations, that limits below ground biomass. However, root/rhizome carbon in Vgrass can be translocated from the root/rhizome to the meristem to support leaf growth or increased respiration requirements. Root/rhizome respiration in the two models is identical.

Since Vgrass simulates the emergence and growth of individual leaves, a method was needed to time leaf initiation. Emergence for the season's first leaf, and subsequent leaves, is based on a time-temperature clock of degree-days. This method has been used in other grass models to predict plant phenology (Kiniry and Bonhomme, 1991; Dofing 1995; Saarikko and Carter, 1996). The determination of when a leaf stops growing and when it is abscised is based on a leaf's integrated daily production-to-respiration ratio. Each event occurs when the leaf's P:R ratio falls below a target value set by a corresponding controlling parameter (defined later).

Vgrass is an incremental step in seagrass modeling by moving from spatially averaged models to an individual based model. *Incremental step* is used here literally since the construction of Vgrass is based on the models of Wetzels and Neckles (1986), and Verhagen

and Nienhuis (1983). Vgrass is literally a scaled version of its ancestors. Wherever possible equations and parameters from the published models were *scaled to an individual plant*. Photosynthesis is based on data from Dennison and Alberte (1986) and general plant physiology data are taken from Nobel (1991). Vgrass is based on published models for two reasons. First, the published models are based on and validated against observational data; reusing their formulations simplifies the validation of Vgrass. Second, it is assumed that the amount of detail from the models and from the Dennison and Alberte (1986) study is sufficient for the research goals of this study.

## 2.3 Model Equations

### 2.3.1 The environment

The physical environment includes light, water depth, water temperature, and light attenuation due to water column attenuation and population self shading. Equations and parameter values for the environment are from Wetzel and Neckles (1986) and are listed in Table 2.1.

#### *Temperature*

$$T_c(\tau_{jd}) = T_{avg} - \left\{ T_{amp} \cos \left[ \frac{2\pi}{365} (\tau_{jd} - 25) \right] \right\} \quad (^\circ\text{C}) \quad (2.1)$$

Photosynthesis and respiration are functions of temperature. Temperature is also used to track degree-days (an integration of time and temperature).

Table 2.1: Definitions and values of model parameters. Environmental values are typical of the southern Chesapeake Bay USA, and identical to Wetzel and Neckles (1986).

Symbol	Purpose	Value	Units
<b>Environmental</b>			
$T_{avg}$	Temperature average	16.25	°C
$T_{amp}$	Temperature amplitude	13.75	°C
$Z_{avg}$	Tidal depth average	1.1	m
$Z_{amp}$	Tidal depth amplitude	0.4	m
$PP_{avg}$	Photoperiod average	11.75	Hr
$PP_{amp}$	Photoperiod amplitude	2.25	Hr
$PAR_{avg}$	PAR average	28.25	$E\ m^{-2}\ day^{-1}$
$PAR_{amp}$	PAR amplitude	16.75	$E\ m^{-2}\ day^{-1}$
$K_d$	Water column attenuation	-1	$m^{-1}$
<b>Time</b>			
$\tau_{jd}$	Julian Day	1.. $n$	Day
$\tau_{hr}$	Hour of the simulation	1.. $x$	Hr
$\tau_{hrd}$	Hour of the day	1..24	Hr
<b>Photosynthesis</b>			
$L_{CA}$	Leaf carbon to area conversion	0.035	$mg\ C\ mm^{-2}$
$\Theta_{PL}$	Photosynthetic temperature coeff.	1.08	-
$K_{EC}$	Photosynthetic carbon conversion	0.0015	$mg\ C\ \mu E^{-1}$
$RC_{max}$	Maximum rate of reaction center	2.0	$\times 10^{-12}\ \mu E\ hr^{-1}$
$a_l$	Leaf aging coefficient	0.5	-
$m$	Chl:area slope	6.1	$\times 10^{-15}\ mm^2\ chl^{-1}$
$b$	Chl:area intercept	-7.5	$\times 10^{-13}\ mm^2$
<b>Respiration</b>			
$\Theta_{RL}$	Leaf Respiration coefficient	1.04	-
$J_{max}$	Maximum leaf age	70	Days
$LR_{max}$	Maximum leaf respiration	0.00054	$mg\ C\ mg\ C^{-1}\ hr^{-1}$
$\Theta_{RR}$	Root respiration coefficient	1.05	-
$\Theta_{RM}$	Meristem respiration coefficient	1.05	-
$RR_{max}$	Maximum root respiration	0.00054	$mg\ C\ mg\ C^{-1}\ hr^{-1}$
$RM_{max}$	Maximum meristem respiration	0.00054	$mg\ C\ mg\ C^{-1}\ hr^{-1}$

*Tidal Height*

$$Z(\tau_{hr}) = Z_{avg} - \left\{ Z_{amp} \sin \left[ \frac{2\pi}{12.4} \tau_{hr} \right] \right\} \quad (\text{m}) \quad (2.2)$$

Tidal height varies water column depth above the plant. Since light is attenuated in the water column (eq. 2.6) it affects light attenuation.

The following equations are for photoperiod ( $PP(\tau_{jd})$ ) and daily PAR ( $PAR(\tau_{jd})$ ).  $PAR(\tau_{jd})$  is daily total irradiance and is used with  $PP(\tau_{jd})$  in equation 2.5 to compute an instantaneous rate at the air:water interface.

*Photoperiod*

$$PP(\tau_{jd}) = PP_{avg} - \left\{ PP_{amp} \cos \left[ \frac{2\pi}{365} \tau_{jd} \right] \right\} \quad (\text{hr}) \quad (2.3)$$

*Daily PAR*

$$PAR(\tau_{jd}) = PAR_{avg} - \left\{ PAR_{amp} \cos \left[ \frac{2\pi}{365} \tau_{jd} \right] \right\} \quad (\text{E m}^{-2} \text{ day}^{-1}) \quad (2.4)$$

*PAR at the air:water interface*

$$PAR(\tau_{hrd})^+ = \frac{10^6}{3600} \left\{ \frac{PAR(\tau_{jd})}{0.63662PP(\tau_{jd})} \right\} \cos \left\{ \frac{\pi}{PP(\tau_{jd})} (\tau_{hrd} - 12) \right\} \quad (\mu\text{E m}^{-2} \text{ s}^{-1}) \quad (2.5)$$

The positive sign indicates non-negative numbers. Values computed as less than zero, become zero.

*Self shading*

Jacobs (1979) shows a relationship between leaf length and shoot density but the re-

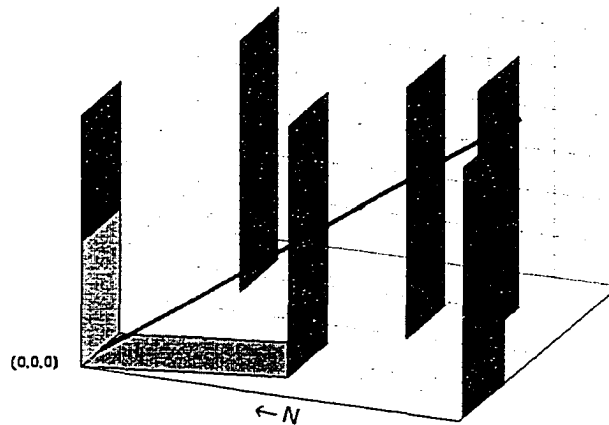


Figure 2.2: Diagram of 3-D self shading model. Each rectangle represents one plant. Solar elevation and azimuth (after refraction at the surface) is shown with the solid line drawn from base of the plant at the origin. The line intersects a plant ( $3^{rd}$  from the left) which is shading the plant at the origin. Its shadow is shown in light gray and shades 50% of the origin plant.

quirement here is to compute a shading factor as a function of leaf geometry and shoot density. A literature review for shading studies did not reveal any empirical relationships directly applicable to this study, so an elementary model of shading was developed.

Shading is estimated from a 3-dimensional representation of an eelgrass bed where rectangles represent individual plants. All rectangles stand vertical and have their surface areas normal to north and south (Figure 2.2). The rectangles are rigid and stationary; they do not bend over for current velocity effects nor do they track the sun. Each rectangle is placed randomly (in  $x$  and  $y$ ) in the virtual bed by selecting two random numbers between 0 and 1000 mm (the bed size is 1000 x 1000 mm). The orientation of the bed places the origin (0,0,0) at the north west corner. An additional rectangle, which will get shaded, is placed at the origin and a second additional rectangle is placed in space to receive 100% of available

light. Daily irradiance is integrated on both of these rectangles as follows.

Julian day and latitude are used to compute sun elevation and azimuth angles at 3 minute intervals (time interval, not degrees of arc) from first light to noon. The 3 minute interval was chosen by first trying larger intervals and then reducing interval size until repeated shading calculations returned similar results. Refraction of light at the air-water boundary is computed using Snell's Law (Kirk, 1994). At each interval a shadow is computed for the shaded rectangle. Shading neighbors are found by intersecting their locations with a line that runs from the origin to the refracted point of entry into the water (Figure 2.2); the closest rectangle on this line is selected. The distance to the closest shading neighbor, the geometries, and the solar zenith, are used to compute the percentage of area that is shaded on the shaded blade. Irradiance is integrated for both the shaded and unshaded blades from first light to noon (symmetry of the irradiance function is assumed for afternoon to dark). Light collected on the shaded blade is divided by the light collected on the unshaded blade and yields a fraction of light collected for that day. This was repeated for all combinations of shoot density, leaf width, leaf length, Julian day, and latitude given in Table 2.2.

For each combination, 300 different bed configurations were averaged. The only thing that changed within the bed configurations was the placement of the individual leaves; placement was randomized. The value of 300 was chosen by increasing the number of combinations until the computed average changed less than 1% from trial to trial. Results were placed in a 5-D lookup table.

Vgrass gets the shade factor ( $\delta$ ) from the 5-D lookup table where shoot density, leaf width, leaf length, Julian day, and latitude are the table ordinates. The values for each

Table 2.2: Ordinate values used to compute the shading array. Values extend beyond published values so that linear interpolation can be done within array boundaries.

Parameter	Values	Units
Shoot density	10, 100, 500, 1000, 1500, 2000, 3000, 5000, 7500, 10,000, 12,500, 15,000	shoots m <sup>-2</sup>
Leaf width	0.1, 0.5, 1, 2, 4, 6, 10, 15, 20, 25, 30, 40	mm
Leaf length	10, 50, 100, 250, 500, 750, 1000, 1250, 1500, 2000, 2500	mm
Julian day	1, 10, 20, 30, 40, 50, 60, 70, 80, 90, 100, 110, 120, 130, 140, 150, 160, 170, 180	day
Latitude	30, 37, 40	°N

ordinate are listed in Table 2.2; a 5-D linear interpolation is used for look-ups that do not match ordinate values. The ranges of these values are slightly beyond published ranges so that interpolation remains inside the ordinate ranges. Each leaf is opaque which may result in an over estimate of shade.

PAR at the leaf's surface can now be computed. This is also the amount of light reaching a PSU (Photosynthetic Unit) since the attenuation of light as it passes from the leaf's surface to the PSU is not considered.

*PAR at leaf surface*

$$PAR_{leaf} = \delta e^{\{K_d Z(\tau_{hr})\} + \log(PAR_{sec})} \quad (\mu E \text{ m}^{-2} \text{ s}^{-1}) \quad (2.6)$$

Equation 2.6 attenuates surface irradiance ( $PAR_{sec}$ ) through plant self shading ( $\delta$ ) and



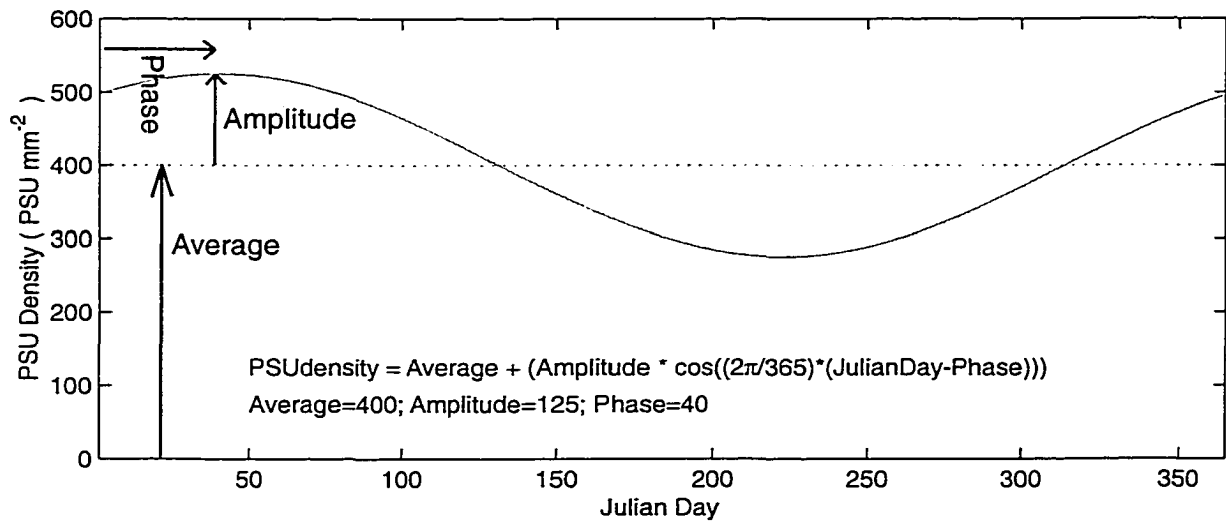


Figure 2.3: Average, Amplitude and Phase of  $\Gamma_{PSU}$ . The cosine form was chosen so that the phase number indicates the Julian day of the positive peak.

water column attenuation ( $K_d$ ). The result is the instantaneous light available at the leaf's surface.

### 2.3.2 Controlling Parameters

Vgrass has 25 parameters that can be varied to manipulate plant behavior. Table 2.3 shows each of the parameters, their purpose, their value for the *nominal* configuration, and their dimensional units. The set of values in this table will be collectively referred to as the nominal configuration. Except for Degree-days-first-leaf all of the parameters are used in triplets to compute a  $\Gamma$  variable (fourth column). An example equation and plot is shown in Figure 2.3.

$\Gamma_{DDF}$  determines how many degree-days will pass before the first leaf of each growing season is allowed to grow. Degree-days is an integration of time and temperature and is

Table 2.3: Controlling parameters for the nominal configuration. Except for *Degree-days first leaf*, each  $\Gamma$  variable is computed from three of the controlling parameters as in Figure 2.3. Space is used in the table to highlight the grouping.

Parameter	Nominal	Units	$\Gamma$ Variable
Degree-days first leaf	6	$^{\circ}\text{C Day}$	$\Gamma_{DDF}$
Degree-days next average	150	$^{\circ}\text{C Day}$	$\Gamma_{DD}$
Degree-days next amplitude	65	$^{\circ}\text{C Day}$	
Degree-days next phase	240	Days	
Shoot density average	1075	Shoots $\text{m}^{-2}$	$\Gamma_{SD}$
Shoot density amplitude	360	Shoots $\text{m}^{-2}$	
Shoot density phase	250	Days	
Leaf width average	5	mm	$\Gamma_W$
Leaf width amplitude	0.1	mm	
Leaf width phase	180	Days	
PSU density average	750	$10^8 \text{ PSU mm}^{-2}$	$\Gamma_{PSU}$
PSU density amplitude	200	$10^8 \text{ PSU mm}^{-2}$	
PSU density phase	60	Days	
PSU antenna average	450	$\text{Chl PSU}^{-1}$	$\Gamma_{ANT}$
PSU antenna amplitude	20	$\text{Chl PSU}^{-1}$	
PSU antenna phase	360	Days	
Stop leaf P:R average	3	Ratio	$\Gamma_{STOP}$
Stop leaf P:R amplitude	5	Ratio	
Stop leaf P:R phase	180	Days	
Abscise leaf P:R average	9	Ratio	$\Gamma_{ABS}$
Abscise leaf P:R amplitude	4	Ratio	
Abscise leaf P:R phase	300	Days	
Shoot:Root average	4	Ratio	$\Gamma_{SR}$
Shoot:Root amplitude	0.3	Ratio	
Shoot:Root phase	50	Days	

used as a temperature clock in plant models for predicting phenological development in maize (Kiniry and Bonhomme, 1991), barley (Dofing 1995), and spring cereals (Saarikko and Carter, 1996). Degree-days are integrated when the temperature is greater than 5 °C.

$\Gamma_{DD}$  establishes when the next leaf will be allowed to start growing. When a new leaf is initiated, whether it be the first leaf of the season or a subsequent leaf, two things happen. The current value of  $\Gamma_{DD}$  is placed into a target variable and the integrator for degrees is set to zero. Degree-days is integrated until the  $\Gamma_{DD}$  target is reached. At that instant the next new leaf is allowed to grow.  $\Gamma_{DD}$  establishes, through temperature and time, the plastichrone interval.

$\Gamma_{SD}$  establishes the current density of plants. This variable is used in the calculation of self shading and to scale the biomass of the individual plant to an areal estimate.

$\Gamma_W$  defines the width of a leaf that is about to start growing. When a new leaf is started, based on  $\Gamma_{DD}$ , the width of the new leaf is set to the current value of this variable.

$\Gamma_{PSU}$  defines the number of PSU's  $\text{mm}^{-2}$  that new leaf will have. The current value of  $\Gamma_{PSU}$  is assigned to a new leaf as it is started (just like  $\Gamma_W$ ) and does not change over time for the leaf. This variable allows PSU density to change on a seasonal basis, but only from leaf to leaf.

$\Gamma_{ANT}$  defines the number of additional chl that will be added to a PSU for use as antenna chl. Just like  $\Gamma_{PSU}$ , the value is assigned to a new leaf as it is started and does not change over the life of the leaf.

$\Gamma_{STOP}$  defines the P:R ratio at which the leaf changes status from growing to mature. This value is assigned to a new leaf as it is started. At midnight of each day, total daily

production and respiration for the leaf are compared to the value of  $\Gamma_{STOP}$  that was assigned to the leaf. If the leaf P:R ratio is equal to or less than this value, the status of the leaf is changed from growing to mature. When a leaf reaches the status of *mature*, the growth equations for the leaf are no longer computed.

$\Gamma_{ABS}$  defines the P:R ratio at which the leaf is abscised from the plant. This is just like  $\Gamma_{STOP}$  except that the status of the leaf changes from mature to dead. At this point the leaf variables are no longer computed and its mass no longer contributes to biomass calculations.

$\Gamma_{SR}$  defines the plant's target shoot-to-root ratio. At each step in the simulation  $\Gamma_{SR}$  is compared to the plant's current shoot-to-root ratio. If the plant's shoot-to-root ratio is less than  $\Gamma_{SR}$ , root growth is limited (the reverse is also true). If the difference between the two ratios is small, neither shoot nor root growth is limited.

### 2.3.3 Photosynthesis

Photosynthesis in the WN86 model is based on production vs. irradiance curves from observational data. To support requirements for future applications of the Vgrass model a slightly more sophisticated, but empirical, photosynthesis model was derived. The goal was to build a model of elementary chlorophyll (chl) dynamics so production vs. irradiance curves are a function of the number of PSU's and the number of antenna chl molecules added to a PSU.

The photosynthetic component of Vgrass is based largely on data from Dennison and Alberte (1986). Data are from *Zostera marina* plants growing over a depth range of 0.5 m

to 7.0 m and with sizes similar to those found in the lower Chesapeake Bay (Orth and Moore, 1986). Data are taken from plants that span a range of high to low light availability; this should allow the model to replicate a full range of photosynthetic adaptation. Photosynthetic data from other studies was not included to simplify validation.

Computing photosynthesis starts with converting leaf structural carbon and the carbon content of chl to leaf area. First, converting structural carbon to leaf area is based on  $1.6 \text{ dm}^2 \text{ gm}^{-1} \text{ DW}$  (Dennison and Alberte, 1986). It is converted to mg C DW using  $0.38 \text{ mg C mg}^{-1} \text{ tissue}$  (Short 1987) and is multiplied by 1.5 to factor in a metabolic construction cost (Poorter and Villar, 1997). The conversion factor,  $L_{CA}$ , is  $0.035 \text{ mg C mm}^{-2}$ . Even though a metabolic construction cost is added, this is still within the margin of published data for *Zostera marina* (Dennison and Alberte, 1982). Second, leaf carbon allocated to chl is computed from  $833 \text{ g C (mol chl}^{-1})$  (Nobel 1991), the leaf's PSU density ( $L_{PSU}$ ), and the amount of chl used for antenna ( $L_{ANT}$ ); these were assigned from  $\Gamma_{PSU}$  and  $\Gamma_{ANT}$  when the leaf started. From these two factors, leaf carbon is converted to leaf area ( $A_{leaf}$ ). Since leaf width was assigned when the leaf first started, length is calculated and used later for self shading.

From  $A_{leaf}$  and  $L_{PSU}$  the total number of PSU's in the leaf are known. A relationship between the number of PSU's and the amount of light energy they can harvest is needed. This is done by estimating an effective PSU area based on  $2.75 \text{ to } 4.25 \text{ mg chl dm}^{-2}$  (Dennison and Alberte, 1986) and from estimates that a PSU is comprised of 150 to 700 total chl molecules (Nobel 1991). From these factors, and appropriate unit conversions, the effective area of the PSU's in the leaf is:

*Leaf Chl Effective area*

$$A_{chl} = m \left\{ A_{leaf} L_{PSU} (L_{ANT} + 150) \right\} + b \quad (\text{mm}^2) \quad (2.7)$$

The coefficients in equation 2.7 are based on the assumptions: 1) that a PSU will have no less than 150 chl molecules, and 2) that the relationship between chl quantity and area can be approximated as linear (See table 2.1 for parameter values).

A photosynthetic rate ( $P_G$ ) is computed by multiplying  $A_{chl}$  by  $PAR_{leaf}$ . Saturation in the production vs. irradiance curve is a function of the number of PSU's in a leaf and the maximum photon processing rate of a reaction center; 1 photons every 5 milliseconds (Nobel, 1991). Carbon from photosynthesis is placed into the leaf mobile carbon state variable. Additionally, there is a feedback in the model so that if leaf mobile carbon becomes excessive, photosynthesis is limited (Bidwell, 1974; Lambers et al. 1998).

Figure 2.4 shows production vs. irradiance curves for various PSU densities and PSU antenna quantities. These curves exhibit behavior as shown in Dring (1982) and are numerically similar to those in Dennison and Alberte (1986). The photosynthetic model achieves this behavior based on a simple empirical model but is sufficient for the Vgrass model. Chl dynamics are much more complex than this.

As in Verhagen and Nienhuis (1983) an age function ( $G_S$ ) is applied to decrease leaf productivity with time. Zimmerman et al. (1995) show that photosynthesis does not change with leaf age. Decreasing production with age, while not specifically calibrated for this purpose, also simulates epiphytic growth which reduces light at the leaf's surface (Penhale,

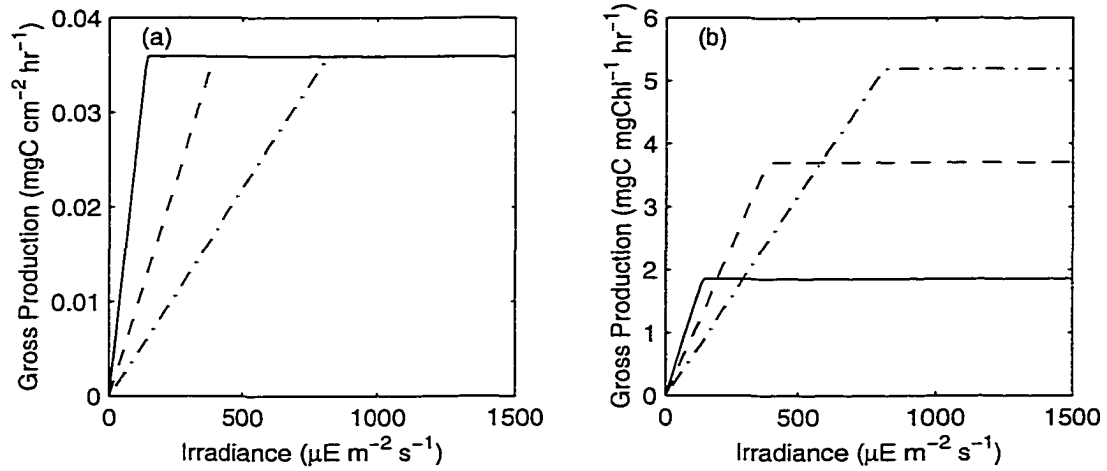


Figure 2.4: Model gross production vs. irradiance curves based on (a) leaf area and (b) chl content computed from the photosynthetic equations. Solid line based on  $2,000 \times 10^8 \text{ PSU mm}^{-2}$  with 550 antenna chl. Dashed line based on  $2,000 \times 10^8 \text{ PSU mm}^{-2}$  with 200 antenna chl. Dot-dash based on  $2,000 \times 10^8 \text{ PSU mm}^{-2}$  with 100 antenna chl.

1977). The effect of temperature on photosynthesis is also modeled as in Verhagen and Nienhuis (1983) and the same coefficient for  $\Theta$  is used here. A coefficient to convert the photosynthetic rate to carbon production,  $K_{EC}$ , is based on 8 Einsteins fixing 1 mole of  $\text{CO}_2$  (Nobel, 1991). Production is:

*Production*

$$P = K_{EC} P_G G_S \Theta_{PL}^{(T_C - 20)} \quad (\text{mg C hr}^{-1}) \quad (2.8)$$

### 2.3.4 Respiration

Respiration is computed for each growing and mature leaf, the meristem, and root/rhizome tissue. All respiration equations follow the form of Verhagen and Nienhuis (1983). Carbon for leaf respiration is taken from leaf mobile carbon and the equation for leaf respiration has an additional term so that respiration increases with age (equation 2.9). Ad-

ditionally, root respiration changes with the photoperiod (Zimmerman and Alberte, 1996). Roots become aerobic 1 hour after the beginning of the day's photoperiod, and become anaerobic 0.5 hrs after the end of the photoperiod. When the roots are anaerobic they respire at 65% of their aerobic rate. Respiration is based on the carbon content of the component ( $C_C$ ), a maximum respiration rate for the component ( $R_{max}$ ), and a temperature coefficient ( $\Theta_R$ ).

*Respiration*

$$R = C_C R_{max} \Theta_R^{(T_C - 20)} x \underbrace{\frac{L_{JD}}{J_{max}}}_{\text{Leaf only}} \quad (\text{mg C hr}^{-1}) \quad (2.9)$$

### 2.3.5 Allocation

The flows of carbon between state variables are: 1) leaf mobile carbon to/from meristem carbon, 2) meristem carbon to leaf structural carbon (leaf growth), 3) meristem carbon to/from the root/rhizome.

The flow of carbon between leaf mobile carbon and the meristem is a simple gradient flow based on Minchin et al. (1993). Leaves with high production have a net flow of carbon to the meristem even though night time respiration requirements may require the flow to reverse.

The flow of carbon from the meristem to leaf structural carbon is based on the growth equation from Verhagen and Nienhuis (1983). Growth is limited if meristem carbon is not available or if the current plant shoot-to-root ratio is higher than the *desired* shoot-to-root ratio which set by  $\Gamma_{SR}$ .

The flow of carbon from the meristem to the root/rhizome is based on the below ground



growth equation from Verhagen and Nienhuis (1983). Root/rhizome growth can be limited by three physical constraints: the availability of carbon from the meristem, the current plant shoot-to-root ratio and  $\Gamma_{SR}$ , and spatial limitations on root growth (from WN86).

$\Gamma_{SR}$  is used as in Grace (1997) to simply allocate carbon to leaf growth or root/rhizome storage based on the plant's current shoot-to-root ratio.

The flow of carbon from the root/rhizome to the meristem is a simple formulation so that if meristem carbon falls to a certain level, root/rhizome carbon can be moved into the meristem. The equations that move carbon between the meristem and root are calibrated such that the meristem always has carbon. If carbon begins to build up in the meristem, it is transported to the root. If meristem carbon is low, carbon is translocated from the root. Ultimately, allocation is dependent on the *desired* shoot-to-root ratio and spatial limitations.

## 2.4 Vgrass Validation

Nearly the entire Vgrass model was built on equations and coefficients from the models of Verhagen and Nienhuis (1983) and Wetzel and Neckles (1986). These models were validated against data from natural systems. Since this model reuses their equations and coefficients and none of the coefficients were *altered* to work in this model, validation of these same equations and coefficients would be redundant. Photosynthetic equations were based on literature estimates, mainly from Dennison and Alberte (1986) and Nobel (1991). Performance of the photosynthetic model was numerically similar to data in Dennison and Alberte (1986) and is shown in Figure 2.4; this similarity verifies the photosynthetic equa-

tions.

Validation of the integrated models was taken in two steps. First, simulation code which initiated, grew, and abscised leaves was monitored to ensure it modeled the leaf phenology. Second, a calibration step was added to show that the model can replicate biomass curves from a third model, BWM99 (Buzzelli et al. 1999). The BWM99 model contains an updated version of the WN86 model as a sub-component of a much larger ecosystem model. The biomass curves from BWM99 are considered to be more accurate (Wetzel, personal conversation) than those from the WN86 model.

## 2.5 Vgrass Calibration

For calibration, the controlling parameters (Table 2.3) were adjusted so that biomass data from Vgrass and BWM99 were similar. The growth and loss of individual leaves causes Vgrass biomass to fluctuate (Figure 2.5); *similarity* involved a visual approximation of the Vgrass biomass trends in relation to the BWM99 biomass data. Also, Vgrass performance was carefully watched so that, for instance, leaf age and the number of leaves growing did not fall outside published data. Essentially, biomass data needed to be comparable while other plant characteristics remained within reported ranges.

In a natural seagrass bed multiple shoots can originate from one plant; in Vgrass, each shoot is considered to be an individual plant. Biomass from Vgrass and BWM99 is compared in Figure 2.5 on both a plant and areal basis. Shoot density data from Moore (1996) is used to scale the BWM99 data down to a plant and, likewise, to scale the Vgrass plant up to an areal estimate. Figure 2.6 shows that the nominal simulation is stable over 5 years. That

Table 2.4: Metrics are computed from the second year of the simulation. Ranges of values are reduced to minimum, average, and maximum values. NPP is Net Primary Production. BIO is the peak biomass obtained during the year. RMS % biomass error is computed as in equation 2.10 but with a modification (see text).

Metric	Min	Avg	Max	Units
First Shoot		70		Julian day
Plastichrone	8	13	30	Days
Leaf Length	20	26	33	cm
Leaf Age	20	28	49	Days
LAI		1.6	5.2	$\text{m}^2 \text{m}^{-2}$
Leaves		22		leaves $\text{y}^{-1}$
NPP Plant		294		$\text{mg C y}^{-1}$
NPP Pop.		343		$\text{g C m}^{-2} \text{y}^{-1}$
BIO Plant		124		$\text{mg C}$
BIO Pop.		149		$\text{g C m}^{-2}$
RMS AG		28.4		RMS % biomass error (MOD)
RMS BG		12.5		RMS % biomass error (MOD)
RMS Plant		26.9		RMS % biomass error (MOD)

is, the biomass peaks from year to year are similar in magnitude, and there is no evident trending.

Table 2.4 lists performance metrics collected from the second year of the simulation. These were collected for comparison to published data and are used later to compare different Vgrass runs. The calculation for RMS % biomass error is done slightly different from standard practice. Computing RMS % biomass error based on equation 2.10 lead to rather high values. Since biomass from Vgrass fluctuates while the BWM99 biomass is relatively smooth, every data point leads to an increase in the summed error. The resulting number quantifies the amount of deviation but gives no indication as to whether or not the trend in the deviations follows the BWM99 data. To capture the trend a slight modification is made to equation 2.10. If Vgrass biomass is greater than BWM99 biomass, the % difference

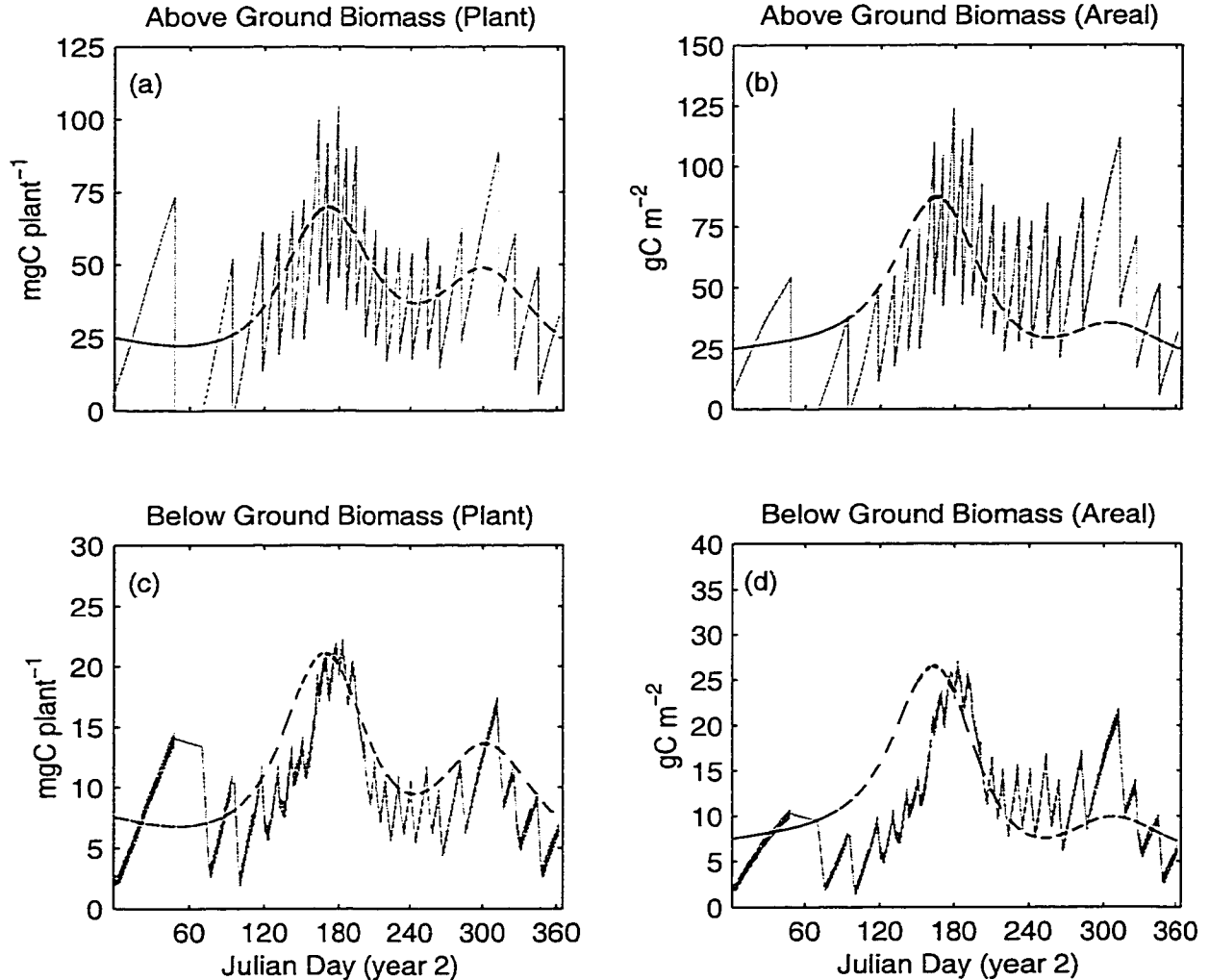


Figure 2.5: Biomass from the nominal configuration compared to BWM99 model biomass. Output from the BWM99 model shown as dashed (smooth) line. Output from the nominal configuration in black/gray (jagged) lines. a) Above-ground and c) below-ground biomass of an individual plant. b) Above-ground and d) below-ground biomass of a square meter of seagrass bed. The Vgrass model simulates individual leaves instead of lumping their biomass into one state variable. The growth and abscission of the individual leaves causes the biomass to fluctuate. Biomass from the single plant is multiplied by shoot density (Moore 1996), and therefore, the areal biomass is subject to the same fluctuations.

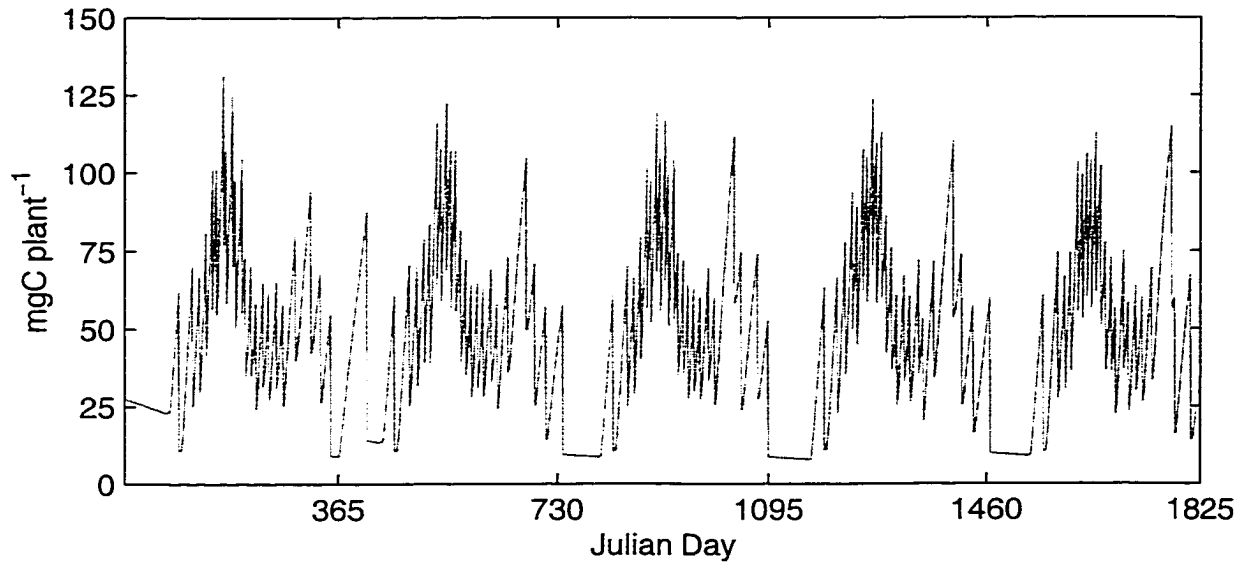


Figure 2.6: Biomass plot of the nominal configuration showing stability over 5 years (i.e. there is no evident trending).

is added in the summation. If *Vgrass* is lower than *BWM99* biomass, the % difference is subtracted. This results in a value that captures the ability of the *Vgrass* model to follow the trend of the *BWM99* even though there may be large excursions. Ideally the positive and negative excursions would average to zero. The resulting values are presented in table 2.4 for above-ground biomass (AG), below-ground biomass (BG), and for AG and BG collectively. Since the below-ground component is modelled in similar fashion to *WN86*, the % error is lower than that experienced by the above-ground calculation.

*Vgrass* plant biomass is typical for the southern Chesapeake Bay. Orth and Moore (1986) show an areal biomass of  $300 \text{ g C m}^{-2}$ . Using a shoot density of  $1,200 \text{ shoots m}^{-2}$  and the  $0.38 \text{ g C (g tissue DW)}^{-1}$  (Short, 1987), peak plant biomass is ca.  $95 \text{ mg C plant}^{-1}$ . Given that the biomass data from Orth and Moore (1986) was based on an average, *Vgrass* plant

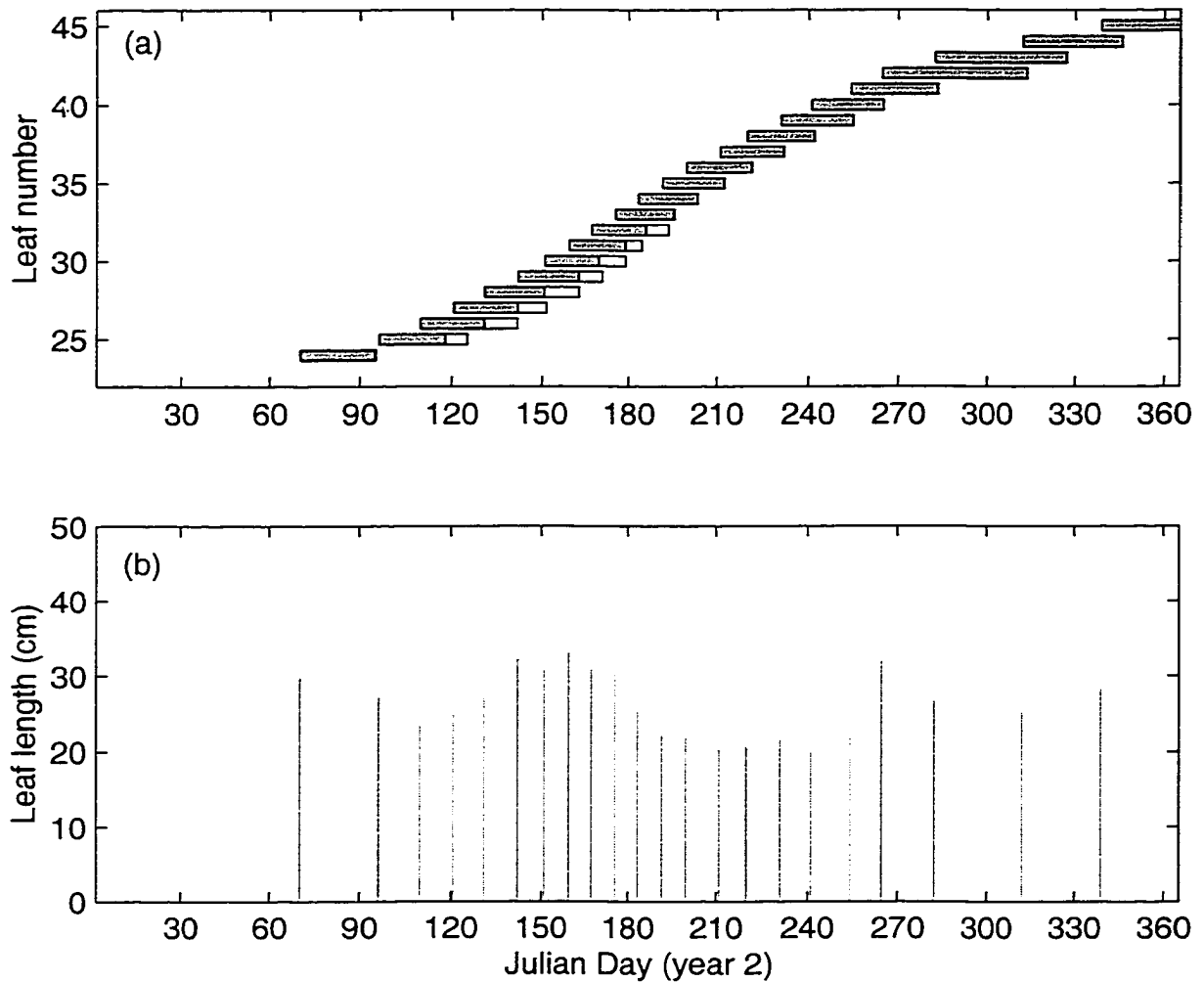


Figure 2.7: Nominal configuration leaf growth. a) each bar represents the start date (left edge), growth stage (left shaded area), mature stage (right unshaded area), and abscission (right edge). b) lines indicate the start date (x axis) and the final length (y axis) of the leaf.

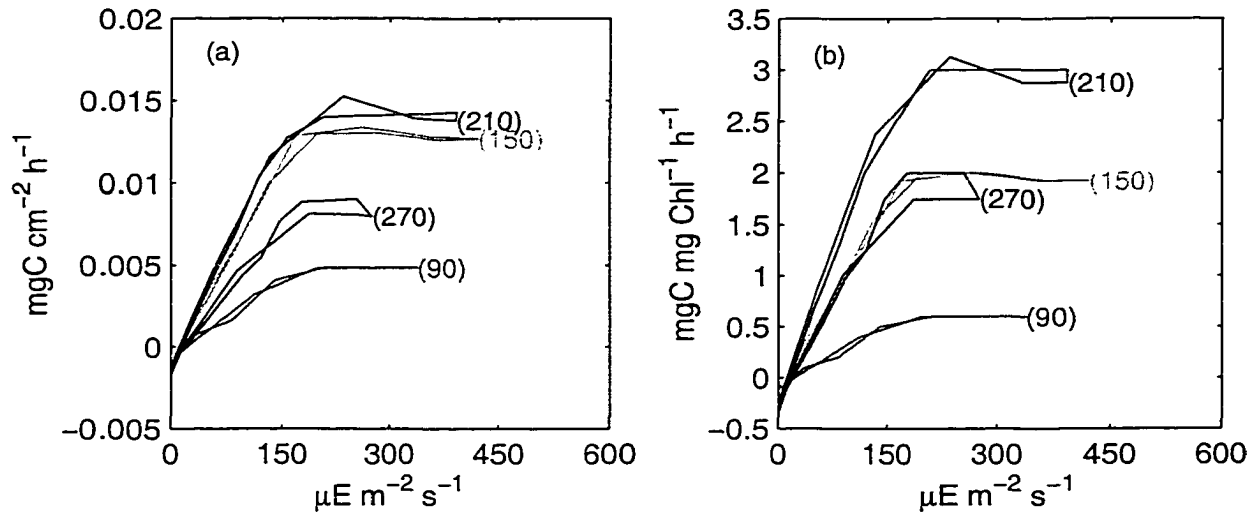


Figure 2.8: Nominal configuration whole-plant production vs. irradiance plots based on leaf area (a) and chl (b). Each line represents 24 hrs of data; the hysteresis is due to production differences between morning and afternoon. The numbers at the end of each line indicate the Julian day of the second year of simulation from which the data were taken.

total biomass (Figure 2.6) is nearly identical.

Figure 2.7a shows leaf longevity and, through overlapping bars, that no more than 3 leaves are attached at a time. Longer plastichrone intervals are seen in the winter and spring seasons (Figure 2.7b) and leaves grow to a longer length during the peak of the growing season. Figure 2.8 shows how  $\alpha$  and  $P_{max}$  through the year. The changes are due to  $\Gamma_{PSU}$  and  $\Gamma_{ANT}$ . These curves show a hysteresis effect that is due to a feedback in Vgrass that limits photosynthesis if leaf mobile carbon exceeds a parameter specified value. Production in the afternoon can be limited if production was high earlier in the day and the plant could not allocate the mobile carbon fast enough to the roots or to new leaf growth.

Table 2.5: RMS % Biomass error for model parameters. Error is % biomass change averaged from 10% increase and 10% decrease in the parameter value.

Symbol	Parameter function	Error
$\Theta_{PL}$	Photosynthetic temperature coefficient	233
$\Theta_{RL}$	Leaf Respiration coefficient	232
$K_{EC}$	Photosynthetic carbon conversion	57
$RC_{max}$	Maximum rate of reaction center	54
$J_{max}$	Maximum leaf age	51
$LR_{max}$	Maximum leaf respiration	50
$L_{CA}$	Leaf carbon to area conversion	49
al	Leaf aging coefficient	45
m	Chl:area slope	43
$\Theta_{RR}$	Root respiration coefficient	36
$\Theta_{RM}$	Meristem respiration coefficient	29
b	Chl:area intercept	25
$RR_{max}$	Maximum root respiration	6
$RM_{max}$	Maximum meristem respiration	6

## 2.6 Sensitivity Analysis

Parameter sensitivity was computed using Root Mean Square (RMS) percent change in biomass (Equation 2.10). Average RMS error, based on Swartzman and Kaluzny (1987), due to a 10% increase and 10% decrease in each parameter's value is shown in Table 2.5.

$$Error = \sqrt{\sum_{t=1}^{8760} \left( \frac{B_{nom}(t) - B(t)}{B_{nom}(t)} \right)^2} \times 100 \quad (\text{RMS \% Biomass error}) \quad (2.10)$$

In equation 2.10, the summation occurs on hourly intervals for the second year of the simulation run.  $B_{nom}(t)$  represents the biomass at time  $t$  for the nominal run, and  $B(t)$  represents biomass during the sensitivity run.

Table 2.5 shows the results of RMS error and the percent biomass change for the model's



constant parameters. The table is sorted in order of decreasing RMS % biomass error. The two most sensitive parameters,  $\Theta_{PL}$  and  $\Theta_{RL}$ , are temperature coefficients for photosynthesis and leaf respiration.  $\Theta_{PL}$  directly affects the only source of carbon input for the model, and  $\Theta_{RL}$  affects a major source of carbon loss in the model. The next parameters in the table,  $K_{EC}$  and  $RC_{max}$  directly affect the conversion of light to carbon and the maximum rate of a reaction center. Like  $\Theta_{PL}$ , these parameters play a direct role in carbon acquisition. Generally, since the models that Vgrass is based on reflect sensitivity to temperature and light it is not surprising that Vgrass is also sensitive to the same.

Table 2.6 shows the results of RMS % biomass error for the controlling parameters. The values used for the controlling parameters are listed in the nominal column of Table 2.3. Since these parameters control model behavior, it is desirable that the model show a moderate level of sensitivity to these parameters. It is interesting to note that the first three parameters directly affect timing events during the plant's life cycle. Taken together these 3 parameters affect when a leaf starts growing, stops growing, and is abscised. A 10% change (36 days) in either of these parameters has more impact on the RMS error than, for instance, changing the number of chl in the PSU. This suggests that the model is more sensitive to event timing than to the averages or amplitudes of the parameters. This should be expected given the seasonal variation in temperature and light and the need to time plant events in phase with these variations. Leaf width average appears low in the table (leaf width average, 22 RMS % biomass error) while leaf width phase and amplitude are at the very bottom. While leaf width affects LAI, and ultimately self shading, it does not appear to be a major influence on leaf biomass. The nominal value for leaf width is 5 mm.

Table 2.6: RMS % Biomass error for each of the controlling parameters. Error is % biomass change averaged from 10% increase and 10% decrease in the parameter value.

Parameter function	Units	Error
Stop leaf phase	Days	85
Abscise leaf P:R phase	Days	58
Degree-days between phase	Days	55
PSU density average	$10^8$ PSU $\text{mm}^{-2}$	51
Stop leaf P:R amplitude	Ratio	50
Abscise leaf P:R average	Ratio	50
Stop leaf P:R average	Ratio	48
PSU antenna average	Chl PSU $^{-1}$	45
Degree-days between average	$^{\circ}\text{C Day}$	43
Shoot density average	Shoots $\text{m}^{-2}$	38
Shoot density amplitude	Shoots $\text{m}^{-2}$	36
PSU density amplitude	$10^8$ PSU $\text{mm}^{-2}$	33
Shoot density phase	Days	33
Degree-days between amplitude	$^{\circ}\text{C Day}$	32
Abscise leaf P:R amplitude	Ratio	32
PSU antenna phase	Days	31
Leaf width average	mm	22
PSU density phase	Days	22
Shoot:Root average	Ratio	21
Degree-days to first leaf	$^{\circ}\text{C Day}$	13
PSU antenna amplitude	Chl PSU $^{-1}$	13
Shoot:Root amplitude	Ratio	6
Shoot:Root phase	Days	6
Leaf width phase	Days	6
Leaf width amplitude	mm	0

Table 2.7: Comparison of Vgrass and data from Orth and Moore (1986) at two different shoot densities. Data from Orth and Moore were estimated from figures. Plant weights were converted to carbon using  $0.38 \text{ g C (g tissue DW)}^{-1}$ .

	Orth and Moore		Vgrass		
	1100	2500	1075	2500	
Shoot Density					Shoots $\text{m}^{-2}$
Leaf Length	40	20	33	27	cm
Max Biomass (Plant)	120	80	124	90	mg C
Max Biomass (Areal)	133	200	149	233	$\text{g C m}^{-2}$

## 2.7 Model Application

Orth and Moore (1986) show year-to-year changes in a seagrass bed after a die-off of seagrass at an inshore site. The die-off was not evident at a nearby offshore site and the die-off was presumed to be caused by a "certain period" of high temperature. In the year after the die-off, shoot density was higher while leaf length was shorter, and above- and below-ground biomass increased. In the year following the recovery, shoot density and leaf length reverted to pre-die-off values (Moore, personal conversation). These year-to-year changes in density, leaf length, and biomass are compared here with the Vgrass model.

The nominal configuration of Vgrass has similar shoot density (1,075 shoots  $\text{m}^{-2}$  average) to the shoot density in Orth and Moore (1986) before the die-off (ca. 1,100 shoots  $\text{m}^{-2}$ ). For comparison, the controlling parameter for shoot density was changed to 2,500 shoots  $\text{m}^{-2}$  in the Vgrass model. Output from Vgrass was compared the observed data at the two shoot densities. Metrics that can be compared between Vgrass and the observed data are shown in Table 2.7.

In a qualitative comparison of the observed data and Vgrass output there is agreement

Table 2.8: Response of Vgrass simulation metrics after a change in shoot density. Metrics are computed from the second year of the simulation. Ranges of values are reduced to minimum, average, and maximum values. NPP is Net Primary Production. BIO is the peak biomass obtained during the year.

Metric	Nominal Configuration			High-Density Configuration			Units
	Min	Avg	Max	Min	Avg	Max	
First Shoot		70			70		Julian day
Plastichrone	8	13	30	8	13	30	Days
Leaf Length	20	26	33	18	22	27	cm
Leaf Age	20	28	49	19	26	37	Days
LAI		1.6	5.2		3.0	8.3	$\text{m}^2 \text{m}^{-2}$
Leaves		22			23		leaves $\text{y}^{-1}$
NPP Plant		294			207		$\text{mg C y}^{-1}$
NPP Pop.		343			536		$\text{g C m}^{-2} \text{y}^{-1}$
BIO Plant		124			90		$\text{mg C}$
BIO Pop.		149			233		$\text{g C m}^{-2}$

in the overall trends. When shoot density is increased, leaf length decreases, plant biomass decreases, and areal biomass increases. Likewise, the relationship between shoot density and leaf length shown here is in agreement with Jacobs (1979); an increase in shoot density leads to a shortening of leaf length.

Figure 2.9 shows lower individual biomass but increased areal biomass with the increase in shoot density when compared to the BWM99 benchmark. It also shows, in similar fashion to Orth and Moore (1986), that an increase in plant biomass is largely due to an increase in below ground biomass. While leaf length is lower in the high-density configuration, it may not be significantly lower as shown in Figure 2.10. It was assumed that the self-shading model would lead to higher than expected shading. The decrease in leaf length here supports this (see discussion).

In the Vgrass model leaf growth is stopped when its daily production to respiration ratio

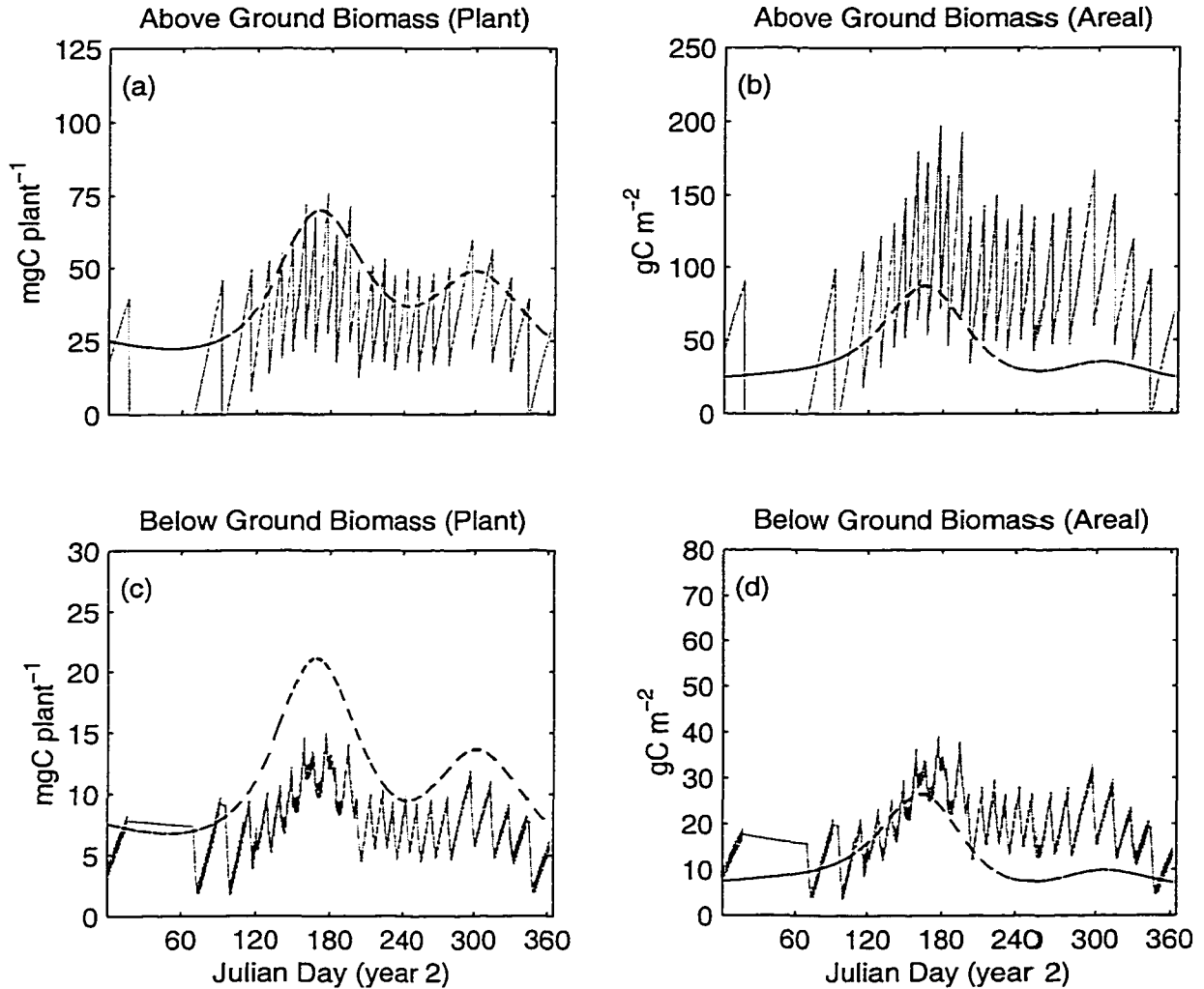


Figure 2.9: Biomass from the high-shoot-density configuration compared to BWM99 model biomass. Output from the BWM99 model shown as dashed (smooth) line. Output from the high-shoot-density configuration in black/gray (jagged) lines. a) Above-ground and c) below-ground biomass of an individual plant. b) Above-ground and d) below-ground biomass of a square meter of seagrass bed. The Vgrass model simulates individual leaves instead of lumping their biomass into one state variable. The growth and abscission of the individual leaves causes the biomass to fluctuate. Biomass from the single plant is multiplied by shoot density (Moore 1996), and therefore, the areal biomass is subject to the same fluctuations.

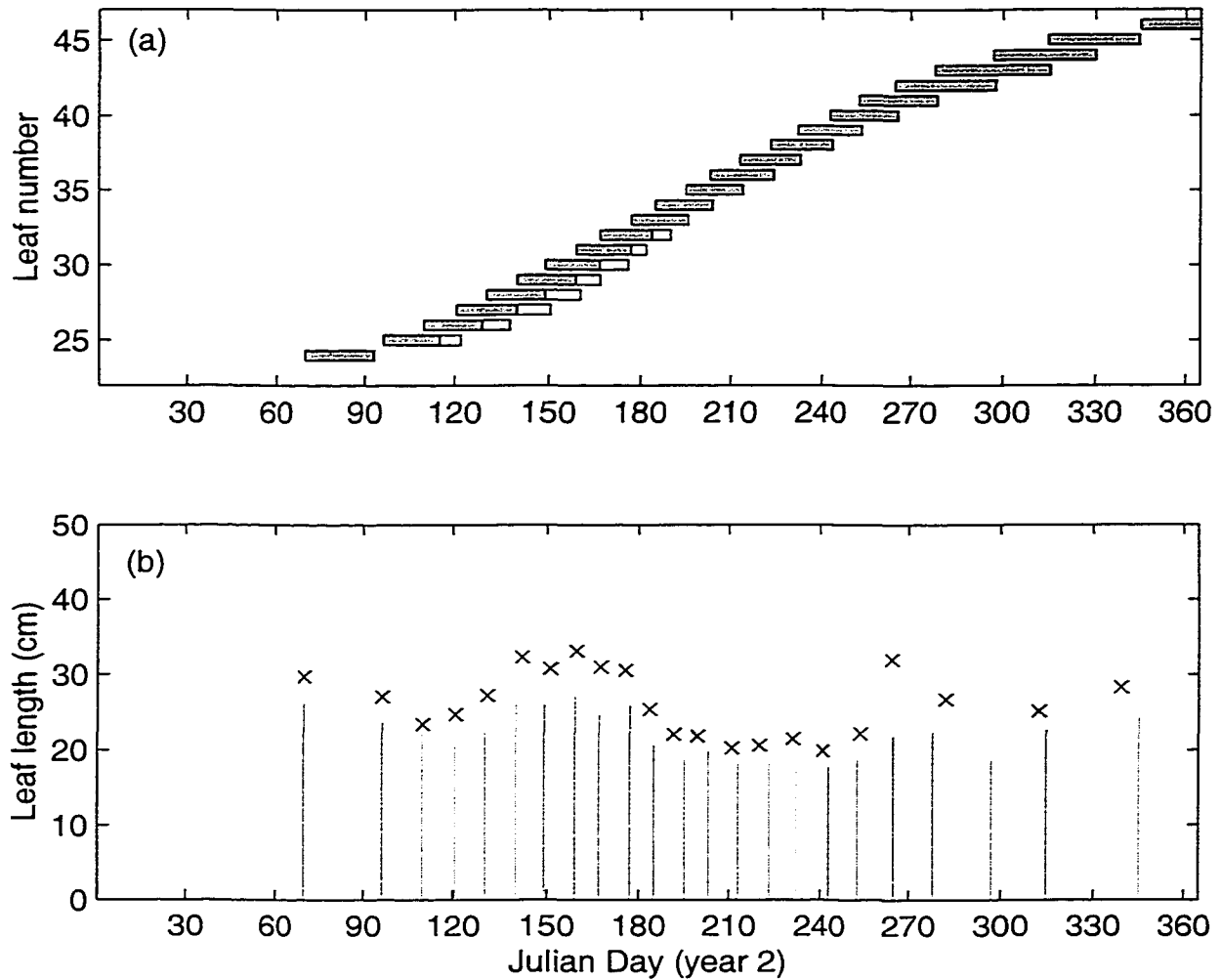


Figure 2.10: High-shoot-density configuration leaf growth. a) each bar represents the start date (left edge), growth stage (left shaded area), mature stage (right unshaded area), and abscission (right edge). b) lines indicate the start date (x axis) and the final length (y axis) of the leaf. The x's represent the lengths and timing of leaves from the nominal configuration.

falls below the value set by  $\Gamma_{STOP}$ . Likewise, a leaf is abscised when its daily production to respiration ratio falls below the value set by  $\Gamma_{ABS}$ . Higher shoot density increases shading and causes the leaves to stop growing and abscise sooner than in the nominal, lower-shoot-density, case. This decreases leaf length, leaf age, and above ground biomass (Table 2.8). Below ground biomass for the plant is maintained, relative to a plant growing at a lower shoot density, since leaf growth is slowed and the root/rhizome tissue growth has not reached limiting values. The individual plant is smaller but when the individual plant biomass is multiplied to an areal basis, areal biomass is higher than the nominal case. The same increases (plant compared to population) are shown with NPP and LAI.

## 2.8 Discussion

The objectives of this study were: 1) to build a seagrass model where plant geometry and shoot density are feedback mechanisms that limit light. 2) to compare output of the Vgrass model with data from Orth and Moore (1986). This chapter reviewed the construction, validation, and sensitivity analysis for a model based primarily on two published models and published photosynthetic data. As with the models ancestors, Vgrass showed sensitivity to light and temperature. Additionally, since the model simulated individual leaves, sensitivity was shown to the timing of leaf events. Since the timing of leaf events is based on degree-days, this indirectly shows sensitivity to temperature.

The environmental equations for Vgrass were taken directly from WN86 and included the use of a constant light attenuation coefficient of  $1 \text{ m}^{-1}$ . A constant value is not realistic in the sense of closely modeling the natural environment. However, modeling the short-

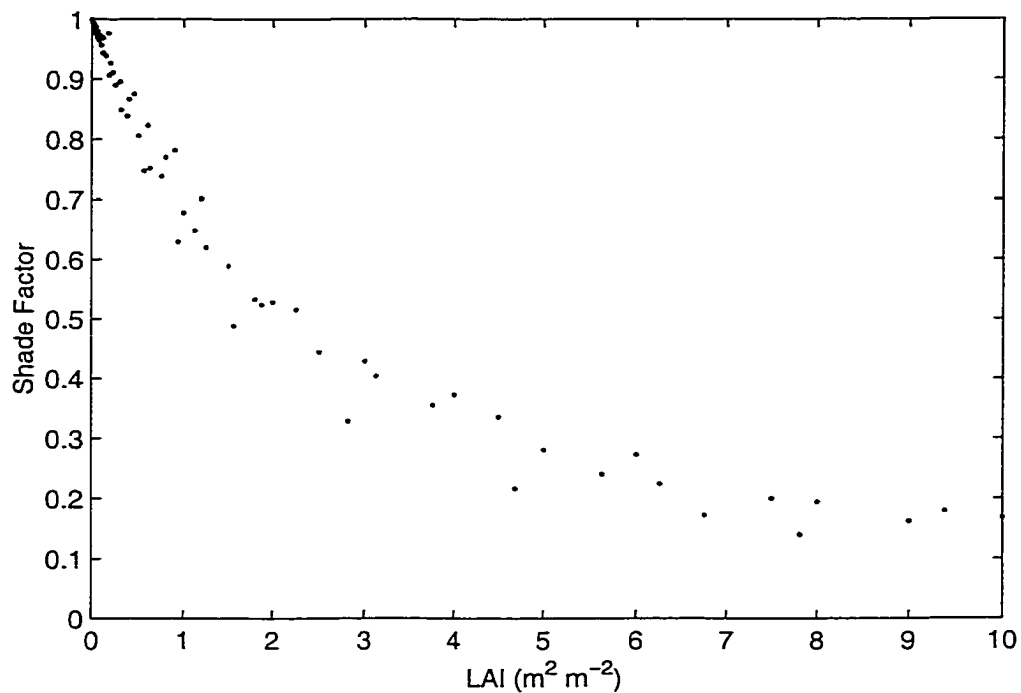


Figure 2.11: Shade Factor ( $\delta$ ) as a function of LAI. Points are average  $\delta$  values for LAI values computed with the self shading model.  $\delta$  continues to drop for LAI values greater than 10.

term dynamics of  $K_d$  may not affect the long-term trends of the models behavior. Zharova (2001) found that using a fixed (field average) value for light attenuation resulted in model behavior similar to when a variable scenario was used. The same might also be said for the daily fluctuations of temperature which are also not typically modeled.

A 3-D model was constructed to compute self-shade based on leaf length, leaf width, shoot density, Julian day, and latitude. This may be a case where a simplified approach may have lead to similar results. Figure 2.11 shows the relationship between LAI and the self shade factor ( $\delta$ ). A curve fit to these data points may have given similar results while eliminating the need for a 5-D linear interpolation.



Phenology in Vgrass is based on a method used in other grass models (Dofing, 1995; Kiniry and Bonhomme 1991; Saarikko and Carter, 1996). Degree-days are integrated and the integrated value indicates the passage of time and temperature. Chemical reactions are temperature dependent and degree-days is used to capture the time and temperature dependence of plant growth. Vgrass uses degree-days to predict the timing of the seasons first leaf and successive leaves. The emergence of the first leaf occurs at the beginning of growing season (Julian day 70) suggesting that degree-days is an effective method for timing *Zostera marina* models. However, the use of degree-days may need to be modified for *Zostera marina* models. Figures 2.7 and 2.10 show a shortening in the plastichrone interval during a time in the season when temperature reaches its highest point. The shortened interval is mathematically correct; increased temperature causes degree-days to integrate quickly. As a result Vgrass initiates new growth at a time in the season when growth may be stressed by higher temperatures. The WN86 model decreases  $P_{MAX}$  (based on field studies) when the temperature is above 25 °C as a means to capture the temperature related limitation. To capture this in the Vgrass model, the degree-days integration should be slowed when temperatures exceed 25 °C. In Vgrass, degree-days are integrated when the temperature exceeds 5 °C. Likewise, stopping the integration when the temperature exceeds 25 °C may result in a reasonable approximation and lengthen the plastichrone interval during periods of high temperature.

Controlling when a leaf stops growing and when a leaf is abscised is accomplished with the variables  $\Gamma_{STOP}$  and  $\Gamma_{ABS}$ . These variables establish a P:R ratio for each of these events and was based on general plant physiology (Lambers et al. , 1998) since no specific published

data were found. For each leaf, production and respiration are integrated throughout the day. At midnight the ratio is calculated. Leaves meeting the  $\Gamma_{STOP}$  value stop growing. Likewise, leaves meeting the  $\Gamma_{ABS}$  value are abscised. The numbers used in the nominal configuration were selected based on a combination that allowed a reasonable leaf age. The average values are  $\Gamma_{STOP}=3$  and  $\Gamma_{ABS}=9$ . These values indicate that a leaf will stop growing at a P:R ratio of 3 and immediately be abscised since the condition for abscission has also been reached. The value of  $\Gamma_{ABS}$  could be anything greater 3 and still give similar results. Further research is needed to improve the model. In an economic evaluation, abscising a leaf when the P:R ratio seems high; the leaf still provides a net income of carbon.

Photosynthesis in Vgrass is empirically derived from data in Dennison and Alberte (1986). The objective was to build a photosynthetic model wherein  $P_{MAX}$  and  $\alpha$ , and thereby production vs. irradiance curves, would become emergent behaviors of chl dynamics; the selection of  $\Gamma_{PSU}$  and  $\Gamma_{ANT}$ . The nominal model shows that this type of emergence is possible but with no real advantage; simple production vs. irradiance curves could have resulted in similar model performance. The role of chl dynamics will become important in a future application of Vgrass.

The data taken from Orth and Moore (1986) in table 2.8 can be compared to *self-thinning* processes discussed in Harper (1977). As the shoot density decreases from 2,500 shoots  $m^{-2}$  to 1,100 shoots  $m^{-2}$ , individual plant mass increases as with other plants (Harper, 1977). In contrast, areal biomass decreases; in other plants areal biomass increases with a decrease in plant density. Harper (1977) shows that self-thinning follows  $w = cp^{-\frac{3}{2}}$  which shows

the relationship between plant mass ( $w$ ) and plant density ( $p$ ). When the relationship is plotted on log-log axes,  $-\frac{3}{2}$  is the slope of the line and  $c$  is the y-axis intercept. When the data from Orth and Moore (1986) is used, a slope of -0.5 is computed for the two plant densities and weights. But since the data are taken from two growing seasons, this value may not represent anything meaningful. If instead, it is assumed that the data reflect a 'self-thinning' pattern and the slope actually is  $-\frac{3}{2}$ , then 2 lines with differing  $c$  exist. As suggested by a shading study in Harper (1977), the transition from 2,500 shoots  $\text{m}^{-2}$  to 1,100 shoots  $\text{m}^{-2}$ , and thereby a change in  $c$ , can be explained by lower light availability during the second year. (A similar change in  $c$  occurs using data from Orth and Moore (1986) from a nearby, offshore site.) Since Vgrass qualitatively followed the data from Orth and Moore (1986), and light levels were the same for each case in Vgrass, a conflict arises. The Vgrass model also shows that LAI decreases by a factor of 2 when shoot density changes from 2,500 shoots  $\text{m}^{-2}$  to 1,100 shoots  $\text{m}^{-2}$ . Meanwhile, LAI for the Orth and Moore (1986) data changes by a factor of only 1.1. This 10% change is probably not significant since it is computed from rough estimates taken from small figures.

Differences in LAI for the Vgrass model can come from two sources. First, from an overestimate of shade in the self shade model. Second, from an overestimate in the conversion of leaf biomass to leaf area. Both may be involved. A Vgrass leaf will stop growing when its P:R ratio drops below the  $\Gamma_{STOP}$  threshold. This threshold will be reached sooner if shade is overestimated relative to the length of the leaves. An overestimate of shade relative to a change in LAI will cause this to happen. As well, if leaf biomass is converted to an overestimate of leaf size, the same will occur. The self-shading model is likely the leading

factor since it is uncalibrated and the conversion from leaf biomass to leaf area is based on published data. Whichever is the cause, it shows up in comparing leaf length between Vgrass and Orth and Moore (1986). In the Orth and Moore (1986) study leaf length changes by a factor of 2 whereas in Vgrass (Table 2.8), leaf length changes by a much smaller factor.

In considering Vgrass' response to a change in shoot density, Jacobs (1979) asserts that shoot density is controlled by insolation. To complicate this, nitrogen supply may play a role in shoot density (Short, 1983) and shoot length (Orth, 1977). Short (1983) suggests that the relationship between shoot density and leaf length is related to both nitrogen supply and light availability. The Vgrass model does not consider nitrogen dynamics in its growth response but is able to show the relationship between shoot density and leaf length for *Zostera marina*. This suggests that nitrogen need not play a major role in this influence. Concurrently, since Vgrass does not consider nitrogen dynamics in plant growth, it cannot suggest that nitrogen plays no role in the relationship between shoot density and leaf length. Harper (1977) shows data from a nutrient related study wherein changes in nutrients and shoot density follow a line of constant  $c$  in the relationship  $w = cp^{-\frac{3}{2}}$ . An experiment like this for *Zostera marina* would likely confirm what Zimmerman et al. (1987) found; that *Zostera marina* growth is not likely limited by N since field N concentrations are above a limiting threshold.

The Short (1983) study expresses the idea that shoot density and leaf length are related to an optimal strategy for harvesting sediment nitrogen and harvesting light. In Orth and Moore (1986) shoot density and leaf length changed after a die-off and then changed back to pre-die-off values. What caused these responses? Is there an optimal growth strategy?

Is it a strategy to optimize the growth of an individual plant or that of the population?

What is optimized?

Vgrass is an incremental step in seagrass modeling. It uses leaf geometry as a feedback mechanism to limit light availability so that above-ground biomass growth becomes an emergent behavior. This is a necessary feature to explore optimal growth since *optimal* implies a trade-off between a cost and benefit. The cost of adding more above-ground biomass to increase light harvesting must be balanced with the amount of shading it will cause. Vgrass was not designed to automatically find that balance point, but does provide a model to study the interaction.

Vgrass, in comparison to its ancestors, carries the assumption that *Zostera marina* growth is largely influenced by light and temperature. Vgrass makes a contribution by showing that leaf phenology may be effectively modeled by incorporating a degree-days time-temperature clock. It is also shown that the limitation of growth through self shading can be modeled as a function of leaf geometry and shoot density; albeit, with a shading model that needs calibration. Adding these features was necessary for future use of the Vgrass model in studying plant growth strategies.

## 2.9 Literature Cited

- Bidwell, R.G.S., 1974. Plant Physiology. Macmillan, NY, 643 pp.
- Buzzelli, C. P., Wetzel, R. L., and Meyers, M. B., 1999. A linked physical and biological framework to assess biogeochemical dynamics in a shallow estuarine ecosystem. Estuarine, Coastal and Shelf Science, 49, 829-851.
- Cowan, G. A., Pines, D., and Meltzer, D., (editors) 1994. Complexity: metaphors, models, and reality. Addison-Wesley, 731 pp.
- Dennison, W. C., and Alberte, R. S., 1982. Photosynthetic responses of *Zostera marina* L. (eelgrass) to in situ manipulations of light intensity. Oecologia, 55, 137-144.
- Dennison, W. C., and Alberte, R. S., 1986. Photoadaptation and growth of *Zostera marina* L. (eelgrass) transplants along a depth gradient. J. Exp. Mar. Biol. Ecol., 98, 265-282.
- Dofing, S. M., 1995. Phenological development-yield relationships in spring barley in a subarctic environment. Can. J. Plant Sci. 75, 93-97.
- Dring, M. J., 1982. The biology of marine plants. Edward Arnold, London, 199 pp.
- Grace, J., 1997. Towards models of resource allocation by plants. In: Bazzaz, F. A., and Grace, J., (Editors), Plant resource allocation. Academic Press, 303 pp.
- Harper, J. L., 1977. Population biology of plants. Academic Press, New York, 892 pp.
- Jacobs, R. P. W. M., 1979. Distribution and aspects of the production and biomass of eelgrass, *Zostera marina*, at Roscoff, France. Aquat. Bot., 7, 151-172.
- Kiniry, J. R., and Bonhomme, R., 1991. Predicting maize phenology. In: Predicting Crop Phenology, CRC Press, Boca Raton.
- Kirk, J. T., 1994. Light and Photosynthesis in Aquatic Ecosystems. Cambridge University Press, Cambridge, 509pp.
- Lambers, H., Chapin III, F. S., and Pons, T. L., 1998. Plant Physiological Ecology. Springer-Verlag New York Inc., New York, 540 pp.
- Minchin, P. E. H., Thorpe, M. R., and Farrar, J. F., 1993. A simple mechanistic model of phloem transport which explains sink priority. J. of Exp. Bot., 44(262), 947-955.

- Moore, K. A., 1996. Dissertation: Relationships between seagrass growth and survival and environmental conditions in a lower Chesapeake Bay tributary. University of Maryland.
- Nobel, P. S., 1991. *Physicochemical and Environmental Plant Physiology*. Academic Press, London, 635 pp.
- Orth, R. J., 1977. Effect of nutrient enrichment on growth of the eelgrass *Zostera marina* in the Chesapeake Bay, Virginia, USA. *Marine Biology*, 44, 187-194.
- Orth, R. J., and Moore, K. A., 1983. Seed germination and the seedling growth of *Zostera marina* L. (eelgrass) in the Chesapeake Bay. *Aquat. Bot.*, 15, 117-131.
- Orth, R. J., and Moore, K. A., 1986. Seasonal and year-to-year variations in the growth of *Zostera marina* L. (eelgrass) in the lower Chesapeake Bay. *Aquat. Bot.* 24, 335-341.
- Penhale, P. A., 1977. Macrophyte-epiphyte biomass and productivity in an eelgrass (*Zostera marina* L.) community. *J. Exp. Mar. Biol. Ecol.*, 26, 211-224.
- Poorter, H. and Villar, R., 1997. The fate of acquired carbon in plants: chemical composition and construction costs. In: Bazzaz, F. A., and Grace, J., (Editors), *Plant resource allocation*. Academic Press, 303 pp.
- Saarikko, R. A., and Carter, T.R., 1996. Phenological development in spring cereals: response to temperature and photoperiod under northern conditions. *European J. of Agronomy*, 5, 59-70.
- Short, F. T., 1980. A simulation model of the seagrass production system. In: R.C. Phillips and C.P. McRoy (Editors), *Handbook of Seagrass Biology; An Ecosystem Perspective*. Garland STPM Press, NY, pp. 277-295.
- Short, F. T., 1983. The response of interstitial ammonium in eelgrass (*Zostera marina* L.) beds to environmental perturbations. *J. Exp. Mar. Biol. Ecol.*, 68, 195-208.
- Short, F. T., 1987. Effects of sediment nutrients on seagrasses: literature review and mesocosm experiment. *Aquat. Bot.*, 27, 41-57.
- Swartzman, G. L., and Kaluzny, S. P., 1987. *Ecological Simulation primer*. Macmillan Publishing Company, New York, 370 pp.

- Verhagen, J. H. G., and Nienhuis, P. H. 1983. A simulation model of production, seasonal changes in biomass and distribution of eelgrass (*Zostera marina*) in Lake Grevelingen. Mar. Ecol. Prog. Ser., 10(2), 195-197.
- Wetzel, R. L., and Neckles, H. A., 1986. A model of *Zostera marina* L. photosynthesis and growth: simulated effects of selected physical-chemical variables and biological interactions. Aquat. Bot., 26, 307-323.
- Zharova, N., Sfriso, A., Voinov, A., and Pavoni, B., 2001. A simulation model for the annual fluctuation of *Zostera marina* biomass in the Venice lagoon. Aquat. Bot., 70, 135-150.
- Zimmerman, R. C., Smith, R. D., and Alberte, R. S., 1987. Is growth of eelgrass nitrogen limited? A numerical simulation of the effects of light and nitrogen on the growth dynamics of *Zostera marina*. Mar. Ecol. Prog. Ser., 41, 167-176.
- Zimmerman, R. C., Kohrs, D. G., Steller, D. L., and Alberte, R. S., 1995. Carbon partitioning in eelgrass. Plant Physiology, 108, 1665-1671.
- Zimmerman, R. C., and Alberte, R. S., 1996. Effect of light/dark transition on carbon translocation in eelgrass *Zostera marina* seedlings. Mar. Ecol. Prog. Ser., 136, 305-309.



## Chapter 3

# Combining Vgrass

# With A Genetic Algorithm

### ABSTRACT

An individual based seagrass model (Vgrass) was coupled with a Genetic Algorithm (GA) to demonstrate the GA in combination with an ecological model. The GA method is described, the interface between the GA and Vgrass is defined, and the GA is used to optimize Vgrass controlling parameters. The goal for the GA was to minimize the RMS error between the biomass curves from Vgrass and a published seagrass model. The exercise demonstrated use of the GA for optimization but more importantly, two model behaviors were noticed that have important implications on model construction. In order for chl allocation to work properly the model had to be modified to include a cost factor so that allocating chl to increase photosynthetic unit density was five times more expensive (in terms of carbon requirements) than allocating chl as antenna chl. The factor of five is a model calibration and may not represent the actual biological cost, but the cost factor must be included for production vs. irradiance curves to replicate natural behavior. This study also showed that models coupled with the GA must be carefully constructed to include both the cost and benefit of any modeled features. Additionally, it is shown how a population of GA solutions can serve as a secondary sensitivity analysis. The additional sensitivity analysis indicates the model's flexibility in reaching the search goals of the GA.

### 3.1 Introduction

Optimization methods have been used in ecological modeling for several beneficial purposes. Drynan and Sandiford (1985) show several linear algebra formulations (or models) that have been used to study economic and biological objectives in fisheries management. While economic and biological complexity lead to differing results from each of the formulations, the authors suggest that results can be used together to assist the fisheries manager. Mohan and Keskar (1991) compare optimal management strategies based on the storage and release of water in a reservoir system. The reservoir system provides irrigation and hydropower production; operational policies for the system are complicated by this dual purpose. The study showed that policy based on release targets was better than policy based on storage targets. Mao and Mays (1994) describe another multi-objective model where the goals are to minimize freshwater inflow to an estuary while maximizing commercial-fish harvest of five fish species. Each of these studies uses goal programming or linear algebra based techniques that require the modeler to provide an initial *guess* at a possible solution. The initial guess can lead to solutions that are locally optimal. That is, the best solution, or global optimum, can be missed unless many initial guesses are tried. It is also notable that the goal programming approach is complex to implement when there are multiple objectives in the goal.

A search algorithm, the Genetic Algorithm (GA), has been used for optimization and has the attribute of being a global search algorithm; there is no single first guess to limit the search around a local optimum. As well, the GA has performed very well on complex problems (Goldberg, 1994). Mitchell (1997) provides a brief history of evolutionary compu-

tation and the GA. In summary, evolutionary computing started in the 1950's and 1960's using operators inspired by natural genetic variation and natural selection. This early work was problem specific and based mainly on mutations of a few parent solutions to generate new solutions closer to the optima. Holland (1975) developed the GA as a means to study adaptation in nature and to bring this feature into computer science. Holland's work introduced a population of candidate solutions and used *selection and crossover* of successful solutions as a means to create new candidate solutions. The method is based on natural selection and has been applied to many areas of science and engineering.

Goldberg (1994) cites four reasons why the GA is an attractive search and optimization method. 1) GA's can solve hard problems quickly and reliably. Most of the evidence for this is empirical but the theory is maturing. 2) GA's are easy to interface to existing simulations and models. As opposed to dynamic programming approaches which must be closely coupled with a simulation, the GA can exist as a separate entity with a simple interface to the simulation. This will be shown here later. 3) GA's are extensible. This means that the GA can be used in situations where there may be several global solutions. In nature these solutions would be considered different species that fulfill a certain ecological niche. This feature is used here and is also demonstrated in Johnson (1996). 4) GA's are easy to hybridize. That is, the GA can be modified to handle problem specific features.

A search for *Genetic Algorithm* in the engineering and science literature will reveal many different applications of the GA method. In ecological modeling the GA has not been used as widely; which is interesting given the method's origin. The GA has been used to calibrate model parameters (Wang, 1997), to study spider-web construction (Krink and

Vollrath,1997), and to study the spatial movements of fish (Huse and Giske, 1999). There are other applications in the literature but these illustrate three different ways that a GA can be applied.

Wang (1997) used a GA to optimize parameters in a rain-runoff model. To test the effectiveness of the GA, the author used the GA to optimize a problem wherein the optimal solution was already known. The GA was able to find a solution very close to the hypothetical optimum. Since most standard methods require an initial starting point, the author also combined the GA with the *univariant search method*. The GA predicted the starting point from which the standard method then found the optimal solution.

Using a GA to calibrate model parameters is actually an optimization problem that could be accomplished with other optimization methods. But the GA can be used for more complex tasks that cannot be done with classical optimization methods. This is shown in the following two examples.

Krink and Vollrath (1997) use a rule-based simulation and a GA to study spider web-building behavior. The rules for the simulation are used to define spiraling, radius, and looping behaviors (geometry rules) from which a *cyber-spider* then spins a web. The GA is used to optimize the web design for prey capture while considering construction cost of the material and the amount of skill, or time, required to build the web. A comparison of real and simulated webs showed no significant differences. Differences that exist might be explained through environmental factors such as gravity; a real spider can move faster going down than up; the cyber-spider did not consider the effects of gravity on movement. This study is an example of a complex simulation that is easily interfaced to a GA. The

simulation is not a set of equations which are then optimized through linear algebra or calculus based methods. In fact, this type of problem may be difficult, if not impossible, to solve with the standard mathematical methods. This is in large part due to the non-linear and discontinuous nature of the underlying simulation. The SIMPLEX method (Nelder and Mead, 1965) requires a continuous solution surface.

In another ecological application of the GA, Huse and Giske (1999) present an individual based fish model where the spatial movement of fish is controlled by a neural network<sup>1</sup>. The neural network controls reactive and predictive behaviors; reactive behaviors search for ideal habitat (temperature and prey) while predictive behaviors enable adaptive response to seasonal changes. In the second year of a fish's life it spawns a number of offspring in proportion to its body size. In their study the GA is not used to optimize, per se. GA methods are used so that offspring are a mix of their *mother's genetic makeup* and that of another member of the population. The new genetic makeup controls a neural network which determines how the offspring will respond to the environment. There is no specific optimization goal other than the implicit goal of survival and reproduction. The authors specifically cite a feature in their model, trophic feedback, that is necessary for proper model function. They also cite that this feature is impossible to implement with dynamic, or goal, programming methods<sup>2</sup>.

---

<sup>1</sup>A neural network takes multiple inputs such as environmental factors, processes them by means of weighting factors and offsets, and provides an output response. The output response is used in this study to control movement of the fish in the simulated environment. The weighting factors and offset are selected by a GA. Neural nets can exhibit very complex behaviors while at a mechanistic level they are a simple combination of multiply and add functions. While the mechanism is simple the numbers used in the process have no interpret-able meaning. One cannot look at a neural net configuration and learn how the net came up with certain behaviors

<sup>2</sup>these authors cite experience with goal-programming techniques in previous work.

As for optimization, there are other methods besides the linear algebra based methods and the GA. There are several reasons for not choosing them. First, classical methods require a first initial guess which can lead to a local optimum. An algorithm could be applied so that many initial guesses could be attempted systematically. This is feasible if there is a limited number of parameters to be optimized. In the application presented here there are 25 parameters that must be optimized and a systematic attempt at trying various starting points would be computationally prohibitive. For example, if each parameter was tested with 10 initial guesses, there would be  $10^{25}$  total initial guesses to optimize. Reducing each parameter to 5 initial guesses only reduces the computational burden to the order of  $10^{17}$  optimizations. In comparison the GA is used here to find local and global optima in fewer than  $10^5$  simulation runs. A second reason for choosing the GA is related to the topography of the solution space. For example, some of the classical optimization routines use hill climbing methods to find the top of the hill, the optimal solution. These methods assume that the hill has a well defined peak on which to converge. If there is no well defined peak the method has trouble converging to the solution. A GA method makes no assumptions as to the shape of the solution space and has the ability to show a population of solutions wherein there may be several local optima.

In addition, other methods are not considered here because of the broad applicability of the GA. Here the GA will be used to calibrate the Vgrass model; an optimization exercise. In Chapter 4, the Vgrass model and GA will be used to study plant allocation strategies; again an optimization exercise. In these optimization exercises it is desired to know if there is a population of solutions close to the optimal solution as opposed to finding one solution.

There is also a desire to use the Vgrass model in an individual based context to study adaptation at the scale of a population. The simplicity of the GA allows all of these studies to proceed with no modification to the Vgrass model and only minor changes in how the GA methods are used. The GA method was chosen for this study because it has been shown to be successful non-linear optimization. Since it works on a population of solutions, as opposed to a singular solutions, this feature allows for a *secondary sensitivity* analysis. It is not the objective of this study to demonstrate the GA as a possibly superior optimization method.

In this study the Vgrass model is coupled with a GA. The purpose of combining the plant model and search method is to enable future study of plant growth strategies. Here the objectives are to show how the model and GA are combined and to demonstrate how the GA can be used to calibrate Vgrass' controlling parameters. To meet these objectives the GA method is described, the interface between Vgrass and the GA is shown, and results from a Vgrass/GA demonstration are reviewed. Coupling Vgrass with the GA resulted in some initially unexpected, but explainable, behaviors related to model construction. The behaviors provide insight to plant physiology and how it should be modeled in optimization studies.

## 3.2 The Simple GA

The GA gets its name because it is a method that mimics the process of natural selection (Holland, 1975; Goldberg, 1989 and 1994; Mitchell, 1997). No inference should be made by the reader that the genetic in GA is in any way manipulating the real genetics of a living

organism. The GA is a search algorithm; genetic is a metaphor. It is accurately termed a search algorithm as opposed to an optimization method since the method is capable of more than optimization. Optimization implies a process that computes a number, or set of numbers, that maximize or minimize a given function. Search has broader application in that it may apply to numeric and symbolic methods. For clarification, a simple symbolic method might use letters in a string such as *ADOEPW* to describe a path through a set of nodes. The first node would represent the initial state, each successive letter would represent changes in state until the goal *W* is achieved.

The simple GA is termed as such because it works with binary values, 1 and 0. In biological terms these are alleles. Alleles are grouped together to form a gene and the combination may be used to represent a value or trait. For example, 1101 could represent the number 13, or perhaps the 13<sup>th</sup> letter of the alphabet. Genes are concatenated to become a chromosome. For the GA, the chromosome may be a set of numbers or symbols. A biological organism may have multiple chromosomes which collectively are called a genome. The simple GA used here has just one chromosome and the genes are used to represent integer values. A set of integers, or *genotype*, is converted to floating point numbers which are used to control the Vgrass simulation. A genotype, in the context of this study, represents a trial *configuration* in a search towards a goal.

The GA process starts with a population of genotypes, or individuals, where the alleles are randomly set to 1 or 0. Each individual is passed to a fitness function (discussed in more detail later) which returns a value that represents the individual's score in its attempt at reaching the goal. After the entire population has been evaluated, individuals are selected



for crossover. Selection is based on a weighted random process wherein individuals with higher fitness have a higher likelihood of being selected as parents. After two individuals are selected as parents, there is a probability that crossover will occur. If crossover does not occur, the individuals are just placed into the next generation. If crossover will occur, a crossover point is randomly selected. The crossover point is the location in the chromosomes where a split will occur, creating a head and tail portion for each of the two parents' chromosomes. Two offspring are made by taking head of one parent and concatenating it with the tail of the other parent. Parents are repeatedly selected and crossed over until another population of trials is produced. After crossover is complete, there is a small probability that each allele will undergo mutation. In this case, the allele value of 1 or 0 is switched.

Generation after generation is produced and tested until the solution is found or it is evident that population fitness is no longer improving. Typically, the average population fitness is tracked and when changes from generation to generation are small or nonexistent, the process is stopped. The best individual from the last generation is usually taken as the solution. Since there is a population of solutions, the best individuals can be selected to see if there is a distribution of genes that lead to highly fit individuals. This will be shown later.

The GA method is based on a collection of processes that make extensive use of random numbers: the first population is generated randomly, selection is a weighted random process, that crossover will occur is a probabilistic event, crossover is based on choosing a crossover point randomly, and mutation occurs randomly. Despite the use of random numbers in the GA method, GA's do converge on a solution. This is largely due to the weighted

random process of selecting parents. The theory behind how the GA method converges is summarized in Goldberg (1994) and Mitchell (1997). Briefly, the GA works because *highly fit* patterns have a higher probability of propagating from generation to generation than the *less fit* patterns. When highly fit patterns are selected and crossover, there is a likelihood that a better pattern will result thus increasing population fitness with each generation.

Use of the word pattern here is important. The GA only manipulates patterns of 1's and 0's based on ranking from another function; it has no information about what it is searching for or optimizing. This feature gives the GA broad applicability since the same GA code that optimizes a plant simulation can also be used to optimize a turbine engine. The only difference between the two problems, from the viewpoint of the GA, is the number of alleles used in the chromosome.

### 3.2.1 Vgrass-GA Interface

This following section describes how the chromosome's 1's and 0's are interpreted and evaluated by a fitness function. Table 3.1 lists the controlling parameters for the Vgrass model along with the values for the nominal configuration and each parameter's dimension. These are the parameters that must be read from the genes of the chromosome.

Table 3.1 also shows the upper and lower limits for each parameter; the GA does not search outside of these ranges. Each range is divided into an integer number of intervals where the interval size is set by the minimum resolution. The upper and lower limit and the resolution are used to determine how many binary digits, or bits, will be needed to represent all possible values. For instance, 3 bits can represent 8 unique values such as the

Table 3.1: Vgrass/GA Controlling parameters interface. The GA search range is defined by the lower and upper limits. Resolution is used with the limits to determine how many bits are necessary to represent the range of values. The 25 sets of bits are concatenated into a 209 bit chromosome which is manipulated by the GA. Floating point numbers are computed from the 25 binary numbers and passed to the GA via a fitness function. The parameter set used for the nominal (NOM) configuration is listed along with values chosen by the GA (GA) in the GA demonstration.

Parameter	Lower Limit	Upper Limit	Min. Res.	Bits	NOM	GA	Units
DD first leaf	2	10	0.1	7	6	8	°C Day
DD next avg.	0	350	1.0	9	150	200	°C Day
DD next amp.	0	100	1.0	7	65	83	°C Day
DD next ph.	0	365	1.0	9	240	311	Days
Shoot dens. avg.	100	12,500	10.0	11	1075	1109	Shoots m <sup>-2</sup>
Shoot dens. amp.	0	2,000	10.0	8	360	364	Shoots m <sup>-2</sup>
Shoot dens. ph.	0	365	1.0	9	250	235	Days
Leaf width avg.	1	25	0.1	8	5	4	mm
Leaf width amp.	0	12	0.1	7	0.1	0.8	mm
Leaf width ph.	0	365	1.0	9	180	178	Days
PSU dens. avg.	10	5000	10.0	9	750	2300	10 <sup>8</sup> PSU mm <sup>-2</sup>
PSU dens. amp.	0	500	1.0	9	200	303	10 <sup>8</sup> PSU mm <sup>-2</sup>
PSU dens. ph.	0	365	1.0	9	60	307	Days
PSU ant. avg.	0	650	2.0	9	450	383	Chl PSU <sup>-1</sup>
PSU ant. amp.	0	300	1.0	9	20	39	Chl PSU <sup>-1</sup>
PSU ant. ph.	0	365	1.0	9	360	20	Days
Stop P:R avg.	0.5	30	0.1	9	3.0	7.8	Ratio
Stop P:R amp.	0	10	0.1	7	5.0	5.1	Ratio
Stop P:R ph.	0	365	1.0	9	180	198	Days
Abscise P:R avg.	0.5	16	0.1	8	9.0	11.3	Ratio
Abscise P:R amp.	0	8	0.1	7	4.0	3.9	Ratio
Abscise P:R ph.	0	365	1.0	9	300	249	Days
Shoot:Root avg.	0.2	10	0.1	7	4.6	4.6	Ratio
Shoot:Root amp.	0	5	0.1	6	0.3	1.5	Ratio
Shoot:Root ph.	0	365	1.0	9	50	330	Days

integers 0 through 7. A multiplier and an offset, based on the upper and lower limits, are used to convert the integer into a real value. This process is the same for all 25 controlling parameters and results in a set 25 real numbers for input to a fitness function.

The fitness function takes the set of parameters and passes them to the Vgrass model. As the model runs, the fitness function tracks key variables in the simulation that are needed to evaluate fitness. For instance, if the goal is to optimize biomass, the fitness function tracks biomass. At the end of the simulation run the fitness function returns, in this example, the highest biomass attained during the simulation. This fitness value is used by the GA during the selection process mentioned earlier.

In summary, the interface between the GA and the Vgrass simulation amounts to three steps. 1) convert the binary chromosome into 25 controlling parameters; 2) the fitness function passes the parameters to Vgrass and monitors Vgrass' progress; 3) after the simulation is complete the fitness function returns a fitness rank to the GA method. This process is repeated for each individual in the population before the GA performs the selection process.

### 3.2.2 GA Demonstration

In this demonstration the GA searches for a configuration of Vgrass controlling parameters that fulfill the goal of minimizing the RMS error between Vgrass' biomass and that of the seagrass component of the model of Buzzelli, et al. (1999)<sup>3</sup>. Shoot density from Moore (1996) was used to convert the BWM99 data to the scale of an individual plant.

The fitness function computed the RMS errors for above ground and below ground

---

<sup>3</sup>Hereafter the Buzzelli, et al. (1999) model is referred to as the BWM99 model.

biomass during the second year of the simulation run. RMS error was computed as:

$$Error = \sqrt{\sum_{t=1}^{8760} \left( B_{BWM99}(t) - B_{Vgrass}(t) \right)^2} \quad (\text{RMS error}) \quad (3.1)$$

RMS error for above ground and RMS error for below ground were added and returned as a fitness rank to the GA. In order to compare plants that would be morphologically similar, the search limits for 6 of the controlling parameters were limited to values similar to the nominal configuration. Allowed ranges were: leaf width (4-6 mm), leaf width average (0-1 mm), leaf width phase (175-185 days), shoot density (975-1175 shoots  $\text{m}^{-2}$ ), shoot density average (330-390 shoots  $\text{m}^{-2}$ ), and shoot density phase (225-275 days). Without these limits it is possible for the GA to find other leaf width and shoot density combinations that meet the fitness goal. These plant configurations would not be as directly comparable to the nominal configuration since the leaf width and shoot density could be very different.

For this study a population was comprised of 450 individuals; the number was chosen subjectively. With a population of 450 individuals, maximum (or minimum) fitnesses were observed in less than 200 generations; all fitness tests were run for 200 generations for similarity. Figure 3.1 shows the maximum and average fitnesses of the population over the 200 generations. The average population fitness decreases quickly at first as individuals with poor fitness values are more likely to be eliminated from the population. The figure also shows the value of the worst individual for each population. Even the value of worst individual for each generation generally improves, while there is the occasional spike caused by mutation or a crossover that leads to a less fit individual.

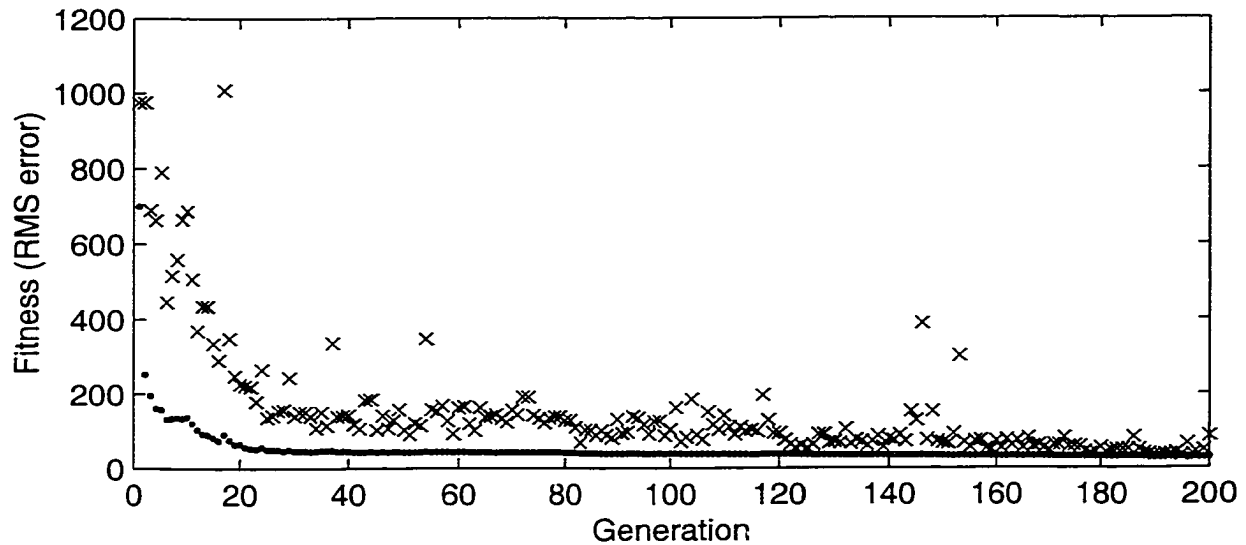


Figure 3.1: Average population fitness (dot) and worst individual fitness (x) from each of the 200 generations. The goal was to minimize the RMS error between the biomass curves from Vgrass and the BWM99 model; smaller values are better.

After the 200 generations were completed the best individual of all the generations was chosen. It would seem the final generation would hold the best individual but that is not always the case. There is nothing notable about the last generation such that its best individual should be chosen over any other individual from any generation. If it were known ahead of time that value X were the best possible, computation would have ended with that generation. The configuration values for the best individual are listed in Table 3.1 in column GA.

Biomass for the GA-selected configuration is similar to that of the BWM99 model and shows stability over a 5 year run (Figures 3.2 and 3.3). Direct comparison of biomass from the GA-selected configuration and the nominal configuration was desired but not visually clear. Plotting the two together leads to a confusing plot of jagged overlapping lines. For that reason the smooth biomass plot from the BWM99 model is used as a benchmark. The

benchmark is a useful reference since not all biomass plots (here and in Chapter 4) cannot use the same plotting limits.

Figure 3.4 shows leaf growth patterns that are typical except for two observations. First, except for one leaf, the leaves do not have a mature stage, they are abscised immediately after the growth stage ends. Second, leaves started in the middle of the growing season are shorter than those in the early and late parts of the growing season. Shorter leaves without a mature stage would seem to decrease the leaf area index (LAI) but Table 3.2 shows that average LAI is similar to the nominal case ( $1.6 \text{ m}^2 \text{ m}^{-2}$  Nominal,  $1.5 \text{ m}^2 \text{ m}^{-2}$  GA-selected). Also, plastichrone intervals are slightly shorter for the GA-selected configuration. (13 days Nominal average, 11 days GA-selected) while the average leaf length slightly longer (26 cm Nominal, 30 cm GA-selected). The GA-selected configuration grows two more leaves (24 vs. 22) while the plastichrone interval was smaller and the average leaf age was shorter (28 days Nominal, 21 days GA-selected).

The similarities and differences between the nominal and GA-selected plants reflect that there are multiple ways that the plant can be configured and still exhibit a similar biomass pattern. One configuration has short leaves in the middle of the growing season but maintains LAI by growing longer leaves in the early and later parts of the growing season. Leaf age is shorter but more leaves are grown by having a slightly smaller plastichrone interval. The differences and similarities between the two configurations show that trade-offs can be made in how the plant is configured while still showing similar biomass patterns. An increase in one attribute can be balanced by decreases in one or several other attributes. As a result the RMS error values for each configuration are numerically similar (Table 3.2).

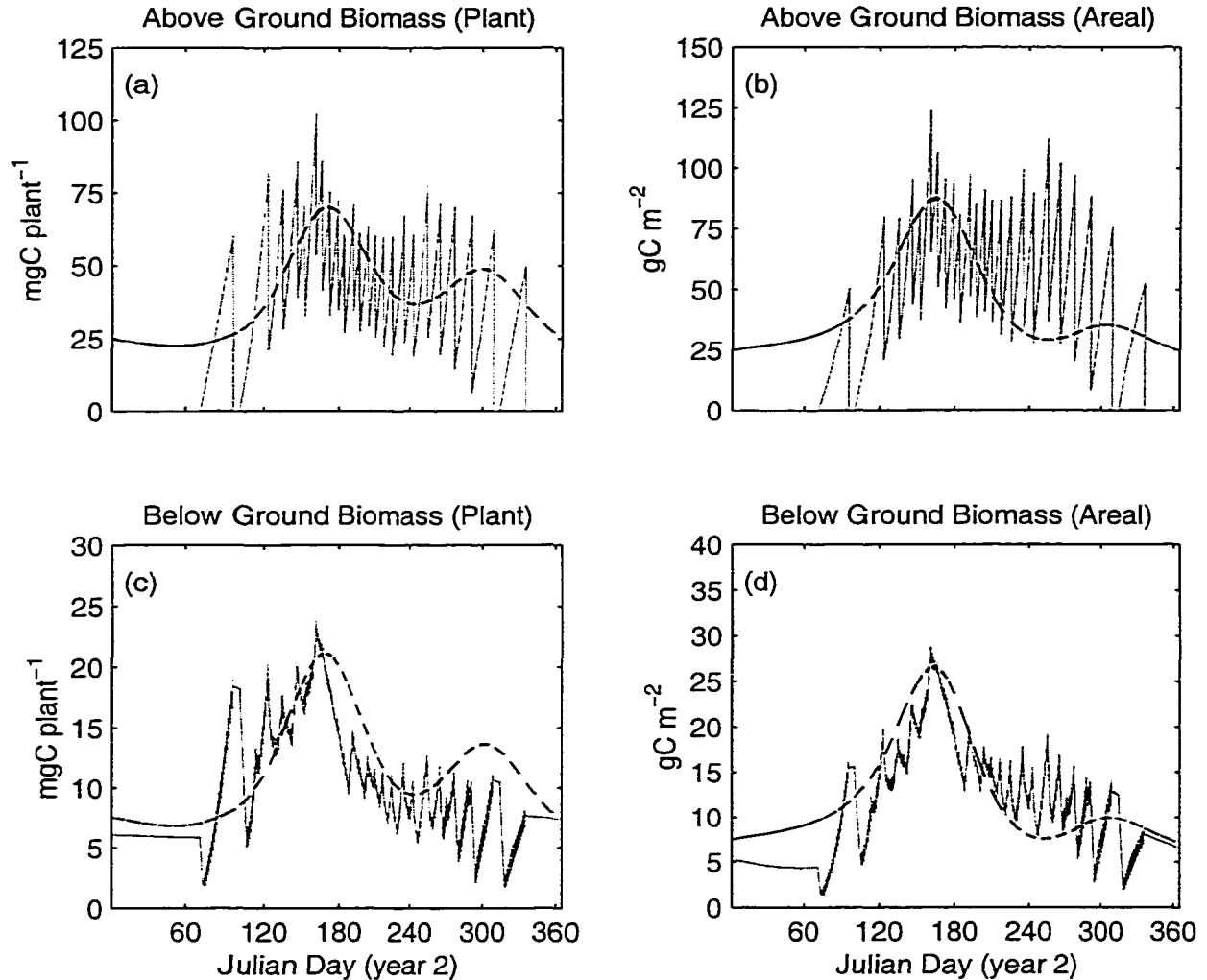


Figure 3.2: Biomass from the GA-selected configuration compared to BWM99 model biomass. Output from the BWM99 model shown as dashed (smooth) line. Output from the GA-selected configuration in black/gray (jagged) lines. a) Above-ground and c) below-ground biomass of an individual plant. b) Above-ground and d) below-ground biomass of a square meter of seagrass bed. The Vgrass model simulates individual leaves instead of lumping their biomass into one state variable. The growth and abscission of the individual leaves causes the biomass to fluctuate. Biomass from the single plant is multiplied by shoot density (Moore 1996), and therefore, the areal biomass is subject to the same fluctuations.



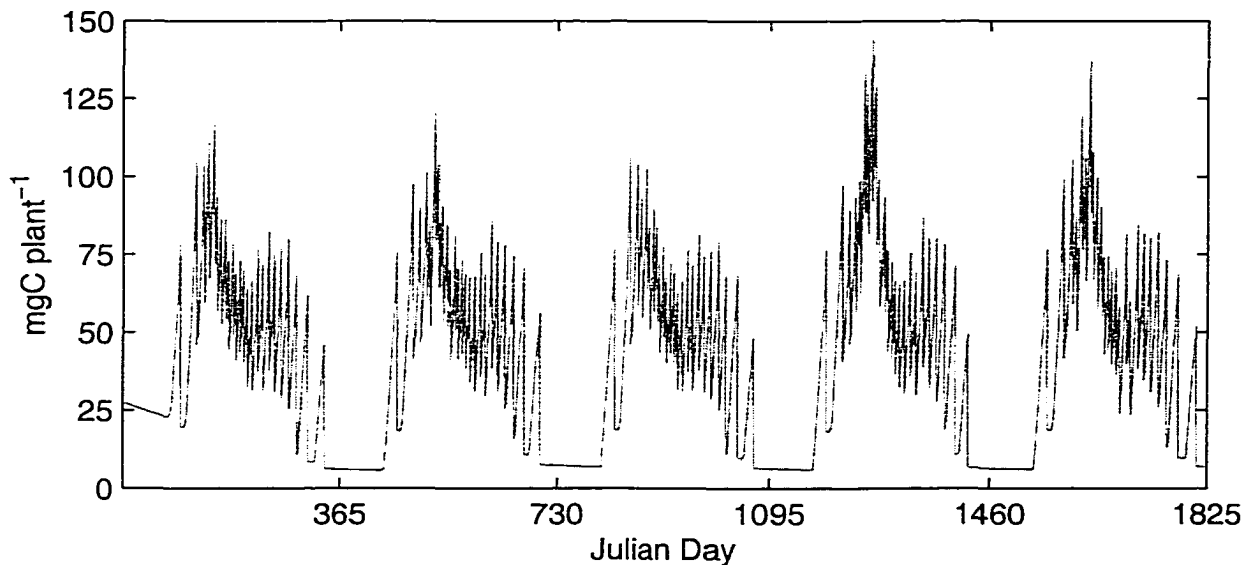


Figure 3.3: Biomass plot of the GA-selected configuration showing stability over 5 years (i.e. there is no evident trending).

Table 3.2: GA-selected configuration performance metrics. The first six metrics are computed from the second year of the simulation. Metrics with a range of values are reduced to minimum, average, and maximum values. NPP is Net Primary Production. BIO is the peak biomass. NPP and BIO are the average of peak values obtained during years 2 through 5 of the simulation. RMS error is computed as in equation 3.1.

Metric	Nominal Configuration			GA-selected Configuration			Units
	Min	Avg	Max	Min	Avg	Max	
First Shoot		70			72		Julian day
Plastichrone	8	13	30	6	11	29	Days
Leaf Length	20	26	33	20	30	46	cm
Leaf Age	20	28	49	18	21	27	Days
LAI		1.6	5.2		1.5	3.9	$\text{m}^2 \text{m}^{-2}$
Leaves		22			24		leaves $\text{y}^{-1}$
NPP Plant		294			417		$\text{mg C y}^{-1}$
NPP Pop.		343			531		$\text{g C m}^{-2} \text{y}^{-1}$
BIO Plant		124			132		mg C
BIO Pop.		149			161		$\text{g C m}^{-2}$
RMS AG		16.9			17.5		RMS error
RMS BG		3.8			3.9		RMS error

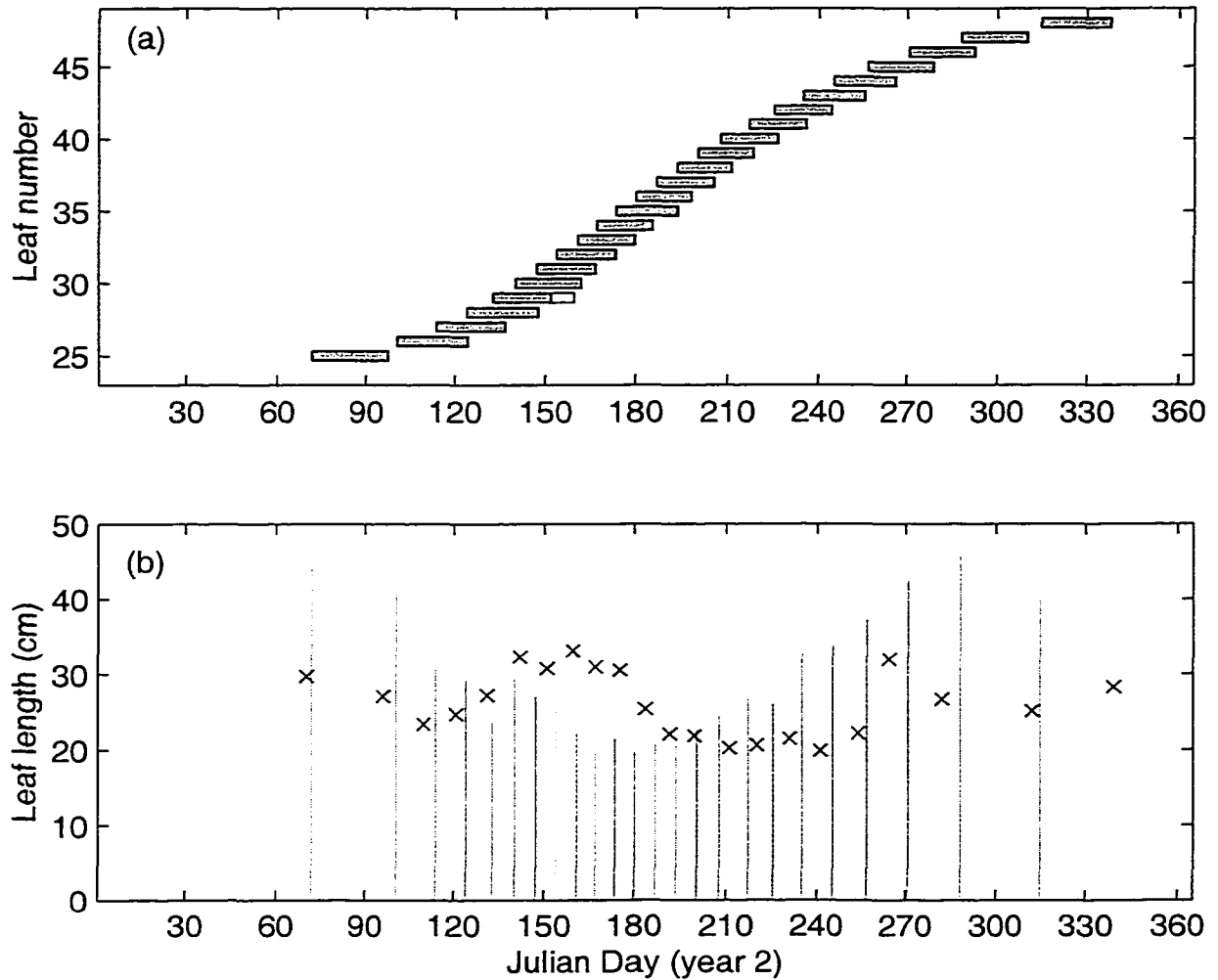


Figure 3.4: GA-selected configuration leaf growth. a) each bar represents the start date (left edge), growth stage (left shaded area), mature stage (right unshaded area), and abscission (right edge). b) lines indicate the start date (x axis) and the final length (y axis) of the leaf. The x's represent the lengths and timing of leaves from the nominal configuration.

Other trade-offs can be shown. The GA-selected plant is more productive on both an individual and areal basis, while the maximum biomass are relatively similar (Table 3.2). This draws the question, how can a plant be more productive while maintaining a similar biomass? Table 3.1 shows that the GA-selected configuration has a PSU density 3 times greater than the nominal configuration. Also, leaf growth in the GA-selected configuration is stopped at a much higher P:R ratio (7.8 GA-selected, 3 Nominal) and abscised at a much higher P:R ratio (11.3 GA-selected, 9 Nominal). The cases where  $\Gamma_{ABS}$  is greater than  $\Gamma_{STOP}$  indicates that a mature leaf stage is not needed to meet the required goal. In these cases the value  $\Gamma_{ABS}$  is virtually meaningless, the leaf is abscised immediately after it stops growing. The increase in chl, and stopping and abscising the leaves early (at high P:R ratios) enhances the net primary production metric. At the same time, stopping and abscising the leaves earlier helps to maintain the biomass pattern.

Figure 3.5 shows production vs. irradiance curves from 4 days of the second year of simulation. The curves show a hysteresis effect which is due to differences in morning and afternoon production rates. The difference in production may not be due to differences in illumination. They are more likely due to higher levels of mobile carbon in the leaf which causes a feedback to inhibit photosynthesis.

### 3.2.3 Goal Sensitivity

A feature of the GA search method is that a population of solutions is used in the search. In any given population there will be several to many individuals with high fitness values. Looking across all generations, a group of highly fit individuals can be culled to see

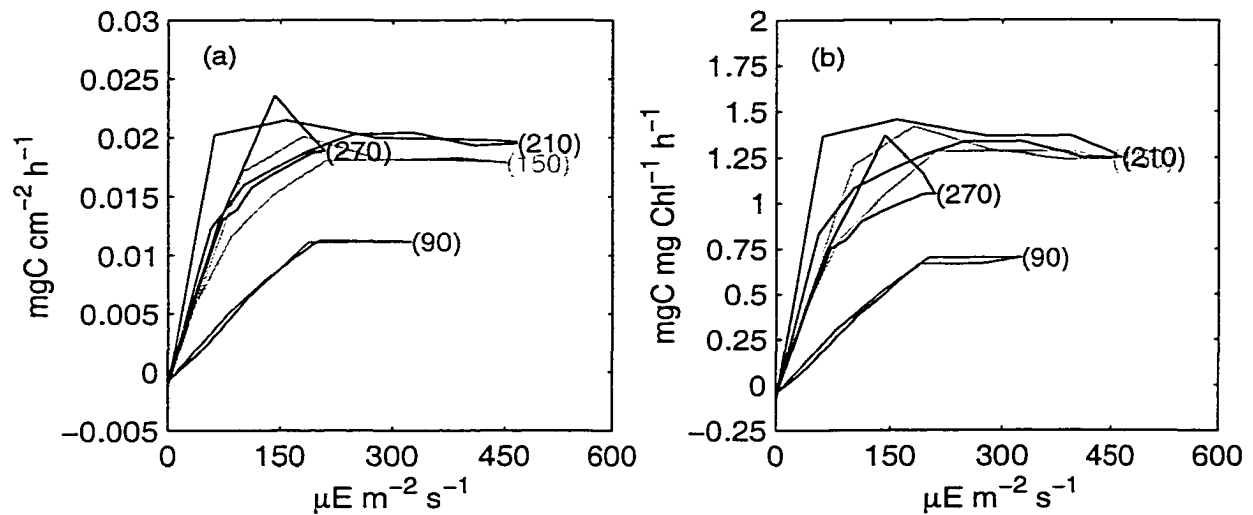


Figure 3.5: GA-Selected configuration whole-plant production vs. irradiance plots based on leaf area (a) and chl (b). Each line represents 24 hrs of data; the hysteresis is due to production differences between morning and afternoon. The numbers at the end of each line indicate the Julian day of the second year of simulation from which the data were taken.

if parameter values are converging to unique optimal values or if some range of variability is evident. Variability for a parameter could indicate that the parameter is not important to the overall fitness value. Expressed another way, a range of acceptable values could indicate that the model is not sensitive to that parameter in terms of reaching the GA's goal.

In this section individuals with a fitness value that was within 10% of the best fitness (the GA-selected configuration) are culled from the entire set of individuals tested over 200 generations. Since it is possible for one individual to exist in several generations, the population was reduced to individuals with unique parameter values. Persistence of an individual through several generations only means that it was selected and may have crossed over with itself. Controlling parameter values from the resulting 121 individuals were combined to make histograms (Figure 3.6).

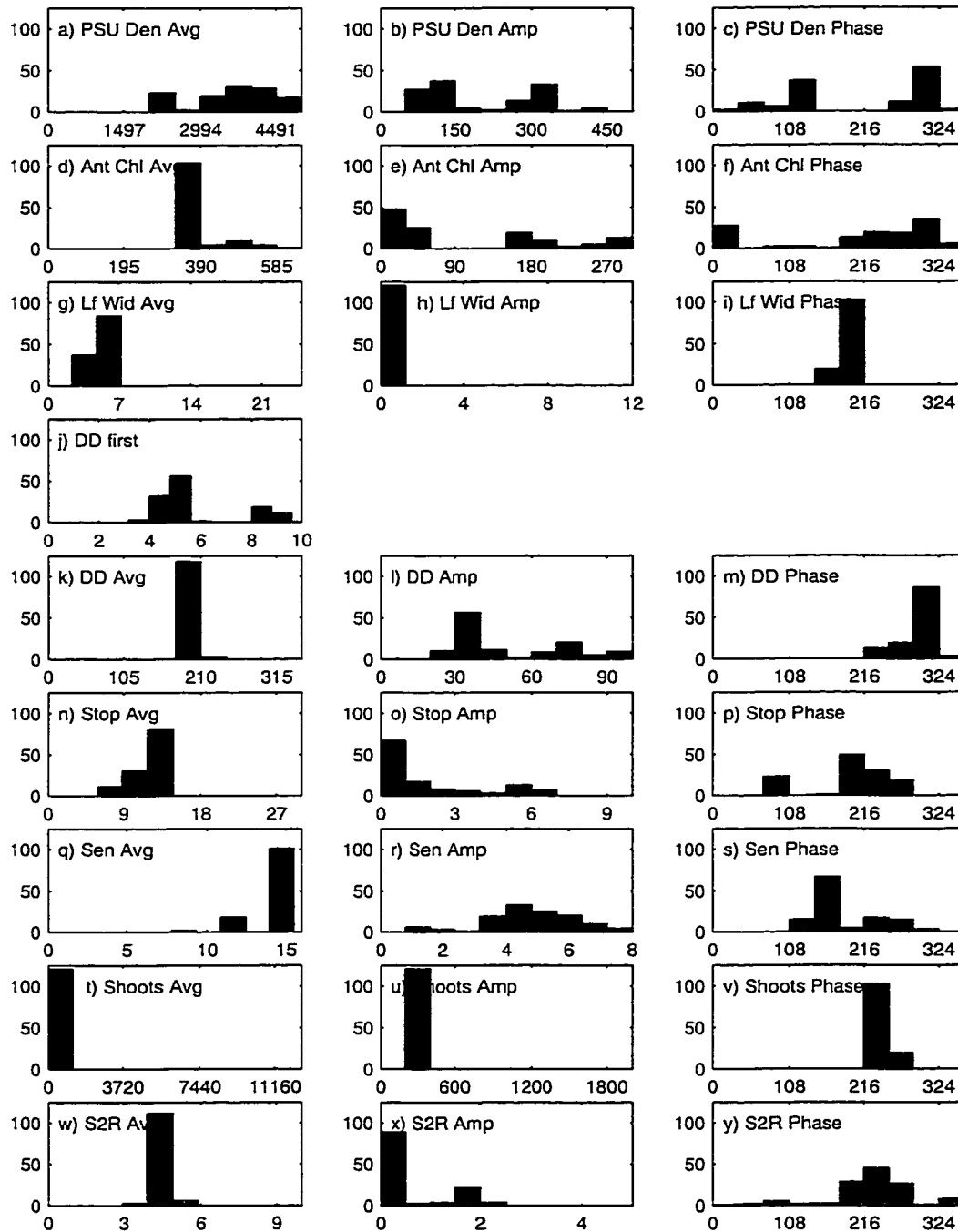


Figure 3.6: Histograms of 121 controlling parameter configurations pulled from the top 10% of individuals over the entire set of 200 generations. The histograms reveal that many different combinations of parameter values lead to high fitness. Y-axis units is number of individuals.

The histograms for leaf width average, amplitude, and phase and shoot density average, amplitude, and phase are not considered here since they were artificially limited to small ranges. Of the remaining 19 histograms, 13 show a bi-modal signature. This indicates that two ranges of values for that parameter can lead to high fitness. Since 13 of the 19 histograms have this behavior it is difficult to show if parameter ranges can be grouped together for the purpose of illustrating trade-offs. For instance, PSU density average has two distinct ranges of values as does degree-days to first leaf. It is difficult to know if high PSU density is related to the first or second set of histogram bars for degree-days to first leaf.

In contrast, 4 of the 19 histograms have pronounced single histogram bars indicating that high fitness is achieved within a small range of values for that parameter. Also, 6 of the 19 parameters have at least one set of histogram bars that shows a wider range of acceptable values for high fitness.

Another 6 of the 19 parameters show a narrow range of possibilities for achieving high fitness. This narrow range suggests that the ability of the GA to achieve the goal is more sensitive to these values. For comparison, are these the same parameters that are also highest in the model's sensitivity analysis? The answer is *no*.

*Stop leaf phase* is first in the sensitivity list of controlling parameters (Table 2.6) but has two histogram peaks in Figure 3.6p. There are 5 parameters that have one histogram bar in Figure 3.6 indicating that the selection range for these parameters is narrow in order to attain high fitness. Meanwhile these same 5 parameters are distributed throughout the Vgrass model sensitivities in Table 2.6. This shows that while Vgrass may be sensitive to a

parameter in the classical sensitivity analysis, that parameter may not have a similar effect when the GA and Vgrass are used in combination.

Biomass data from each of the 121 configurations was averaged together and is shown in Figure 3.7. The biomass curve shows perturbations caused by the growth and abscission of individual leaves even though 121 plants have been averaged. The perturbations are due to *degree-days between average*, amplitude, phase (Figure 3.6k-m) each having a narrow range of selection. This further demonstrates that the timing of leaf events is critical to matching the biomass curve of the BWM99 model.

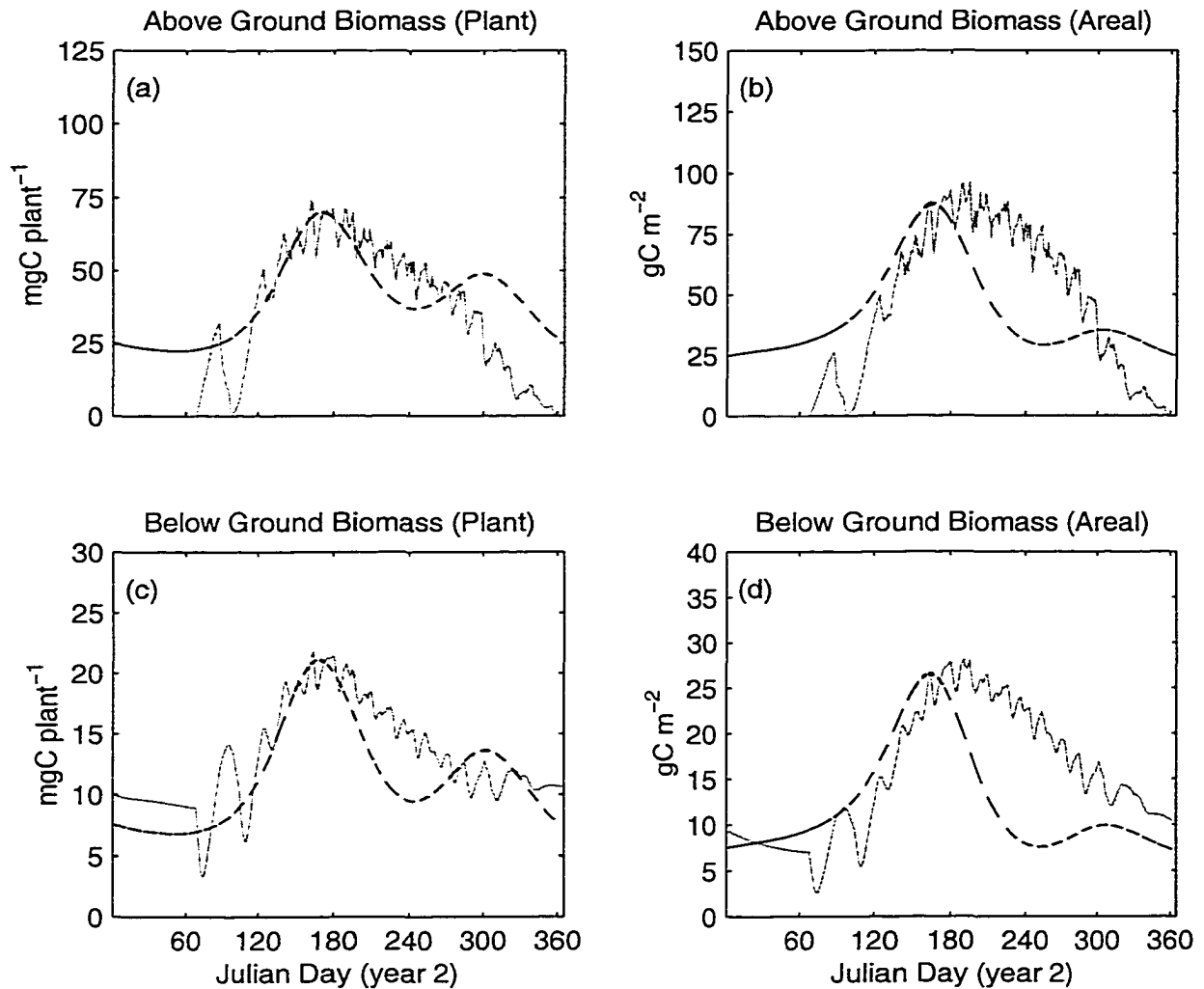


Figure 3.7: Average biomass of the top 121 configurations compared to BW99 model biomass. Output from the BW99 model shown as dashed (smooth) line. Output from the configuration in black/gray (jagged) lines. a) Above-ground and c) below-ground biomass of an individual plant. b) Above-ground and d) below-ground biomass of a square meter of seagrass bed. The Vgrass model simulates individual leaves instead of lumping their biomass into one state variable. The growth and abscission of the individual leaves causes the biomass to fluctuate. Biomass from the single plant is multiplied by shoot density (Moore 1996), and therefore, the areal biomass is subject to the same fluctuations.



### 3.3 Discussion

To summarize, this chapter covered the integration of Vgrass with a GA. The GA method was described and the Vgrass-GA interface was shown. To demonstrate the Vgrass-GA combination the GA was used to select Vgrass controlling parameters that lead to a minimum in RMS error between biomass in the Vgrass model and biomass from the BWM99 model. Initially the GA was introduced as an optimization method but in this project one of the GA's features was used to show the GA to be capable of more than optimization. Since the GA works with populations of solutions, a subset of highly fit individuals was culled and the individuals were compared. The result was a *sensitivity* analysis of Vgrass' controlling parameters in relation to their selection ranges and goal fitness.

When the GA and Vgrass were first used together a couple of unexpected, but explainable, behaviors were noticed. First, equation 2.7 (computing chl area) does not consider the relative cost differences of chl used for building reaction centers and chl used for antenna. When the GA selected PSU density and PSU antenna parameters, the values resulted in production vs. irradiance (PI) curves that did not have the typical shape. Normally production increases in proportion to light until the photosynthetic apparatus is saturated. When irradiance exceeds the saturation level, production remains fixed with increases in irradiance;  $P_{max}$ . At high irradiance production can be inhibited and can decrease with an increase in irradiance. In early GA selected configurations production increased in proportion to irradiance, but only up to  $P_{max}$ . The photosynthetic apparatus never saturated. Likewise, there was never an overabundance of chl. This behavior is explainable in the context of chl construction cost (carbon) and the benefit (or energy) derived from the investment.

Chl is part of the structural leaf carbon and therefore imposes a construction and respiration cost. Higher concentrations of chl in a leaf result in a more expensive leaf with a higher respiration rate. The construction and respiration costs kept the GA from selecting chl near its upper limit; energy collection was matched for energy requirements. This trade off affected total chl, but there was no trade off in how chl was allocated to increase PSU density or to increase the number of antenna chl. Since there was no difference in the cost of adding more reaction centers or adding more antenna chl, the GA chose to add more chl as reaction centers to meet energy collection requirements. As a question, if there is no difference in cost in allocating chl to the reaction center or antenna, then why build PSU's that saturate? Saturation implies that there is an excess of chl absorbing light that cannot be processed by the number of reaction centers. The excess chl increase the respiration load without the benefit of increased energy collection. The simple chl allocation model shows that it is more expensive to build chl into a PSU than to add chl as antenna.

In order for the GA to select PSU parameters such that saturation was observed in the P vs. I curve, a carbon cost factor was introduced. After trial and error it was found that if reaction center chl was 5 times more expensive than antenna chl, the GA would select PSU parameters that lead to more normal P vs. I curves. This cost factor is a calibrated factor and may not reflect the relative cost differences of chl in real plants. The chl allocation model is not realistic in how the cost of chl is computed; it only accounts for the amount of carbon in a chl molecule and not the supporting apparatus required for electron transport, etc. Figure 3.5 shows the P vs. I curve for the GA-selected model.

While a cost factor of 5 did lead to more normal P vs. I curves, how the cost factor

is applied may not be totally correct. Table 3.1 shows that the PSU density for the GA-selected configuration is 3 times greater than the nominal configuration (2,300 vs.  $750 \times 10^8$  PSU  $\text{mm}^{-2}$ ). If the cost factor of 5 is reasonable, then the total cost of chl and its corresponding respiration load needs to be increased. In a biological plant it is not just a matter of chl allocation but also a matter of additional proteins and lipids required to build PSU complexes and supporting membranes (Björkman, 1981). Here the allocation of chl is greatly simplified and represents the total cost of the various supporting materials.

In another instance of combining the GA and the Vgrass model, unrealistic biomass values were noted in the leaf biomass. Above ground biomass values were 3 to 6 orders of magnitude higher than expected. Structural leaf carbon was within expected ranges while the mobile carbon pool was accumulating large amounts of carbon. There was no mathematical limit on the mobile carbon concentration and with the goal of *maximize biomass* (this involved testing for future application of the Vgrass-GA combination), the GA used this mathematical *feature* to attain the goal. To fix the problem a feedback was introduced to limit photosynthesis as the concentration of mobile leaf carbon increased. This is an example of how a model may behave well under normal circumstances even though the model may have underlying structural problems. Proper use of a GA with a model can be a way to find these problems. Given the proper goal, the GA will exploit mathematical weakness' in the model in order to achieve the goal.

These two examples illustrate something about the plant and the model. In all cases where a plant can experience a benefit (more leaf area to harvest more light) there must also be a cost (increased shading). Analyzing plant behavior without regard to both would

be short-sighted. For the model, both cost and benefit must be included or replaced with a more empirical relationship. Vgrass' ancestors modeled the relation between production and irradiance as an empirical, but experimentally derived, relationship. Here chl dynamics were initially modelled in a fashion that considered the benefit of adding more chl without including the cost. While the formulation was functional for nominal runs, the flaw in the formulation was quickly revealed when an optimization criterium was applied. This was shown again in the case where mobile carbon built up in the leaf tissue, there was no cost factor to inhibit the build up of mobile carbon.

The Vgrass-GA combination, and the results obtained from it, illustrate a different approach in model construction and demonstrate a fundamental benefit of applying the GA method to an ecological simulation. First, Vgrass was constructed so as to consider the cost and benefit of adaptable features (leaf area vs. shading). Vgrass' ancestors are built mostly from a combination of empirical functions that re-integrate experimental findings. Their approach provides insight to *what-if* scenarios, but predictions on how a plant responds to environmental change are limited to predictions in biomass change (this is not a negative critique, the models fulfill their purposes). When Vgrass was run at two shoot densities (Chapter 2), Vgrass was able to show a reduction in leaf length due to the reduction of light availability. This relationship was shown because Vgrass modeled the cost and benefit of adding more leaf tissue.

To the second point, adding the GA to a model provides additional insight to the model's construction and its ability to replicate natural behavior. Two cases were cited above showing that an early version of Vgrass included only one half of the cost-benefit relationship

for chl dynamics and in the accumulation of mobile carbon in leaf tissue. Applying the GA to a model that performed well in the nominal case quickly revealed that the model was missing half of the cost-benefit feature. Also, when the cost-benefit feature is complete, the Simulation-GA combination provides a method to exercise the cost-benefit relationships. In the case of Vgrass the cost-benefit relationship in chl dynamics was used to show that chl added to the reaction center must cost 5 times that of chl added as antenna.

There is another benefit to applying the GA to an ecological simulation. The GA carries a population of potential solutions through many generations. During this process a family of individuals are found that achieve high fitness values. In this study 121 individuals in 90,000 trials were found to have a fitness score within 10% of the *best* individual. Plotting histograms of the controlling parameters revealed that some parameters had a narrow range in the selection process, some had multiple ranges of selection, and others revealed a wide range of suitable values. This suggests two things. First, for highly non-linear ecosystem simulations there may be no point in attempting to optimize model parameters in the classical sense of finding one optimal solution. In terms of expressing the solution surface as a contour, or topography, there may not be a global maximum in the form a well defined peak. Instead, highly fit solutions may be found along a mountain range. The GA is able to identify the mountain range of solutions while the solution surface may have cliffs or discontinuities. In contrast, standard methods look for a peak on a surface that cannot have discontinuities, or cliffs. For instance, the Simplex method requires a continuous surface and a unique minimum in the vicinity of the search. (Nelder, 1965). Second, the histograms reveal a secondary *sensitivity* analysis that can be performed on the simulation. In the case

of matching biomass curves, the histograms reveal that some parameters can vary by more than others in achieving high fitness value. But it cannot be captured in a classical % RMS error calculation. Some of the parameters display multiple ranges of acceptable values. In this study it was shown that the parameters for computing *degree-days between leaves* were important to matching biomass curves. This makes intuitive sense since matching a biomass curve would depend on the timing of leaf initiation.

In this study the Vgrass model was combined with a GA to, mainly, show how the GA could be implemented as an optimization routine. In the process of combining the GA and Vgrass model several important things were illustrated. First, combining the GA and model can be used to reveal information regarding plant physiology. Here it was shown that in order for chl parameter selection to yield realistic production vs. irradiance curves, the cost of allocating chl to increase PSU density is 5 times higher than the cost of allocating chl for use as antenna chl. Second, model construction is critical to proper function with the GA since the GA can exploit weakness in model design. Here it was shown that while the model behaved well in normal circumstances, the GA made use of a weakness in the model in order to achieve its goal. Third, when using a GA to optimize a model, a family of solutions can indicate parameters that are key in reaching the optimization goal. The parameters that are important to reaching the goal, may not be the parameters that exhibit higher sensitivity in a standard sensitivity analysis.

### 3.4 Literature Cited

- Björkman, O., 1981, Responses to different quantum flux densities. In: *Physiological Plant Ecology I: Responses to the physical environment*. Ed: Lange, O. L., Nobel, P. S., Osmond, C. B., and Ziegler, H. Springer-Verlag, New York, 625 pp.
- Buzzelli, C. P., Wetzel, R. L., and Meyers, M. B., 1999. A linked physical and biological framework to assess biogeochemical dynamics in a shallow estuarine ecosystem. *Estuarine, Coastal and Shelf Science*, 49, 829-851.
- Drynan, R. G., and Saniford, F., 1985. Incorporating economic objectives in goal programming for fishery management. *Marine Resource Economics*, 2(2), 175-195.
- Goldberg, D. E., 1989. *Genetic Algorithms in search, optimization, and machine learning*. Reading, Massachusetts: Addison-Wesley.
- Goldberg, D. E., 1994. Genetic and evolutionary algorithms come of age. *Comm. of the ACM*, 37(3), 113-119.
- Holland, J. H., 1975. *Adaptation in natural and artificial systems*. University of Michigan Press. (Second edition: MIT Press, 1992.)
- Huse, G., Strand, E., and Giske, J., 1999. Implementing behaviour in individual-based models using neural networks and genetic algorithms. *Evol. Eco.* 13, 469-483.
- Jacobs, R. P. W. M., 1979. Distribution and aspects of the production and biomass of eelgrass, *Zostera marina*, at Roscoff, France. *Aquat. Bot.*, 7, 151-172.
- Krink, T., and Vollrath, F., 1997. Analysing spider web-building behaviour with rule-based simulations and genetic algorithms. *J. theor. Biol.*, 185, 321-331.
- Johnson, C. M., 1996. A grammar-based technique for genetic search and optimization. Dissertation, College of William and Mary, Williamsburg, VA.
- Mao, N., and Mays, L. W., 1994. Goal programming models for determining freshwater inflows to estuaries. *J. Water Res. Plng. and Mgmt.*, 120(3), 316-329.
- Mitchell, M., 1997. *An introduction to genetic algorithms*. MIT Press, Cambridge, Massachusetts, 209 pp.
- Nelder, J. A., and Mead, R., 1965. A Simplex method for function maximization. *Computer J.*, 7, 308-313.

- Mohan, S., and Keskar, J. B., 1991. Optimization of multipurpose reservoir system operation. 27(4), 621-629.
- Moore, K. A., 1996. Dissertation: Relationships between seagrass growth and survival and environmental conditions in a lower Chesapeake Bay tributary. University of Maryland.
- Wang, Q. J., 1997. Using genetic algorithms to optimize model parameters. *Env. Mod. Soft.*, 12(1), 27-34.



## Chapter 4

# Testing Plant Growth Strategies

### ABSTRACT

The Genetic Algorithm (GA) is used with the Vgrass model to demonstrate a computational framework capable of testing plant growth strategies. The GA searches for configurations of Vgrass controlling parameters best able to meet the following strategies: optimization of relative growth rate, optimization of biomass, optimization of net primary production, and longevity. The first three strategies are tested at the spatial scale of an individual plant and at the scale of a population of plants; comprising 6 total tests. The final strategy is based on plant longevity. For each of the seven tests, the GA selected distinct configurations of controlling parameters and each configuration lead to distinct plant growth patterns. The plant growth patterns reveal that the simulated plant is following the given strategy even though the growth patterns are not biologically realistic. The ability to find distinct configurations for each growth goal demonstrates the ability of the computational framework to address this type of problem. Ecologically, the results indicate that plants do not pattern their configuration or allocation behaviors to attain some *maximization of growth* strategy.

## 4.1 Introduction

Plant allocation hypotheses span a full range of time scales from short, on the order of days, to evolutionary, on the order of generations.

In a short time scale, the multiple limitation hypothesis predicts that plant morphology and physiology adjust so that all resources become simultaneously limiting (Kastner-Maresch and Mooney, 1994; Bloom et al. 1985). Kastner-Maresch and Mooney (1994) favor the hypothesis that allocation occurs at a short time scale by stating that a plant must adapt an allocation strategy to varying short-term environmental conditions. As an example that allocation can change on a short time scale, Zimmerman et al. (1996) show that limpets grazing on the epidermis of *Zostera marina* induce carbon limitation and alter allocation. Grazed plants lose less than 10% of their tissue by volume and do not produce lateral shoots in the spring-summer period of maximum growth. The relatively small amount of tissue that was lost supported CO<sub>2</sub> uptake and photosynthesis. That small amount must be important since plants that are not grazed allocate 800% more carbon to their roots.

Gleeson and Tilman (1992) review assumptions and predictions made by a model of optimal allocation and include an important point: short-term hypotheses only consider plant behavior at a single point in time. Any observation of non-optimal behavior fails to consider that the plant may be optimizing allocation for long-term benefits. That optimal allocation occurs over a longer scale is supported by Abrahamson and Caswell (1982). Plants show adaptations for nutrient uptake, water conservation, temperature tolerance, pollinator attraction, herbivore avoidance, seed dispersal, etc. One of these factors cannot be singled out as the crucial item for determining allocation. All constraints must be considered. As

an example, some plants sacrifice growth for reproduction (Poorter and Garnier, 1999). This is also supported by Grime (1977) noting that shade tolerant plants that show little or no response to increased shading are probably more concerned with long-term survivability in deep shade than with maximizing light interception and dry-matter production.

At an even longer time scale, studies have shown that plants allocate resources in a fashion that leads to evolutionary stability for the species. At this scale studies include: allocation to attractive structure for animal-pollinated flowers (Sakai, 1993), allocation to flower and seed size (Sakai and Sakai, 1995), seed vs. clonal reproduction (Takada and Nakajima, 1996; Sakai, 1995), allocation to growth and reproduction (Kozlowski and Janczur, 1994), and optimal strategies for the fraction of individuals entering diapause in a stochastic environment (McNamara, 1994). This list is not exhaustive but complements the list of allocation studies to help show the range of time scales that have been considered. Each of these studies use mathematical models to show optimal allocation and support the model with biological evidence.

It seems logical to assume that a plant must optimize allocation at all time scales since there is biological evidence to support hypotheses at each of the different time scales. Optimal allocation typically refers to allocation that supports an evolutionary stable strategy (Givnish, 1983a). Evolutionary stability requires allocation to reproduction vs. allocation to plant growth so it is easy to understand why long-term models focus on allocation to reproduction. But what is optimized at the shorter time scales? Givnish (1983a) presents a collection of papers that show the importance of form and function in the growth cycle and competitive abilities of the plant. Studies range from the scale of stomatal conductance

(Givnish, 1983b), to the orientation and support of leaves in the canopy (Fisher, 1983). Growth is necessary to support the higher level purpose of reproduction (Lambers et al. 1998), but how is allocation optimized at all of the various time and space scales? *If growth is the goal, what is the strategy for optimizing growth and how can it be tested?*

The goal of the study was to build and demonstrate a computational framework capable of testing several plant growth strategies. The computational framework consists of an individual based model of *Zostera marina* (Vgrass) coupled with a Genetic Algorithm (GA). In this combination, the Vgrass model has a set of parameters that control allocation and the GA searches for a combination of these parameters necessary to attain one of several plant growth goals. Further, the objective of this study is not to demonstrate a mechanism that supports a plant growth strategy, but instead to explore the result of a plant growth strategy.

## 4.2 Vgrass/GA

The Vgrass model has 25 controlling parameters which are formulated into nine  $\Gamma$  variables (Table 2.3). Of the nine variables, seven directly affect allocation: leaf initiation ( $\Gamma_{DDF}$  and  $\Gamma_{DD}$ ), leaf growth and abscission ( $\Gamma_{STOP}$ , and  $\Gamma_{ABS}$ ), light harvesting ( $\Gamma_{PSU}$ , and  $\Gamma_{ANT}$ ), and shoot to root ratio ( $\Gamma_{SR}$ ). Each of these variables affects allocation empirically since no attempt is made to explain the underlying plant mechanisms. The assumption is made that regardless of the underlying mechanisms, these variables adequately reflect the outcome of the mechanisms.

Chapter 3 describes how the GA is interfaced to the Vgrass model. For these studie's,

there are two notable differences. First, the fitness function in Chapter 3 measured the RMS error between the biomass of the simulation and that of the BWM99 model. Here that fitness function is replaced with seven fitness functions (each done separately) that evaluate the model's ability at attaining each of the given goals (these goals, or strategies, are enumerated later). The second change allows the model's performance to be evaluated at the scale of a plant or a population of plants. In evaluating the model at the plant scale, the shoot density selection range is limited to: shoot density (975-1175 shoots  $\text{m}^{-2}$ ), shoot density average (330-390 shoots  $\text{m}^{-2}$ ), and shoot density phase (225-275 days). This effectively eliminates these variables as part of the selection process since shoot density is virtually the same for all model evaluations. This forces the individual plant to coexist in a population of identical peers at a shoot density similar to that of seagrasses in the southern Chesapeake Bay (Moore, 1996). Results from these model runs represent those of an individual plant. In order to evaluate the allocation strategy at the population level, the shoot density parameter selection is open to the full range given in Table 3.1. This allows the model's performance to be evaluated at the scale of a population and parameter selection reflects the result of a population of plants attempting to achieve the goal collectively. This is not to suggest that a population of natural plants could work together but the results of the computational exercise do have implications for human manipulated plant populations.

The four growth strategies are: optimization of relative growth rate (RGR), optimization of biomass (BIO), optimization of net primary production (NPP), and longevity (LONG). RGR, BIO, and NPP are optimized for an individual plant and for a population of plants. Longevity is tested as an optimization goal for a population wherein persistence is the

measure of fitness. In total, there are 7 strategies tested. The selection of these goals is subjective. Biomass, relative growth rate, and net primary production are growth measurements commonly reported in the plant literature. In contrast to these goals, allocation to achieve longevity is a *good enough* approach. That is, a plant only needs to be good enough in its allocation strategy to attain population persistence: energy spent on being too much better is wasted. The criteria used for longevity is for the simulation to run for 20 years.

Due to the different ranges of biomass data from each of the seven strategies it was impossible to use identical axis limits on all of the biomass plots. While it would be desirable to compare all of the model output to the nominal run of Chapter 2, the resulting plot would not be legible due to the excursions caused by individual leaves growing and abscising. To help the reader compare data, biomass data from the BWM99 model (Buzzelli et al., 1999) is used here as a benchmark and appears as a dashed line in the biomass plots. This was done since data from the nominal configuration was similar to that of the BWM99 model.

For all of the Vgrass/GA runs, 200 generations of 450 individuals were accomplished. The selection of these numbers is subjective but based on observations of how long it took for the GA to find an optimal solution. The number of individuals in a population was a multiple of 30 to balance the computational load over 30 CPU's running in parallel. The number of generations and individuals are actually larger than necessary to ensure that an optimal solution was found within the 200 generations. The best individual, or set of parameters, was then run through the simulation program again in order to collect performance metrics and data for a standard set of tables and plots.

### 4.3 Optimization Goal:

#### Maximization of Relative Growth Rate

RGR was computed as the percent change in total plant biomass over a 2-week period. RGR values for the 26, 2-week periods of the second simulation year were added together and returned to the GA as the fitness rank. The GA searched for a configuration of controlling parameters best capable of maximizing the sum of the 26 RGR values.

Two tests were run. First, RGR was maximized for an individual plant (RGR-Plant), that is, biomass for an individual plant was used in the RGR calculation. In the second run RGR was maximized for a population of plants (RGR-Population). In this case biomass for the individual was scaled up to a population by multiplying biomass with shoot-density. Results of the searches are shown in Table 4.1.

##### 4.3.1 Strategy One: RGR-Plant

Biomass for the RGR-Plant configuration is about half that of the nominal configuration (Figures 4.1 and 4.2). In comparing metrics in Table 4.2 to the nominal configuration, the average RGR-Plant plastichrone interval is longer (19 days vs. 13 days), leaf lengths are shorter (17 cm vs. 26 cm), average leaf age is shorter (16 days vs. 28 days), leaf area index (LAI) is lower ( $0.9 \text{ m}^2 \text{ m}^{-2}$  vs.  $1.6 \text{ m}^2 \text{ m}^{-2}$ ), and the number of leaves grown is less (16 leaves vs. 22 leaves).

Leaves for the RGR-Plant configuration are shorter, younger, and fewer in number than the nominal configuration (Figure 4.3). PSU density and antenna chl counts (Figure 4.4a

Table 4.1: GA selected configurations for RGR-Plant and RGR-Population growth strategies compared to the nominal configuration. Each column represents the individual that attained the highest fitness for the indicated test. Since the binary chromosome is 209 bits long, the individual should be the best of  $2^{209}$  or on the order of  $10^{62}$  possible configurations.

Parameter	Nominal	RGR Plant	RGR Pop.	Units
Degree-days first leaf	6	6	9	°C Day
Degree-days next average	150	237	315	°C Day
Degree-days next amplitude	65	98	8	°C Day
Degree-days next phase	240	226	67	Days
Shoot density average	1075	991	506	Shoots $m^{-2}$
Shoot density amplitude	360	364	234	Shoots $m^{-2}$
Shoot density phase	250	226	12	Days
Leaf width average	5.0	8.3	8.9	mm
Leaf width amplitude	0.1	9.3	7.4	mm
Leaf width phase	180	172	264	Days
PSU density average	750	3879	2671	$10^8$ PSU $mm^{-2}$
PSU density amplitude	200	406	391	$10^8$ PSU $mm^{-2}$
PSU density phase	60	120	241	Days
PSU antenna average	450	552	463	Chl PSU $^{-1}$
PSU antenna amplitude	20	42	58	Chl PSU $^{-1}$
PSU antenna phase	360	63	26	Days
Stop leaf P:R average	3.0	27.1	16.8	Ratio
Stop leaf P:R amplitude	5.0	0.9	0.7	Ratio
Stop leaf P:R phase	180	262	164	Days
Abscise leaf P:R average	9.0	15.2	14.5	Ratio
Abscise leaf P:R amplitude	4.0	0.1	7.9	Ratio
Abscise leaf P:R phase	300	237	276	Days
Shoot:Root average	4.0	2.7	0.4	Ratio
Shoot:Root amplitude	0.3	0.2	1.3	Ratio
Shoot:Root phase	50	15	344	Days



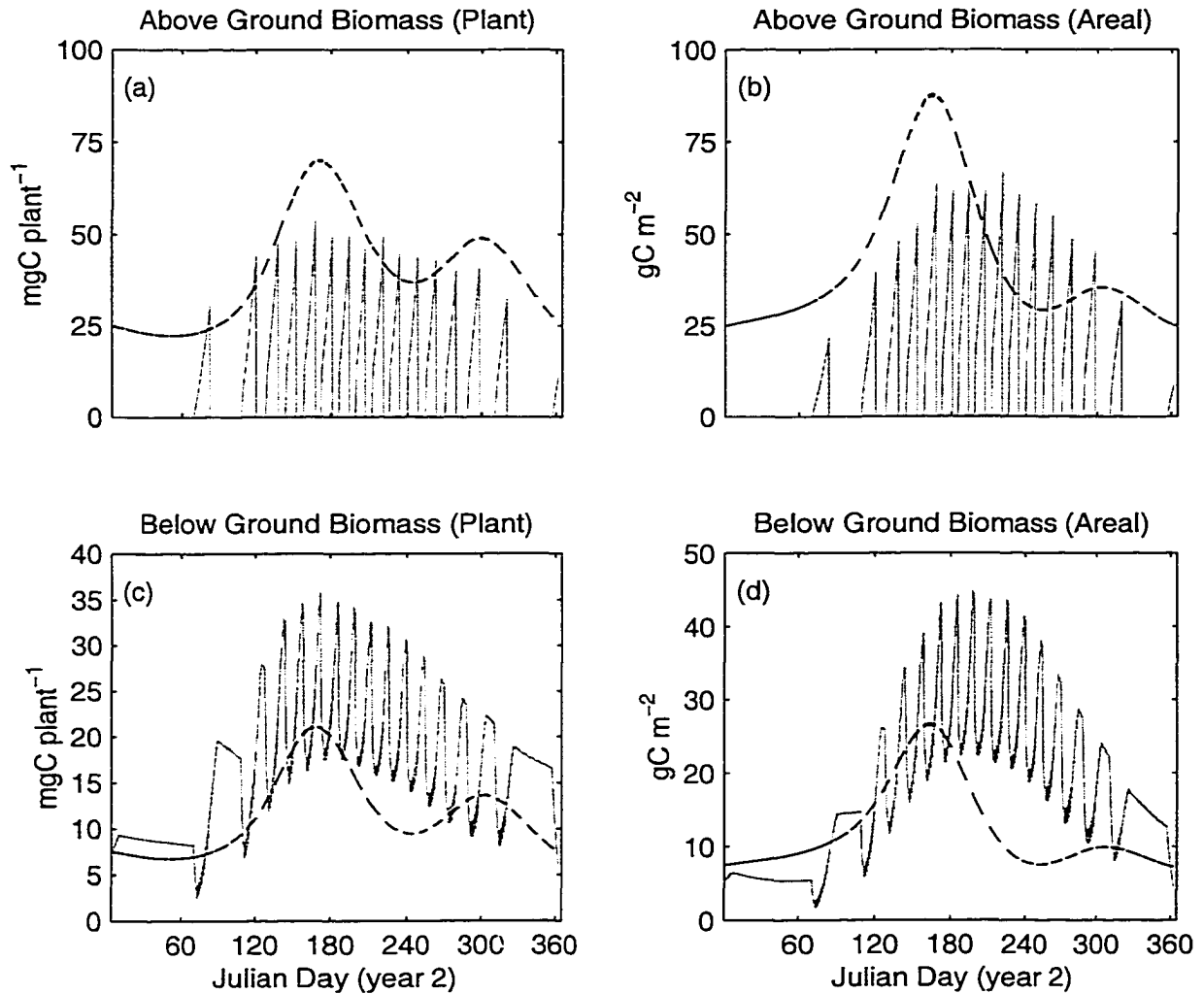


Figure 4.1: Biomass from the RGR-Plant configuration compared to BWM99 model biomass. Output from the BWM99 model shown as dashed (smooth) line. Output from the RGR-Plant configuration in black/gray (jagged) lines. a) Above-ground and c) below-ground biomass of an individual plant. b) Above-ground and d) below-ground biomass of a square meter of seagrass bed. The Vgrass model simulates individual leaves instead of lumping their biomass into one state variable. The growth and abscission of the individual leaves causes the biomass to fluctuate. Biomass from the single plant is multiplied by shoot density (Moore 1996), and therefore, the areal biomass is subject to the same fluctuations.

Table 4.2: RGR-Plant configuration performance metrics. The first six metrics are computed from the second year of the simulation. Metrics with a range of values are reduced to minimum, average, and maximum values. NPP is Net Primary Production. BIO is the peak biomass. NPP and BIO are the average of peak values obtained during years 2 through 5 of the simulation.

Metric	Nominal Configuration			RGR-Plant Configuration			Units
	Min	Avg	Max	Min	Avg	Max	
First Shoot		70			70		Julian day
Plastichrone	8	13	30	13	19	46	Days
Leaf Length	20	26	33	8	17	58	cm
Leaf Age	20	28	49	14	16	21	Days
LAI		1.6	5.2		0.9	2.0	$\text{m}^2 \text{m}^{-2}$
Leaves		22			16		leaves $\text{y}^{-1}$
NPP Plant		294			263		$\text{mg C y}^{-1}$
NPP Pop.		343			310		$\text{g C m}^{-2} \text{y}^{-1}$
BIO Plant		124			79		$\text{mg C}$
BIO Pop.		149			98		$\text{g C m}^{-2}$

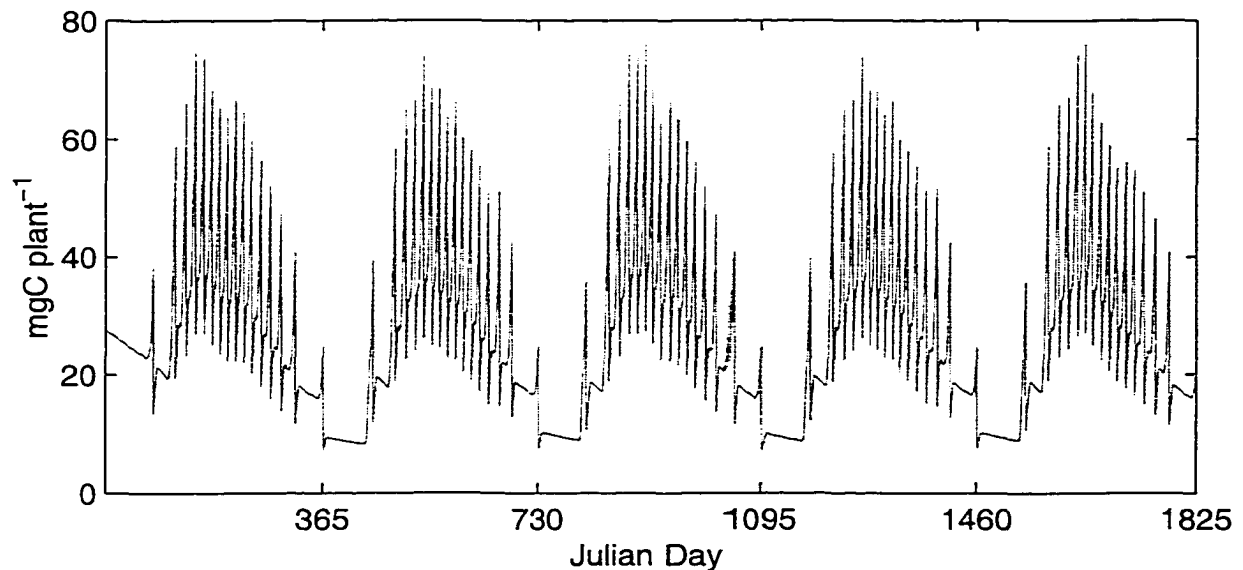


Figure 4.2: Biomass plot of the RGR-Plant configuration showing stability over 5 years (i.e. there is no evident trending).

and 4.4b) are higher but not high enough to elevate NPP or BIO. NPP for the plant and areal basis are lower for the RGR-Plant configuration (263 mg C  $y^{-1}$  and 310 g C  $m^{-2} y^{-1}$  vs. 294 mg C  $y^{-1}$  and 343 g C  $m^{-2} y^{-1}$ ). Peak biomass for the plant and areal basis are also lower (79 mg C and 98 g C  $m^{-2}$  vs. 124 mg C and 149 g C  $m^{-2}$ ).

Leaf length for the RGR-Plant configuration is shorter during the growing season (Figure 4.3) while leaf width reaches 15 mm (Figure 4.4c). This leads to a smaller LAI and allows more light to reach the leaf's surface. Figure 4.5 shows a peak irradiance approaching 600  $\mu E m^{-2} s^{-1}$ , while the nominal configuration peak irradiance was around 450  $\mu E m^{-2} s^{-1}$ .

Maximizing RGR at the scale of 2-weeks calls for a strategy where biomass at the end of each 2-week period is greater than at the beginning. But since the RGR values for each 2-week period are added together, biomass at the end of the year should be greater than at the beginning. A careful look at the data for Figure 4.2 shows that at the end of Day 365 the plant abscises a leaf and causes a biomass drop. On Day 366 when RGR begins to be measured for year 2, biomass starts at around 10 mg C for the plant. On the last day of year 2, plant biomass is near 20 mg C so that an increase is computed for the year. Immediately after RGR is computed for the year a leaf is abscised, so that biomass begins at a lower level for the next year.

The GA has chosen a combination of degree-days between leaves, P:R for stopping growth, and P:R for abscission (Table 4.1) that produce this behavior (Figure 4.4d, e, and f). These factors are of primary importance when considering plant behavior along with the GA goal to maximize RGR. The ratios P:R stop and P:R abscise are higher than in the

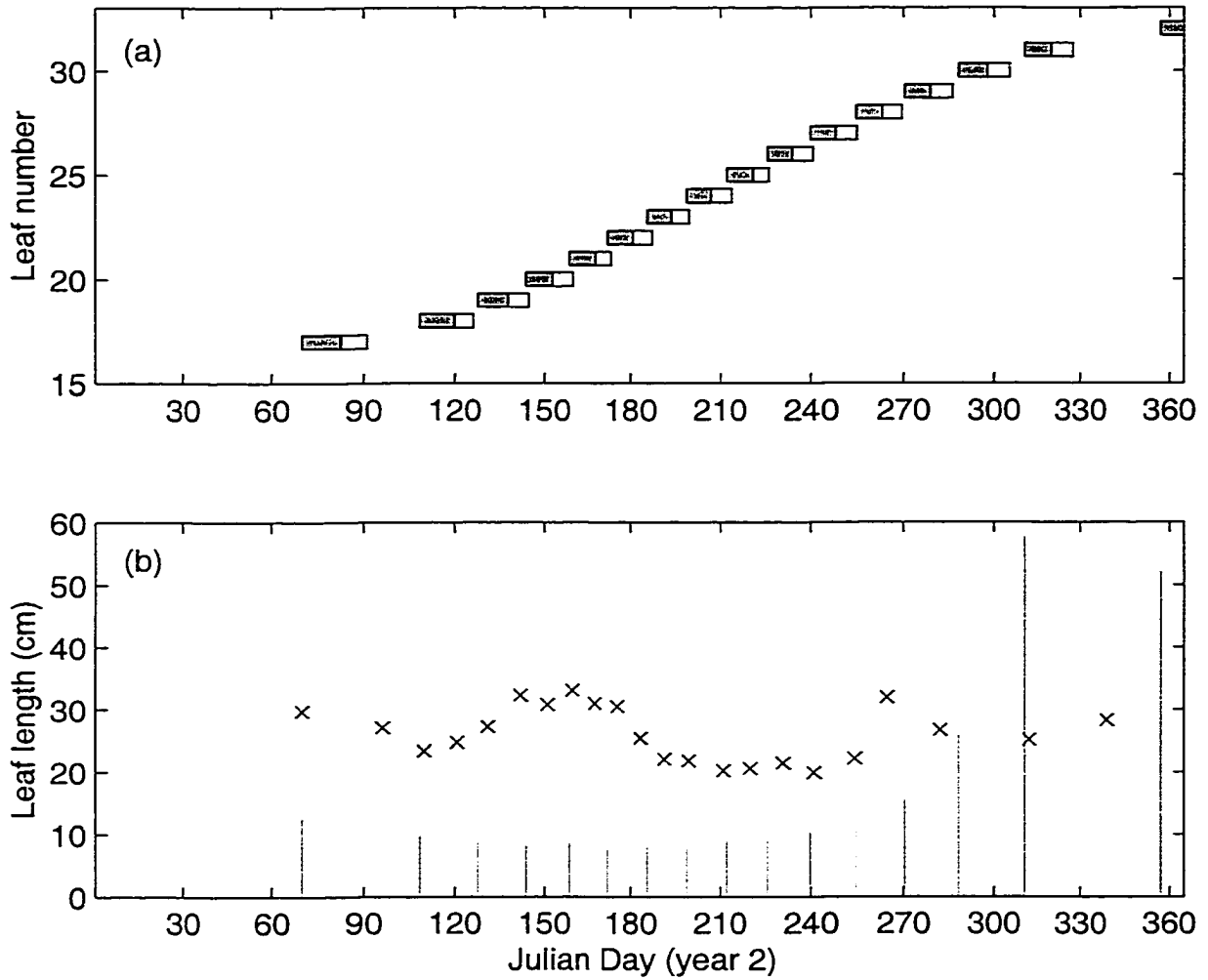


Figure 4.3: RGR-Plant configuration leaf growth. a) each bar represents the start date (left edge), growth stage (left shaded area), mature stage (right unshaded area), and abscission (right edge). b) lines indicate the start date (x axis) and the final length (y axis) of the leaf. The x's represent the lengths and timing of leaves from the nominal configuration.

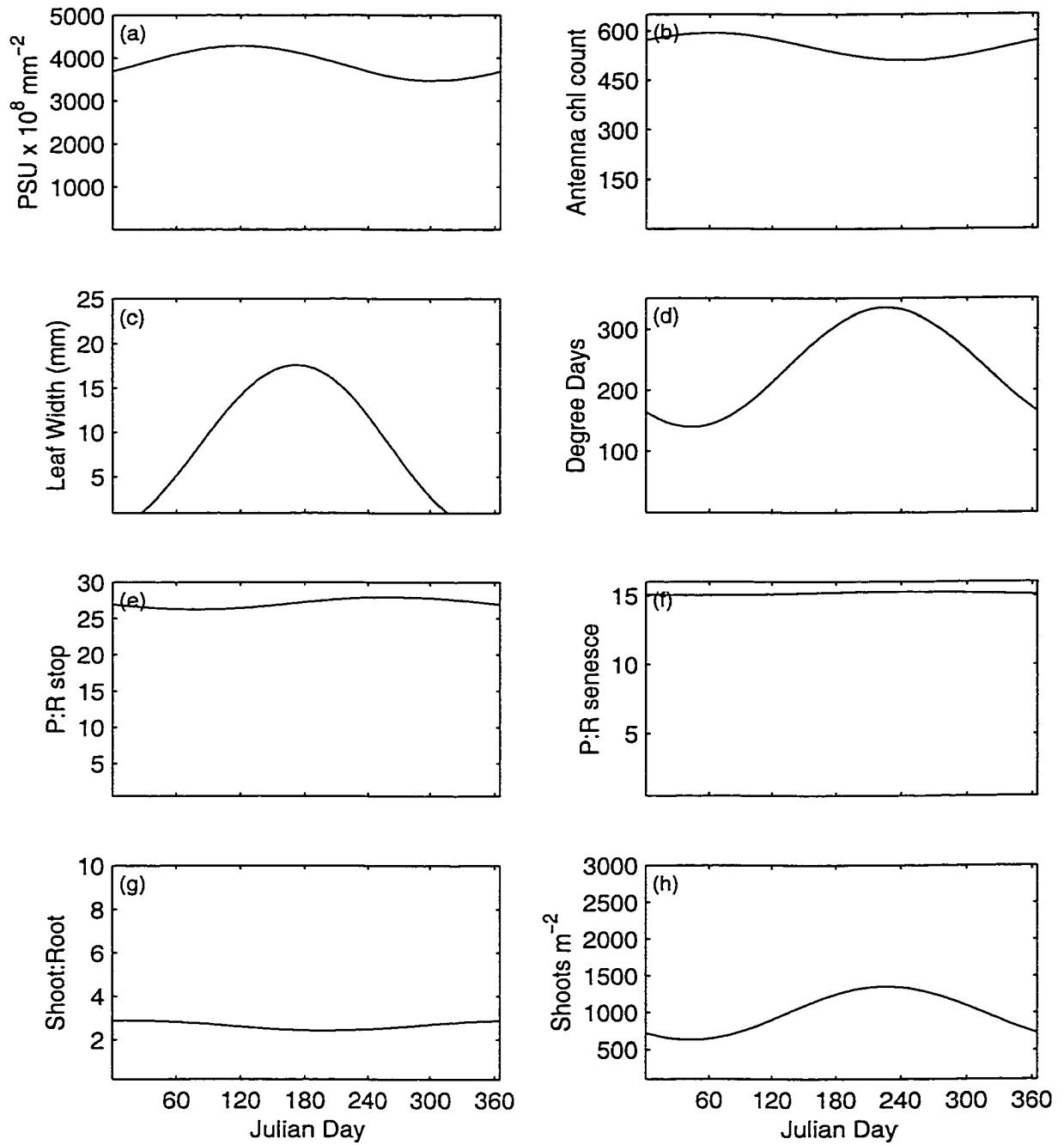


Figure 4.4: RGR-Plant configuration  $\Gamma$  variable plots. Each curve is computed from its  $\Gamma$  variable (Table 2.3) as in Figure 2.3.

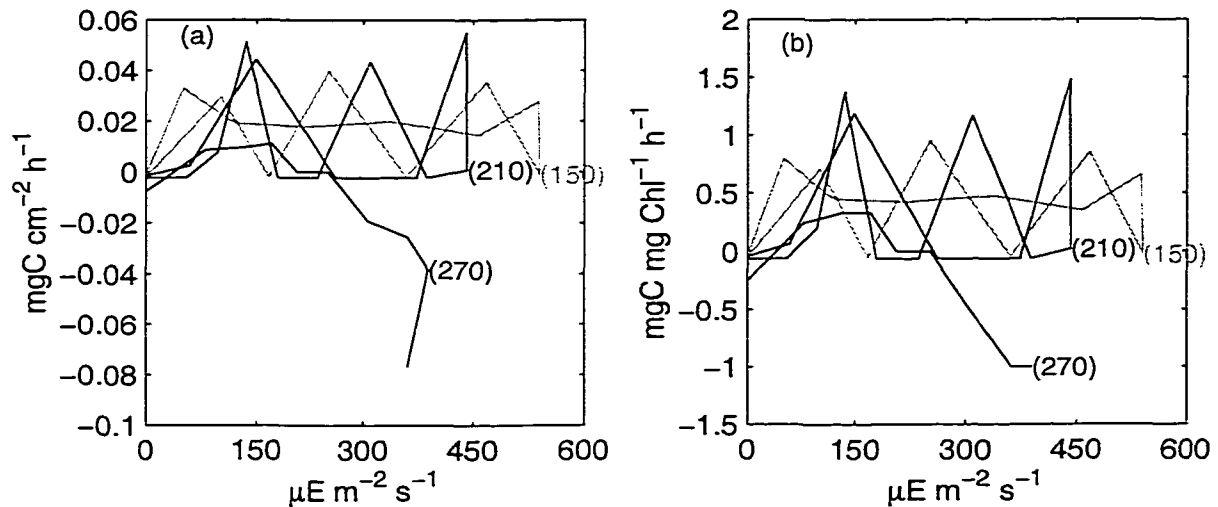


Figure 4.5: RGR-Plant configuration whole-plant production vs. irradiance plots based on leaf area (a) and chl (b). Each line represents 24 hrs of data; the hysteresis is due to production differences between morning and afternoon. The numbers at the end of each line indicate the Julian day of the second year of simulation from which the data were taken.

nominal configuration, and the PI curves are erratic (Figure 4.5). The erratic PI behavior shows that the PSU's are over productive relative to the plant's ability to use the carbon for storage or growth. Mobile carbon increases in the leaves faster than the meristem can take the mobile carbon and reallocate it to leaf growth or root/rhizome storage. The model has a feedback equation to limit photosynthesis when leaf mobile carbon reaches a parameter set value. The PI curves show cycling behavior as mobile carbon is overproduced and then used. These factors suggest that the timing of leaf events, and therefore biomass, is more important than balancing the leaf's production with the plant's ability to use that production. This seems backwards compared to normal plant growth although the behavior is directly related to how the growth strategy is measured. The excessive production leads to high internal concentrations of mobile carbon and poor P vs. I curves. The simulated

plant is using the mobile carbon pool to store excess mobile carbon so that when it is needed for leaf growth it is readily available; resupply from the roots is slower. In order to maximize fitness (relative to the goal) the leaves are abscised at the end of one RGR measurement period and another begins growing (Figure 4.3). This timing leads to positive RGR values. Growth of the new leaf can be maximized if the mobile carbon pool contains readily available carbon.

The goal was to maximize RGR by adding RGR measurements every two weeks. The goal places emphasis on biomass and the timing of its gain and loss, not on the plant's ability to balance production with the plants ability to use that production. Both of the P:R ratios ( $\Gamma_{STOP}$ , and  $\Gamma_{ABS}$ ) are near the high end of the allowable range indicating that higher values would be chosen if possible.

### 4.3.2 Strategy Two: RGR-Population

While plant above ground biomass for the RGR-Population configuration is somewhat higher than that of the nominal configuration, below ground biomass is much higher (Figure 4.6). The configuration is stable for a 5 year run (Figure 4.7) even though peak total plant biomass is roughly 4 times greater than the nominal configuration (536 mg C vs. 124 mg C), and biomass on an areal basis is slightly higher (170 g C m<sup>-2</sup> vs. 149 g C m<sup>-2</sup>) as shown in Table 4.3.

The first leaf for the RGR-Population configuration starts 2 days later than the nominal configuration (Table 4.3) and the plastichrone interval is longer (18 vs. 13 days). Early in the year leaves grow to longer lengths (up to 67 vs. 33 cm, Figure 4.8) and are wider (up to

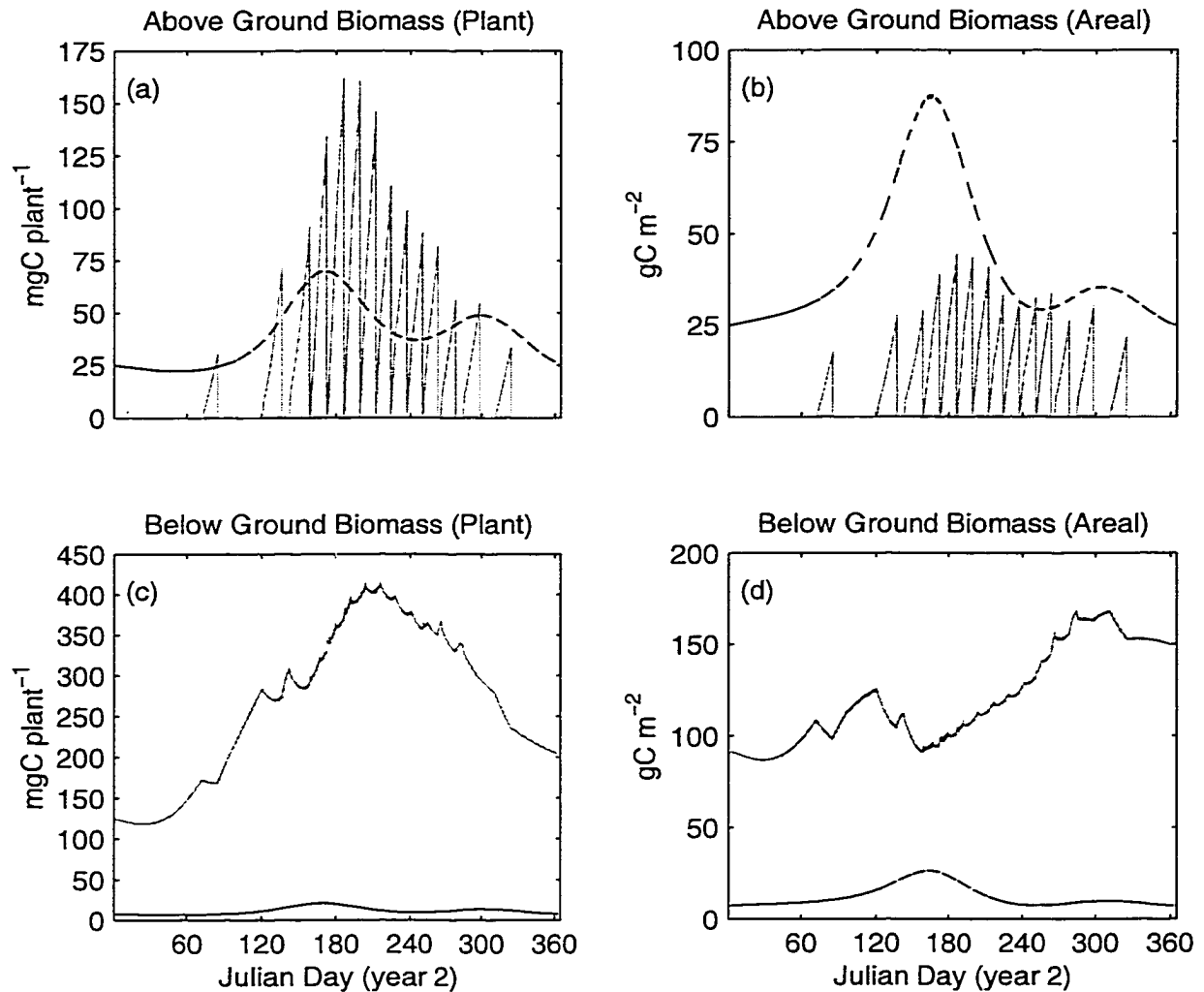


Figure 4.6: Biomass from the RGR-Population configuration compared to BWM99 model biomass. Output from the BWM99 model shown as dashed (smooth) line. Output from the RGR-Population configuration in black/gray (jagged) lines. a) Above-ground and c) below-ground biomass of an individual plant. b) Above-ground and d) below-ground biomass of a square meter of seagrass bed. The Vgrass model simulates individual leaves instead of lumping their biomass into one state variable. The growth and abscission of the individual leaves causes the biomass to fluctuate. Biomass from the single plant is multiplied by shoot density (Moore 1996), and therefore, the areal biomass is subject to the same fluctuations.



Table 4.3: RGR-Population configuration performance metrics. The first six metrics are computed from the second year of the simulation. Metrics with a range of values are reduced to minimum, average, and maximum values. NPP is Net Primary Production. BIO is the peak biomass. NPP and BIO are the average of peak values obtained during years 2 through 5 of the simulation.

Metric	Nominal Configuration			RGR-Population Config.			Units
	Min	Avg	Max	Min	Avg	Max	
First Shoot		70			72		Julian day
Plastichrone	8	13	30	12	18	48	Days
Leaf Length	20	26	33	7	32	67	cm
Leaf Age	20	28	49	14	19	27	Days
LAI		1.6	5.2		0.7	1.9	$\text{m}^2 \text{m}^{-2}$
Leaves		22			14		leaves $\text{y}^{-1}$
NPP Plant		294			30		$\text{mg C y}^{-1}$
NPP Pop.		343			-32		$\text{g C m}^{-2} \text{y}^{-1}$
BIO Plant		124			536		$\text{mg C}$
BIO Pop.		149			170		$\text{g C m}^{-2}$

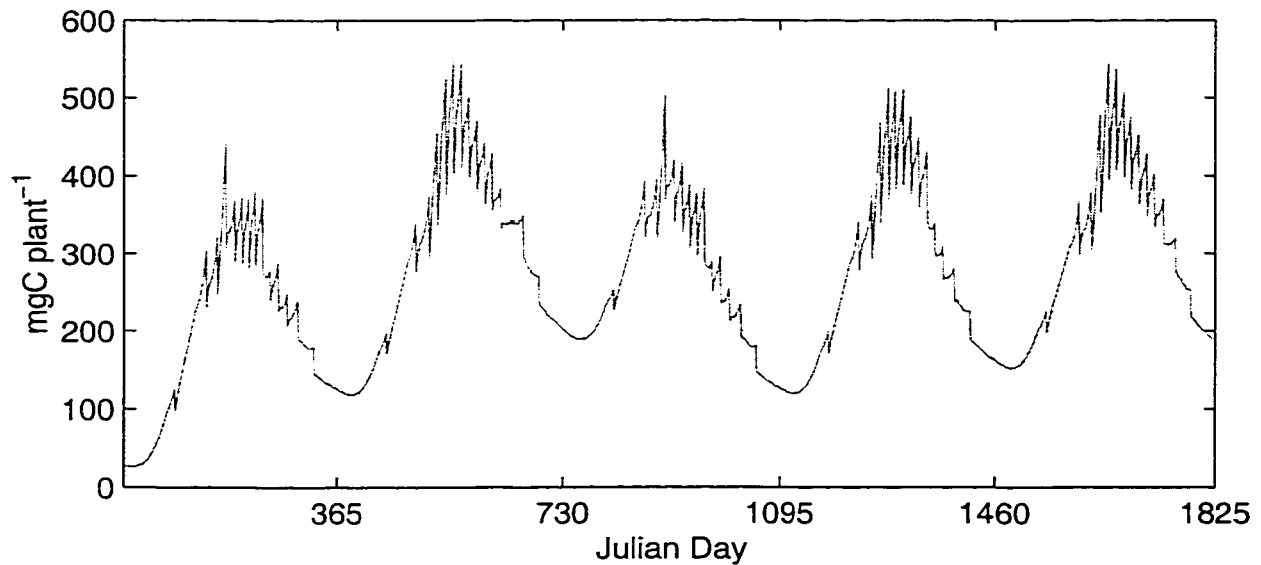


Figure 4.7: Biomass plot of the RGR-Population configuration showing stability over 5 years (i.e. there is no evident trending).

15 mm vs. 5 mm, Figure 4.10c) midyear than nominal. There are fewer leaves grown each year (14 vs. 22 leaves) and they abscise at a younger age (19 vs. 28 days). New leaves grow to shorter and shorter lengths as the season continues (Figure 4.8). Shoot density (Figure 4.10h) is lowest during the period of the growing season when light is at its peak. The lower shoot density and shorter leaves help to lower LAI ( $0.7$  vs.  $1.6 \text{ m}^2 \text{ m}^{-2}$ ) and increase light availability at the leaf surface (Figure 4.9) to nearly  $600 \mu\text{E m}^{-2} \text{ s}^{-1}$  (vs.  $450 \mu\text{E m}^{-2} \text{ s}^{-1}$ ) during the middle of the year.

PSU density and antenna chl levels are within normal limits (Figure 4.10a and 4.10b), and the PI curves for days 90 and 150 have a relatively normal shape. By day 210, below ground biomass has reached its limit. With storage limited, the PI curves for days 210 and 270 show that more carbon is being collected than can be processed.

NPP (Table 4.3) for the RGR-Population configuration is substantially lower than that of the nominal configuration ( $30 \text{ mg C y}^{-1}$  and  $-32 \text{ g C m}^{-2} \text{ y}^{-1}$  vs.  $294 \text{ mg C y}^{-1}$  and  $343 \text{ g C m}^{-2} \text{ y}^{-1}$ ). Larger than nominal below ground biomass is a factor in the lower NPP value as it introduces a large respiration demand. While NPP is positive for the plant, it is negative on an areal basis. This is due to how the GA used shoot density ( $\Gamma_{SD}$ ) and shoot-to-root ratio ( $\Gamma_{SD}$ ) in achieving the RGR-Population goal. Figure 4.6c shows plant below-ground biomass decreasing after Julian day 200 while Figure 4.6d shows areal below-ground biomass increasing. The GA has selected parameters such that shoot density increases (Figure 4.10h) after Julian day 200. Shoot density is used by the GA to increase areal below-ground biomass.

To attain the goal of maximizing RGR at the population level, the GA should select

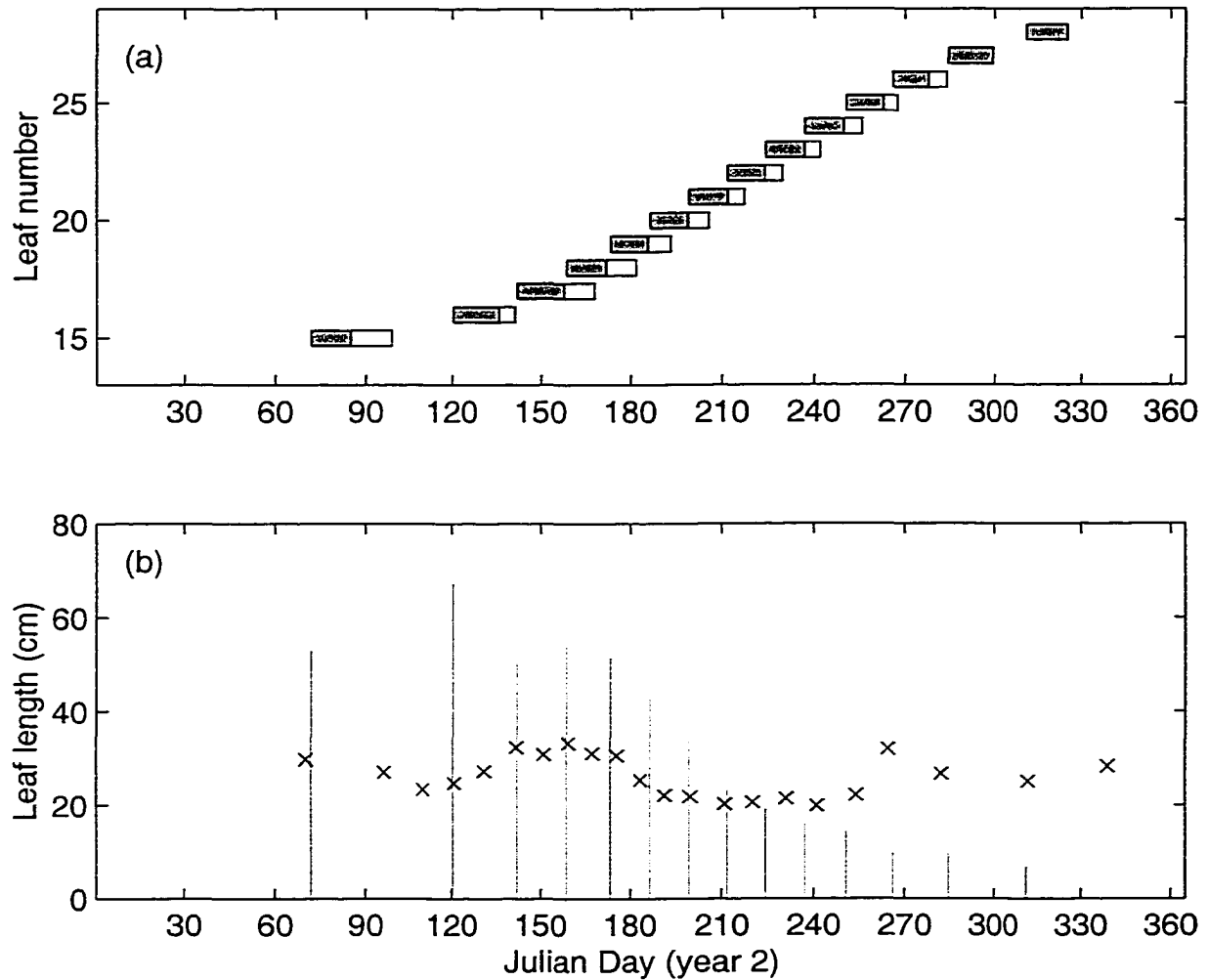


Figure 4.8: RGR-Population configuration leaf growth. a) each bar represents the start date (left edge), growth stage (left shaded area), mature stage (right unshaded area), and abscission (right edge). b) lines indicate the start date (x axis) and the final length (y axis) of the leaf. The x's represent the lengths and timing of leaves from the nominal configuration.

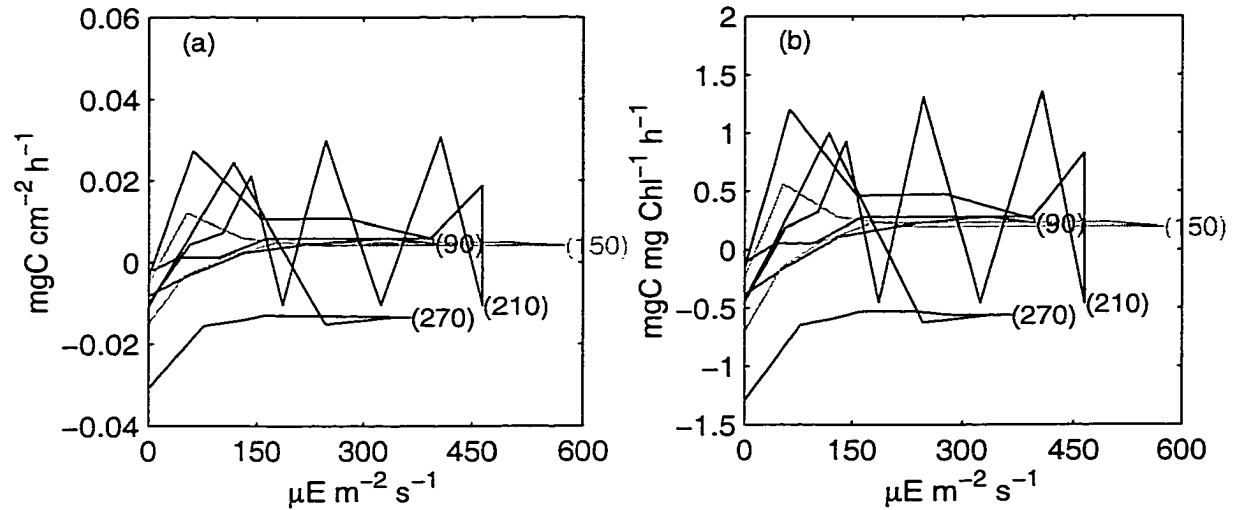


Figure 4.9: RGR-Population configuration whole-plant production vs. irradiance plots based on leaf area (a) and chl (b). Each line represents 24 hrs of data; the hysteresis is due to production differences between morning and afternoon. The numbers at the end of each line indicate the Julian day of the second year of simulation from which the data were taken.

parameters that lead to higher areal biomass at the end of year 2 than at the beginning. Figure 4.6b and 4.6d show that above ground biomass does not contribute directly to this goal; all of the biomass gain takes place below ground. Figure 4.10g shows that the GA selected for the Shoot:Root ratio to be less than 1 (it does not reach zero) from about day 70 to day 240. This gives priority to below ground growth. The GA also selected for degree-days between leaves to be near the maximum allowed in the search. This would help reduce the number of leaves grown in a season to just the number needed to harvest enough energy to push below ground biomass to its limit. Increasing shoot density also helps to increase areal biomass at the end of the growing season. Shoot density for the RGR-Population configuration is nearly 100 days out of phase with the nominal configuration. In effect, shoot density is used to allow a few plants to grow large root storage during the middle of

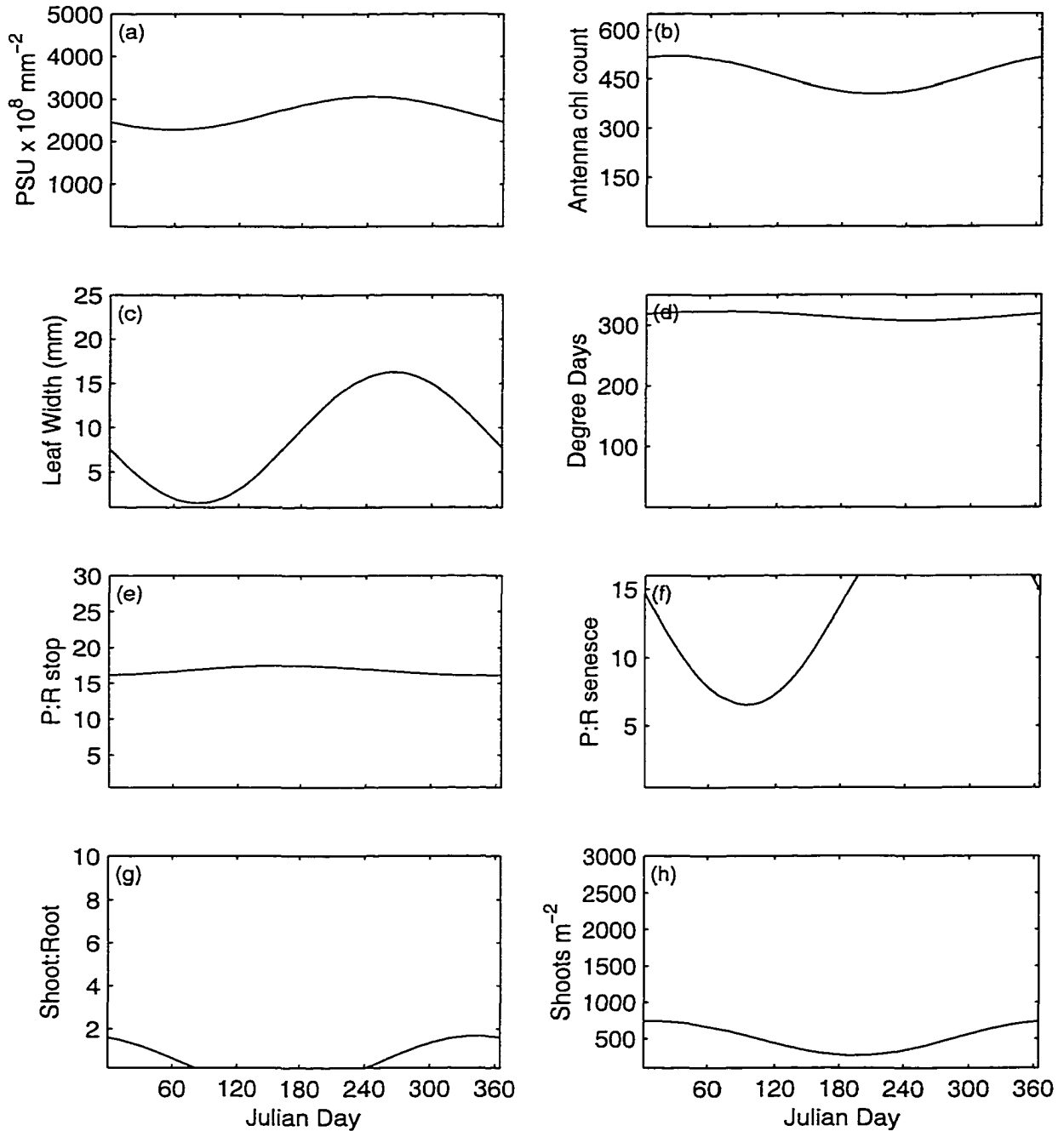


Figure 4.10: RGR-Population configuration  $\Gamma$  variable plots. Each curve is computed from its  $\Gamma$  variable (Table 2.3) as in Figure 2.3.

the year. Shoot density increases at the end of the growing season, artificially increasing the areal below ground biomass. *Artificial* is used here in the sense that shoot density is increased mathematically but the carbon required by the *new* plants does not come from existing plants. Since the GA was able to control shoot density, it used it to help achieve its goal.

### 4.3.3 RGR-Plant vs. RGR-Population

In comparing the RGR-Plant to RGR-Population attributes in Tables 4.2 and 4.3, nearly all of the average values are similar. There is a 2 day difference between first shoot initiation, 1 day difference in average plastichrone interval, 3 day difference in average leaf age, almost no difference in LAI, and a difference of 2 leaves grown during the year.

The differences lie in the average leaf length (17 cm vs. 32 cm, plant vs. population), and in the NPP and Maximum Biomass metrics. Both NPP metrics (plant and areal) for the RGR-Plant configuration are higher than those of the NPP metrics for the RGR-Population configuration (263 mg C y<sup>-1</sup> and 310 g C m<sup>-2</sup> y<sup>-1</sup> vs. 30 mg C y<sup>-1</sup> and 32 g C m<sup>-2</sup> y<sup>-1</sup>). In contrast, the maximum biomass metrics are higher for the RGR-Population configuration than for the RGR-Plant configuration (536 mg C and 170 mg C vs. 79 g C m<sup>-2</sup> and 98 g C m<sup>-2</sup>).

In selecting for a plant that optimizes RGR, the GA emphasizes the timing of leaf initiation, time to maturity, and timing of abscission. This is done in favor of balancing PSU size and number with the plant's ability to use the harvested carbon and leads to higher NPP. In selecting for a population of plants that optimize RGR for the population,

the GA selects plants that build biomass in the root (low Shoot:Root), while minimizing the number of leaves needed to accomplish the task. The photosynthetic apparatus balances well with growth and storage requirements until storage has reached its maximum. The GA also takes advantage of the fact that mass is not conserved when plant biomass is scaled to areal biomass. The GA controls shoot density and uses this to numerically increase plant population. The increase in population is not the result of existing plants using some of their biomass to produce new plants.

## 4.4 Optimization Goal:

### Maximization of Biomass

The fitness function for maximization of biomass tracked biomass through years 2–5 of the simulation and recorded each year’s maximum value. The four maximum biomass values were averaged and returned to the GA as the fitness value. The GA searched for a configuration of controlling parameters capable of maximizing the average of the four yearly peak biomass values. While maximizing biomass was the primary goal of the GA, taking the average of 4 biomass peaks constrained the solutions to those capable of surviving five years. Rephrased, the goal is *maximize biomass in a fashion that leads to at least 5 years of simulated life*.

Two tests were run. First, biomass was maximized for an individual plant (BIO-Plant), that is, biomass for an individual plant was used in BIO calculation. In the second run mass was maximized for a population of plants (BIO-Population). In this case biomass for the individual was scaled up to a population by multiplying biomass with shoot density. Results of the searches are shown in Table 4.4.

#### 4.4.1 Strategy Three: BIO-Plant

Biomass for the BIO-Plant configuration far exceeded biomass of the nominal configuration (Figures 4.11 and 4.12). Leaves start growing 2 days earlier than the nominal configuration (Table 4.5). On average the plastichrone interval is shorter than nominal (10 days vs. 13 days) but has a maximum value of 144 days (30 days nominal). The effect



Table 4.4: GA selected configurations for BIO-Plant and BIO-Population growth strategies compared to the nominal configuration. Each column represents the individual that attained the highest fitness for the indicated test. Since the binary chromosome is 209 bits long, the individual should be the best of  $2^{209}$  or on the order of  $10^{62}$  possible configurations.

Parameter	Nominal	BIO Plant	BIO Pop.	Units
Degree-days first leaf	6	4	2	°C Day
Degree-days next average	150	90	46	°C Day
Degree-days next amplitude	65	66	41	°C Day
Degree-days next phase	240	290	7	Days
Shoot density average	1075	975	1535	Shoots $m^{-2}$
Shoot density amplitude	360	356	1992	Shoots $m^{-2}$
Shoot density phase	250	272	326	Days
Leaf width average	5.0	21.1	4.2	mm
Leaf width amplitude	0.1	1.7	7.1	mm
Leaf width phase	180	72	293	Days
PSU density average	750	4600	4698	$10^8$ PSU $mm^{-2}$
PSU density amplitude	200	347	413	$10^8$ PSU $mm^{-2}$
PSU density phase	60	89	60	Days
PSU antenna average	450	573	640	Chl PSU $^{-1}$
PSU antenna amplitude	20	29	241	Chl PSU $^{-1}$
PSU antenna phase	360	25	94	Days
Stop leaf P:R average	3.0	0.8	1.5	Ratio
Stop leaf P:R amplitude	5.0	9.5	5.6	Ratio
Stop leaf P:R phase	180	11	39	Days
Abscise leaf P:R average	9.0	2.5	13.1	Ratio
Abscise leaf P:R amplitude	4.0	5.9	0.8	Ratio
Abscise leaf P:R phase	300	207	26	Days
Shoot:Root average	4.0	6.9	9.3	Ratio
Shoot:Root amplitude	0.3	3.3	2.0	Ratio
Shoot:Root phase	50	169	250	Days

Table 4.5: BIO-Plant configuration performance metrics. The first six metrics are computed from the second year of the simulation. Metrics with a range of values are reduced to minimum, average, and maximum values. NPP is Net Primary Production. BIO is the peak biomass. NPP and BIO are the average of peak values obtained during years 2 through 5 of the simulation.

Metric	Nominal Configuration			BIO-Plant Configuration			Units
	Min	Avg	Max	Min	Avg	Max	
First Shoot		70			68		Julian day
Plastichrone	8	13	30	2	10	144	Days
Leaf Length	20	26	33	6	15	36	cm
Leaf Age	20	28	49	149	174	216	Days
LAI		1.6	5.2		37	103	$\text{m}^2 \text{m}^{-2}$
Leaves		22			26		leaves $\text{y}^{-1}$
NPP Plant		294			-196		$\text{mg C y}^{-1}$
NPP Pop.		343			-1,280		$\text{g C m}^{-2} \text{y}^{-1}$
BIO Plant		124			2,947		$\text{mg C}$
BIO Pop.		149			3,912		$\text{g C m}^{-2}$

of these values is shown in Figure 4.13 as leaves are started at the beginning of the season and survive into the latter part of the growing season. The minimum age for a leaf is 149 days for the BIO-Plant compared to the nominal configuration having a maximum leaf age of 49 days. There is also a large mid-season gap where no new leaves are started. Leaves continue to grow through the entire mid-season and are abscised during their growth stage (i.e. they never reach maturity). Since the P:R abscise ratio is greater than the P:R stop, leaves stop growing at the appropriate P:R stop ratio but then are immediately abscised.

Leaf length is similar to the nominal case (up to 36 cm vs. 33 cm) while leaf width is greater (21.1 mm vs. 5.0 mm, Table 4.4). Only 4 more leaves are used (26 vs. 22) but since most are growing at the same time LAI is considerably higher (up to  $103 \text{ m}^2 \text{ m}^{-2}$  vs.  $5.2 \text{ m}^2 \text{ m}^{-2}$ ). The high LAI lowers peak light intensities after day 90 to less than

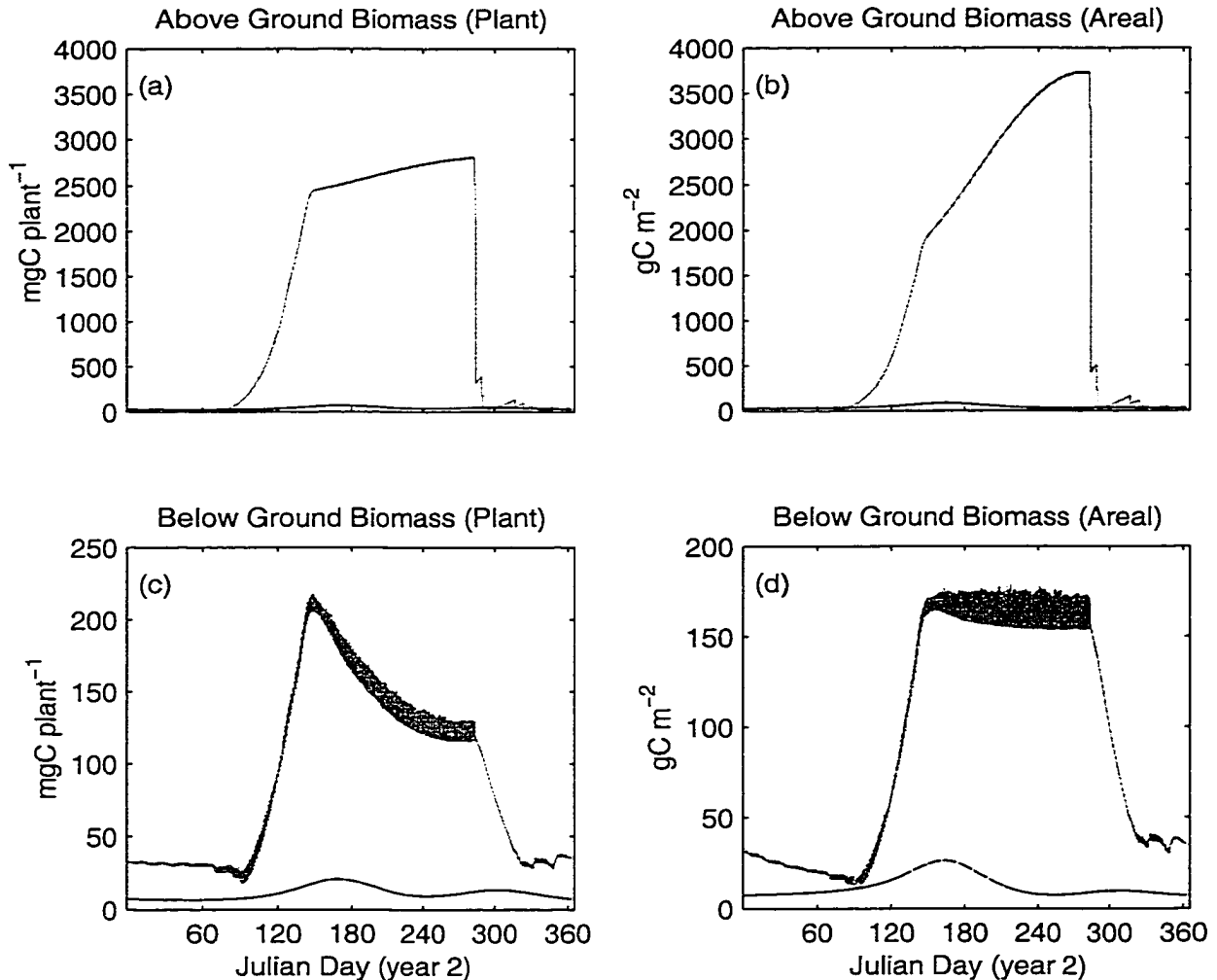


Figure 4.11: Biomass from the BIO-Plant configuration compared to BWM99 model biomass. Output from the BWM99 model shown as dashed (smooth) line. Output from the BIO-Plant configuration in black/gray (jagged) lines. a) Above-ground and c) below-ground biomass of an individual plant. b) Above-ground and d) below-ground biomass of a square meter of seagrass bed. The Vgrass model simulates individual leaves instead of lumping their biomass into one state variable. The growth and abscission of the individual leaves causes the biomass to fluctuate. Biomass from the single plant is multiplied by shoot density (Moore 1996), and therefore, the areal biomass is subject to the same fluctuations.

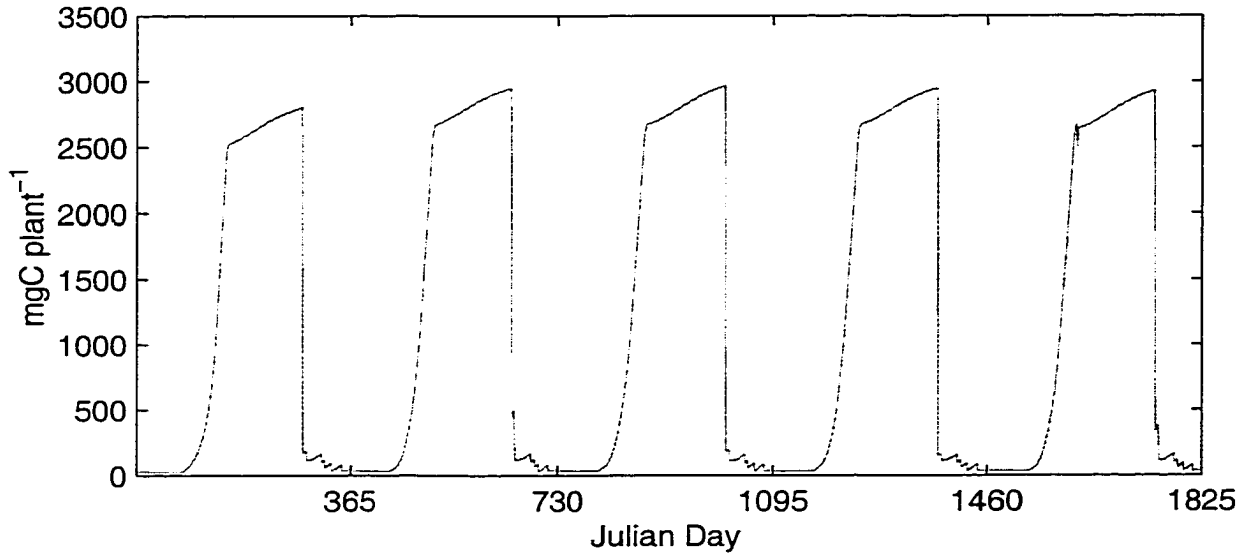


Figure 4.12: Biomass plot of the BIO-Plant configuration showing stability over 5 years (i.e. there is no evident trending).

$200 \mu\text{E m}^{-2} \text{s}^{-1}$  ( $450 \mu\text{E m}^{-2} \text{s}^{-1}$  for nominal).

The goal for the GA with BIO-Plant is to produce as large a plant as possible regardless of the cost. To accomplish this, PSU density and antenna chl are at (or near) their maximum values to elevate energy collection (Figure 4.15). The value of degree-days between leaves causes leaf growth patterns seen in Figure 4.13. This is reinforced by the  $\Gamma_{STOP}$  value of less than 1 that is assigned to each of these leaves, Figure 4.15f. As such, leaves started early actually are abscised after they have respired more carbon than they produced.

In comparing Figure 4.15e and Figure 4.15f it is notable that the phase of  $\Gamma_{STOP}$  and  $\Gamma_{ABS}$  are nearly 180 days out of phase with each other. A leaf will be assigned a low  $\Gamma_{STOP}$  ratio or a low  $\Gamma_{ABS}$  ratio. As such either a leaf will stop growing at a very low P:R ratio or, if  $\Gamma_{STOP}$  is high,  $\Gamma_{ABS}$  would cause the leaf to be abscised at a very low P:R ratio. The phasing of these two parameters will always lead to leaves that have very low P:R ratios

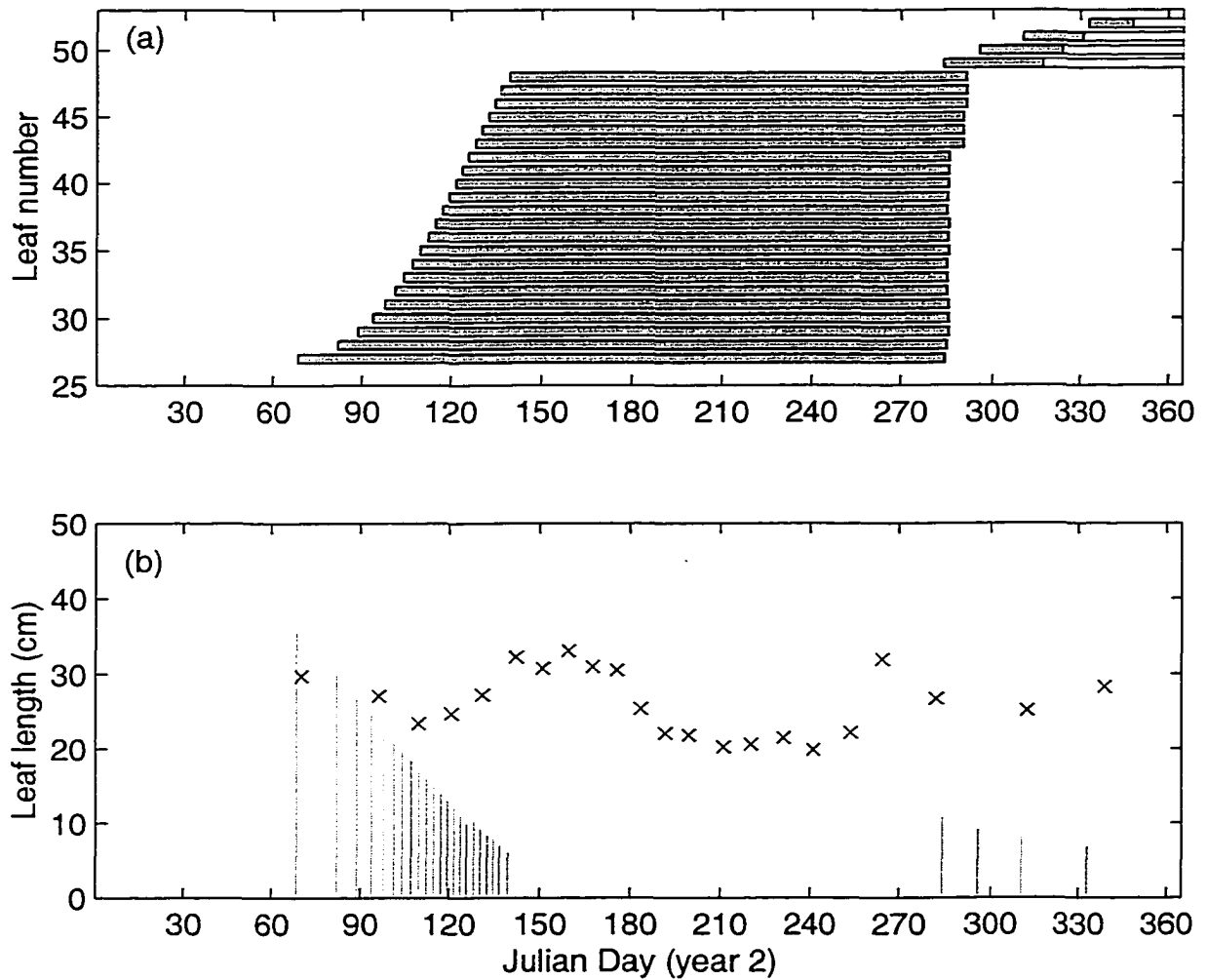


Figure 4.13: BIO-Plant configuration leaf growth. a) each bar represents the start date (left edge), growth stage (left shaded area), mature stage (right unshaded area), and abscission (right edge). b) lines indicate the start date (x axis) and the final length (y axis) of the leaf. The x's represent the lengths and timing of leaves from the nominal configuration.

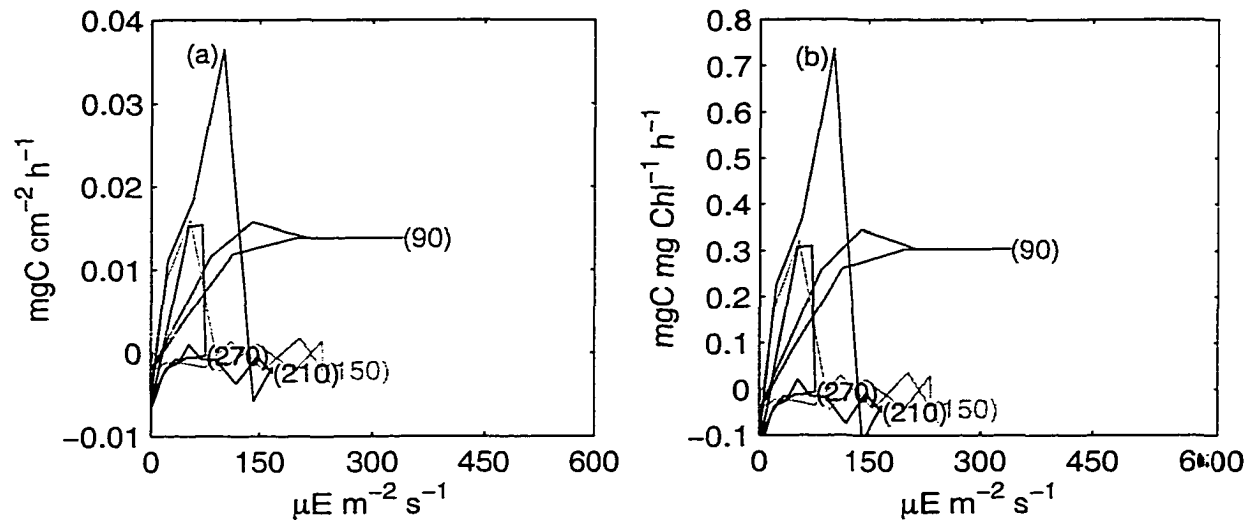


Figure 4.14: BIO-Plant configuration whole-plant production vs. irradiance plots based on leaf area (a) and chl (b). Each line represents 24 hrs of data; the hysteresis is due to production differences between morning and afternoon. The numbers at the end of each line indicate the Julian day of the second year of simulation from which the data were taken.

before they are abscised.

The NPP values in Table 4.5 indicate that the GA has selected a plant configuration which optimizes biomass regardless of cost; the NPP values are negative. The negative values should be accompanied by biomass plots that show a plant which is losing carbon (but Figure 4.12 shows no net loss of carbon from year to year. The negative values were traced to an accounting error in computing NPP. The situation only arises in this and the BIO-Population configuration. Carbon for leaf respiration is taken from the leaf's mobile carbon state variable. Photosynthesis and carbon flow from the meristem are the only other flows that can add to the leaf's mobile carbon state variable. Leaves for this configuration become very old (up to 216 days) and photosynthesis and respiration are negatively affected by leaf age. Photosynthesis decreases and respiration increases to the point that photosynthesis and

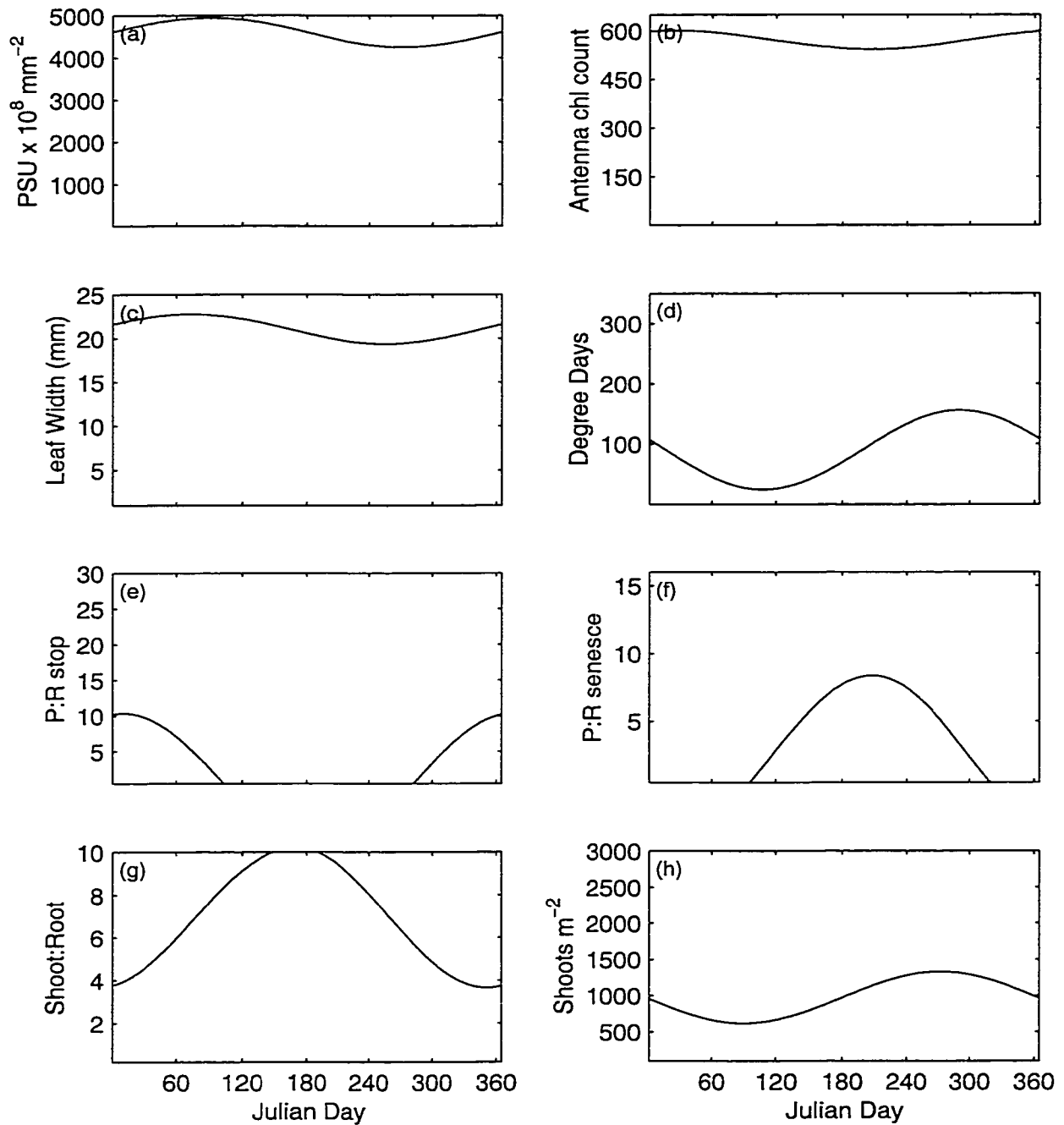


Figure 4.15: BIO-Plant configuration  $\Gamma$  variable plots. Each curve is computed from its  $\Gamma$  variable (Table 2.3) as in Figure 2.3.

meristem resupply cannot meet the leaf's respiration demand. In the model, leaf respiration is logged before the flows are computed; the respiration demand is computed into NPP even though the leaf never respire the carbon. Mass balance is maintained in the model and the leaf is not allowed to respire at this elevated rate.

This accounting error did not show up during nominal runs when carbon was mass balanced; the situation of high leaf respiration did not occur and was not anticipated. When this error was noticed, code was added to the model to print a statement when the condition occurred during model execution. All GA configurations were run with this modification to see if the situation occurred with other configurations. This error only happened when running the BIO-Plant and BIO-Population configurations and therefore does not affect results obtained for the other configurations.

#### 4.4.2 Strategy Four: BIO-Population

Biomass levels for the BIO-Population configuration far exceed those of the nominal configuration (Figure 4.16 and Figure 4.17) but the configuration is stable over 5 years. Table 4.6 shows that leaf growth is started 4 days earlier (day 66 vs. day 70), leaf ages are greater (up to 230 days vs. 49 days), and nearly the same number of leaves are used (23 vs. 22). Leaf length is greater (up to 1,307 cm vs. 33 cm) while leaf width is very thin (1 mm) for leaves started before Julian day 140 (Figure 4.18b and Figure 4.20c). Leaf age and size lead to high LAI (up to  $469 \text{ m}^2 \text{ m}^{-2}$  vs. up to  $5.2 \text{ m}^2 \text{ m}^{-2}$ ) but the timing of leaf initiation helps light availability at the leaves surfaces to be higher than nominal (up to  $600 \mu\text{E m}^{-2} \text{ s}^{-1}$  vs.  $450 \mu\text{E m}^{-2} \text{ s}^{-1}$ ) early in the growing season (Figure 4.19).



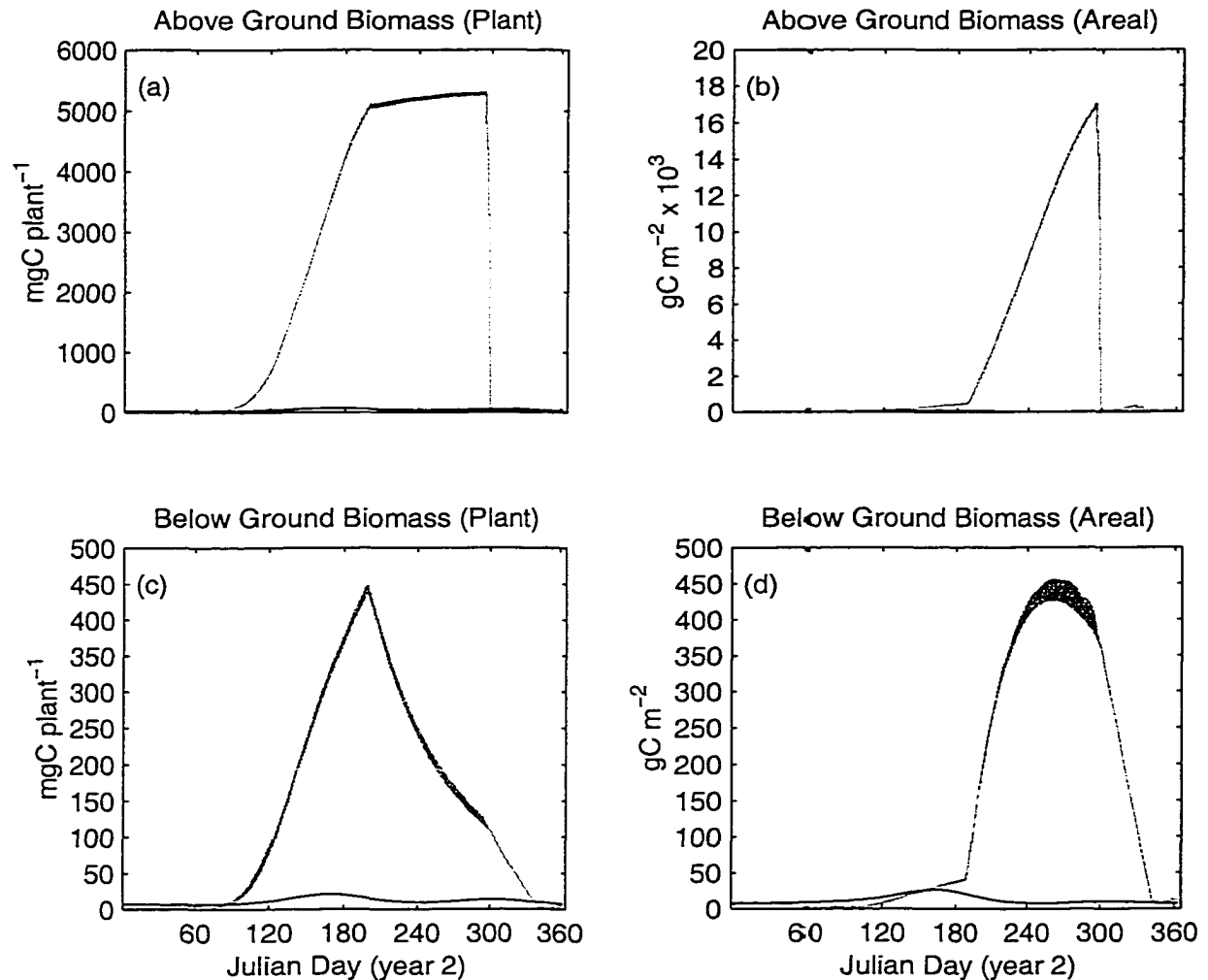


Figure 4.16: Biomass from the BIO-Population configuration compared to BWM99 model biomass. Output from the BWM99 model shown as dashed (smooth) line. Output from the BIO-Population configuration in black/gray (jagged) lines. a.) Above-ground and c.) below-ground biomass of an individual plant. b.) Above-ground and d.) below-ground biomass of a square meter of seagrass bed. The Vgrass model simulates individual leaves instead of lumping their biomass into one state variable. The growth and abscission of the individual leaves causes the biomass to fluctuate. Biomass from the single plant is multiplied by shoot density (Moore 1996), and therefore, the areal biomass is subject to the same fluctuations.

Table 4.6: BIO-Population configuration performance metrics. The first six metrics are computed from the second year of the simulation. Metrics with a range of values are reduced to minimum, average, and maximum values. NPP is Net Primary Production. BIO is the peak biomass. NPP and BIO are the average of peak values obtained during years 2 through 5 of the simulation.

Metric	Nominal Configuration			BIO-Population Config.			Units
	Min	Avg	Max	Min	Avg	Max	
First Shoot		70			66		Julian day
Plastichrone	8	13	30	1	12	160	Days
Leaf Length	20	26	33	8	634	1,307	cm
Leaf Age	20	28	49	21	150	230	Days
LAI		1.6	5.2		97	469	$\text{m}^2 \text{m}^{-2}$
Leaves		22			23		leaves $\text{y}^{-1}$
NPP Plant		294			-19		$\text{mg C y}^{-1}$
NPP Pop.		343			-7,718		$\text{g C m}^{-2} \text{y}^{-1}$
BIO Plant		124			5,531		$\text{mg C}$
BIO Pop.		149			17,361		$\text{g C m}^{-2}$

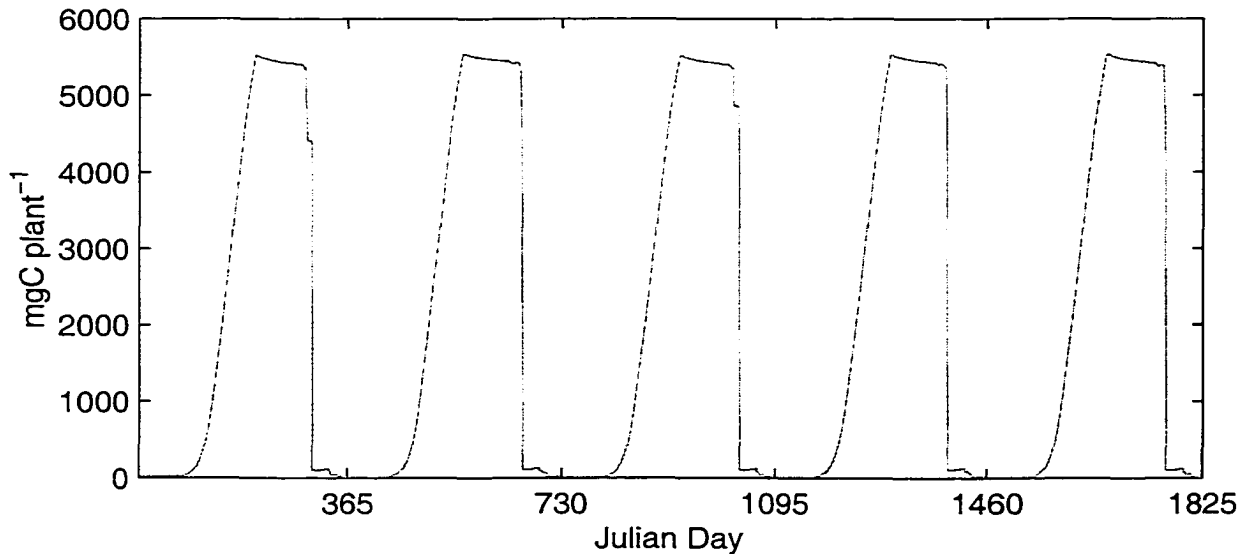


Figure 4.17: Biomass plot of the BIO-Population configuration showing stability over 5 years (i.e. there is no evident trending).

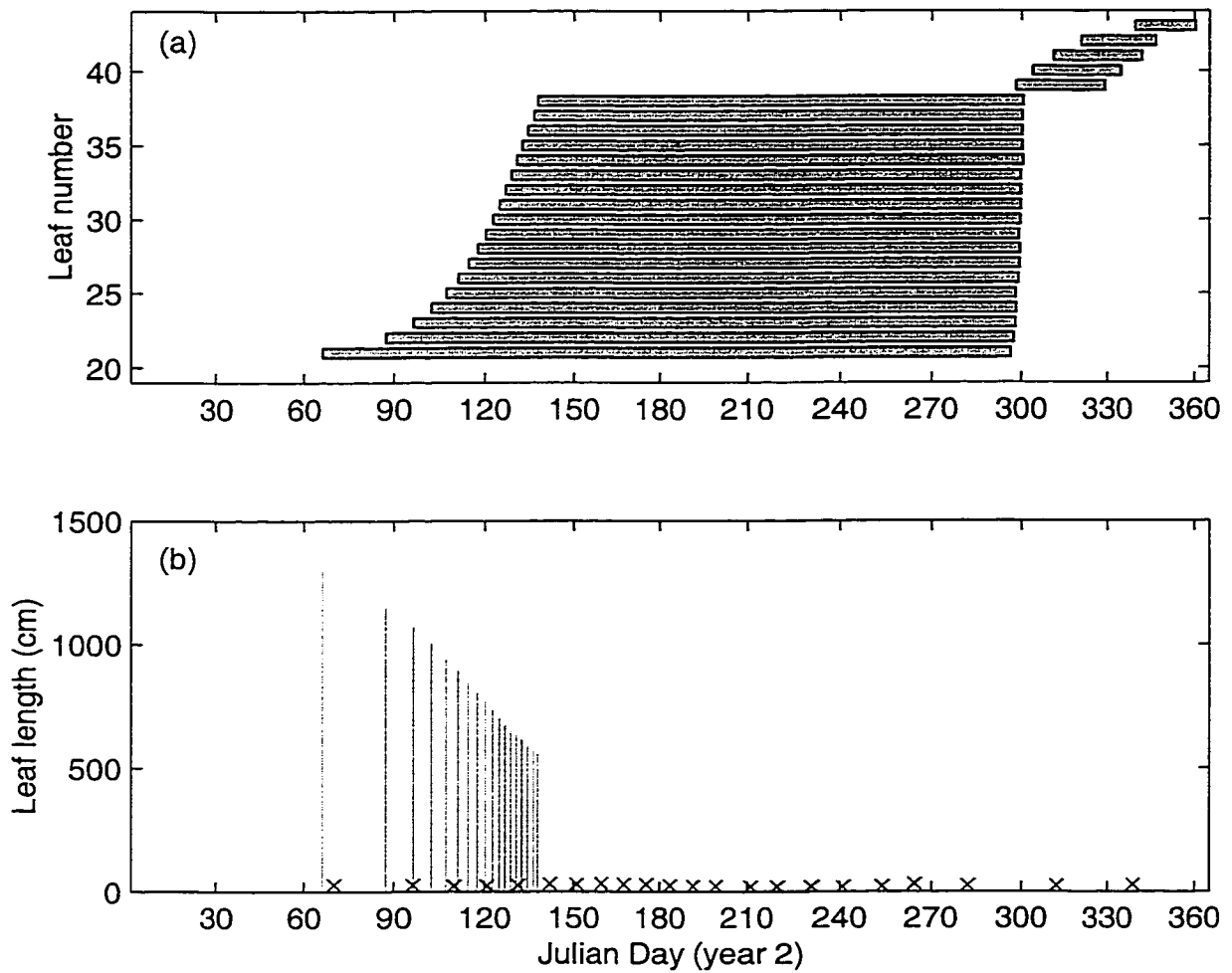


Figure 4.18: BIO-Population configuration leaf growth. a) each bar represents the start date (left edge), growth stage (left shaded area), mature stage (right unshaded area), and abscission (right edge). b) lines indicate the start date (x axis) and the final length (y axis) of the leaf. The x's represent the lengths and timing of leaves from the nominal configuration.

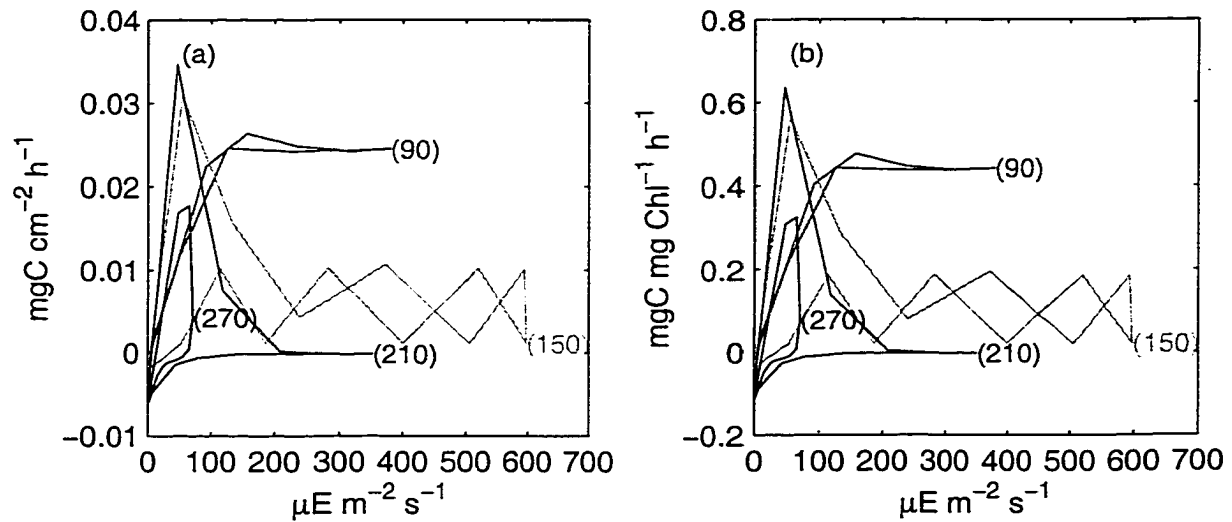


Figure 4.19: BIO-Population configuration whole-plant production vs. irradiance plots based on leaf area (a) and chl (b). Each line represents 24 hrs of data; the hysteresis is due to production differences between morning and afternoon. The numbers at the end of each line indicate the Julian day of the second year of simulation from which the data were taken.

The goal for BIO-Population is to achieve a high biomass peak on an areal basis regardless of the cost. To accomplish this PSU density and antenna chl parameters are at (or near) their maximum values (Figure 4.20a and 4.20b). The P:R abscise ratio is rather high (near 15) but must be ignored in favor of P:R stop. The timing of maturity (P:R stop) and abscission (P:R abscise) requires leaf growth to stop before the leaf may be abscised. In this configuration, leaf growth stops at a low P:R ratio (less than 5); the leaf is then considered mature. Any mature leaves whose P:R ratio is less than P:R abscise are immediately abscised. Since all leaves have a P:R stop ratio less than the P:R abscise ratio, the leaves are immediately abscised when the P:R stop condition arises. As was noted in the BIO-Plant configuration, there is an accounting error for NPP when leaves respire at a rate higher than what photosynthesis and the flow of carbon from the meristem can supply.

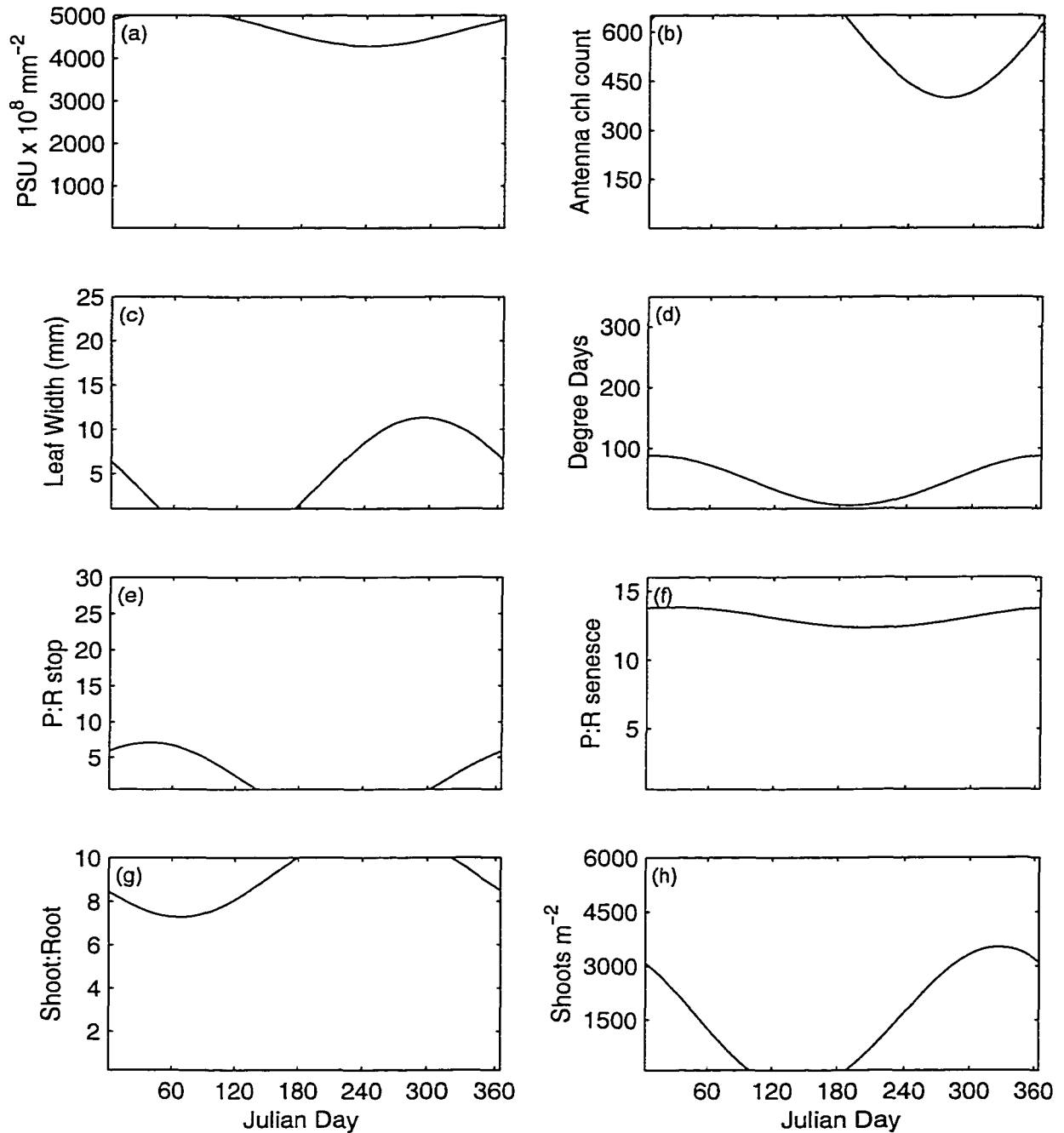


Figure 4.20: BIO-Population configuration  $\Gamma$  variable plots. Each curve is computed from its  $\Gamma$  variable (Table 2.3) as in Figure 2.3.

The BIO-Population configuration produces an areal biomass maximum of  $17,361 \text{ g C m}^{-2}$  ( $149 \text{ g C m}^{-2}$  nominal). No other configuration produces nearly as much biomass. Normally, below ground biomass is constrained to  $175 \text{ g C m}^{-2}$  but notice in Figure 4.16d that below ground biomass peaks near  $450 \text{ g C m}^{-2}$ . Figure 4.20h shows that between days 100 and 180 shoot density is very small ( $100 \text{ shoots m}^{-2}$ ). Just before and during this period, most leaves are started (Figures 4.18a and 4.18b). This timing allows the plants to individually grow large shoot and root biomass which peak just after Julian day 180 (Figure 4.16a and 4.16c). The below ground biomass is within the spatial limit of  $175 \text{ g C m}^{-2}$ . Just after Julian day 180, the shoot density rises (Figure 4.20h) and artificially pushes areal biomass (below ground and above ground) to high values. Biomass is inflated artificially because the GA has control over shoot density; the GA selected shoot density to achieve the goal of maximizing biomass. Note that while areal biomass is increasing up to ca. day 240 (Figure 4.16b and 4.16d), total individual plant biomass is decreasing (Figures 4.16a and 4.16c, Figure 4.17). After Julian day 180, individual plant biomass decreases sharply due to the large respiration demand from old leaves and a large root biomass.

#### 4.4.3 BIO-Plant vs. BIO-Population

Both BIO-Plant and BIO-Population configurations start a group of leaves early and then keep them over the entire midyear growing season. Both configurations use about the same number of leaves (26 BIO-Plant and 23 BIO-Population). Plant and areal biomass values are unrealistically large (over  $2,500 \text{ mg C plant}^{-1}$  for BIO-Plant, over

5,000 mg C plant<sup>-1</sup> for BIO-Population, vs. 100 mg C plant<sup>-1</sup> for the nominal configuration), and each configuration has a high shoot:root ratio. Leaves are abscised immediately after reaching maturity and have a long life span (up to 216 days and up to 230 days).

The configurations differ in that the BIO-Plant configuration uses short and wide leaves and the BIO-Population uses long narrow leaves. Leaf size leads to a smaller LAI for the BIO-Plant configuration (103 vs. 469).

It appears that the BIO-Population configuration leads to a plant capable of attaining a higher peak biomass than that of the BIO-Plant configuration (5,531 mg C vs. 2,947 mg C). The BIO-Population plant does reach a higher biomass, but shoot density plays a role in limiting plant size for the BIO-Plant configuration. Shoot density for the BIO-Plant configuration is limited so that shoot densities remain similar to the nominal model (approximately 1,100 shoots m<sup>-2</sup>). Meanwhile the BIO-Population configuration lowers its shoot density to 100 shoots m<sup>-2</sup> for Julian days 100 through 180. The BIO-Population plants may grow larger below ground biomass (and concurrently, above ground biomass) before running up against the spatial constraint of 175 g C m<sup>-2</sup> for the below ground tissue. If the BIO-Plant test was given a lower shoot density, it most likely would grow much larger plants.

## 4.5 Optimization Goal:

### Maximization of Net Primary Production

Net primary production (NPP) was computed as the difference between total yearly integrated production and total yearly integrated respiration. NPP was computed for years 2 through 5 of the simulation, and the average of those four years was taken. The GA searched for a set of controlling parameters that were best able to maximize the average NPP from 4 years of simulation. As in the BIO tests, the 4 year average also requires the solution to be stable for at least 5 total years.

NPP was maximized at the spatial scales of plant (NPP-Plant) and population (NPP-Population). Results of the searches are shown in Table 4.7.

#### 4.5.1 Strategy Five: NPP-Plant

Compared to the nominal configuration, biomass for NPP-Plant is very high (Figures 4.21 and 4.22). In comparing plant performance metrics from Table 4.8, the range of plastichrone interval is similar to the nominal configuration (5 to 29 days vs. 8 to 30 days) but the leaves are kept around for much longer periods of time (up to 107 days vs. 49 days). Leaves for the NPP-Plant configuration grow up to 1,222 cm (Figure 4.23) vs. 33 cm for the nominal case but are very narrow (1 mm, Figure 4.25c). Leaf length, width, and age together determine LAI values that are also quite high (up to  $125 \text{ m}^2 \text{ m}^{-2}$  vs.  $5.2 \text{ m}^2 \text{ m}^{-2}$ ).

Even though the leaves are quite long, peak irradiance is over  $300 \mu\text{E m}^{-2} \text{ s}^{-1}$  (Figure 4.24). As a result of the leaf area and light availability, NPP for an individual plant and NPP



Table 4.7: GA selected configurations for NPP-Plant and NPP-Population growth strategies compared to the nominal configuration. Each column represents the individual that attained the highest fitness for the indicated test. Since the binary chromosome is 209 bits long, the individual should be the best of  $2^{209}$  or on the order of  $10^{62}$  possible configurations.

Parameter	Nominal	NPP Plant	NPP Pop.	Units
Degree-days first leaf	6	6	3	°C Day
Degree-days next average	150	159	155	°C Day
Degree-days next amplitude	65	48	49	°C Day
Degree-days next phase	240	314	314	Days
Shoot density average	1075	985	12,209	Shoots $m^{-2}$
Shoot density amplitude	360	364	1,563	Shoots $m^{-2}$
Shoot density phase	250	273	206	Days
Leaf width average	5.0	1.1	24.9	mm
Leaf width amplitude	0.1	0.1	0.1	mm
Leaf width phase	180	68	321	Days
PSU density average	750	4922	4903	$10^8$ PSU $mm^{-2}$
PSU density amplitude	200	338	77	$10^8$ PSU $mm^{-2}$
PSU density phase	60	238	77	Days
PSU antenna average	450	636	623	Chl PSU $^{-1}$
PSU antenna amplitude	20	26	19	Chl PSU $^{-1}$
PSU antenna phase	360	280	124	Days
Stop leaf P:R average	3.0	2.5	4.8	Ratio
Stop leaf P:R amplitude	5.0	0.1	6.2	Ratio
Stop leaf P:R phase	180	327	164	Days
Abscise leaf P:R average	9.0	1.7	1.0	Ratio
Abscise leaf P:R amplitude	4.0	0.6	0.1	Ratio
Abscise leaf P:R phase	300	291	167	Days
Shoot:Root average	4.0	9.2	9.0	Ratio
Shoot:Root amplitude	0.3	2.8	4.8	Ratio
Shoot:Root phase	50	226	203	Days

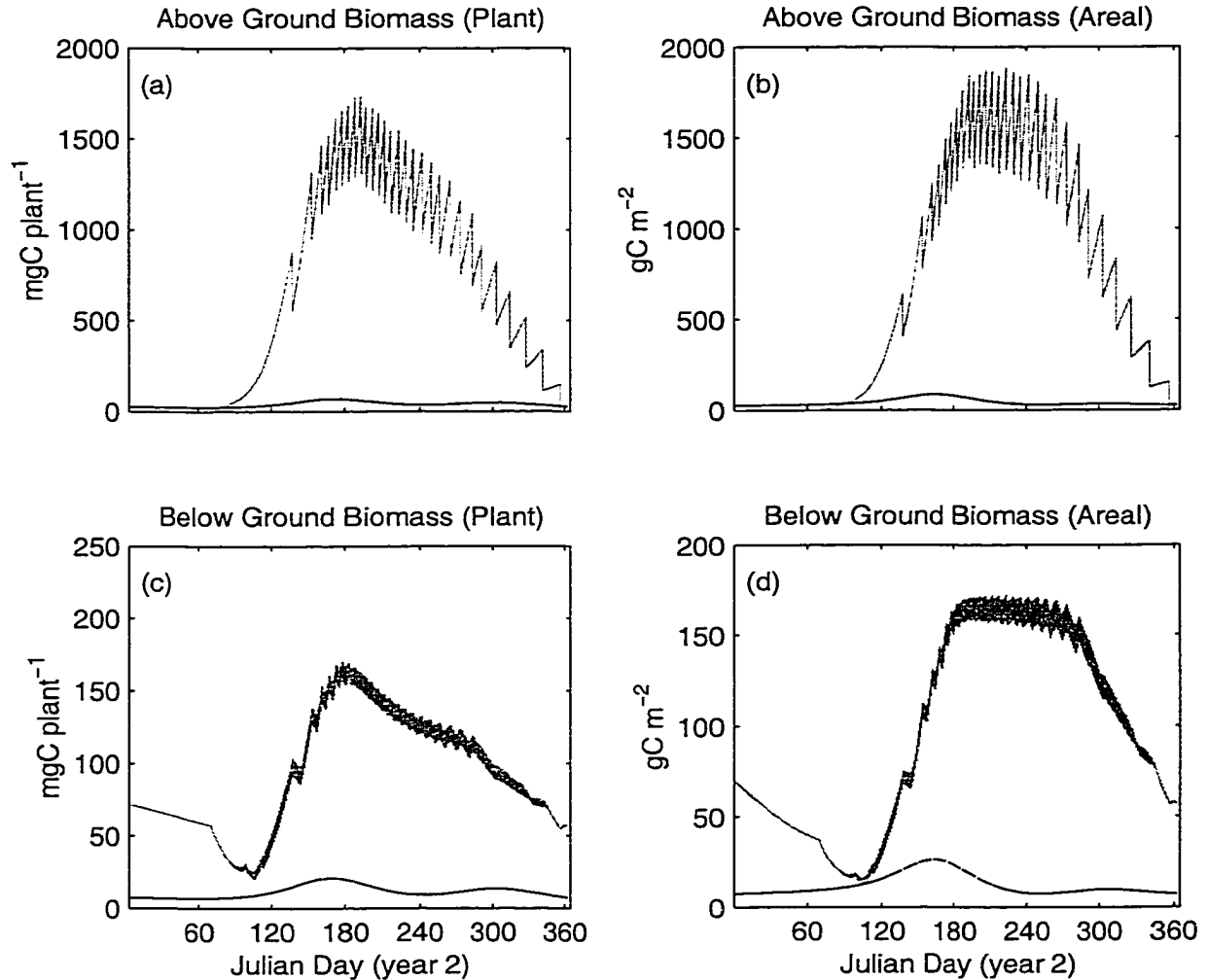


Figure 4.21: Biomass from the NPP-Plant configuration compared to BWM99 model biomass. Output from the BWM99 model shown as dashed (smooth) line. Output from the NPP-Plant configuration in black/gray (jagged) lines. a) Above-ground and c) below-ground biomass of an individual plant. b) Above-ground and d) below-ground biomass of a square meter of seagrass bed. The Vgrass model simulates individual leaves instead of lumping their biomass into one state variable. The growth and abscission of the individual leaves causes the biomass to fluctuate. Biomass from the single plant is multiplied by shoot density (Moore 1996), and therefore, the areal biomass is subject to the same fluctuations.

Table 4.8: NPP-Plant configuration performance metrics. The first six metrics are computed from the second year of the simulation. Metrics with a range of values are reduced to minimum, average, and maximum values. NPP is Net Primary Production. BIO is the peak biomass. NPP and BIO are the average of peak values obtained during years 2 through 5 of the simulation.

Metric	Nominal Configuration			NPP-Plant Configuration			Units
	Min	Avg	Max	Min	Avg	Max	
First Shoot		70			70		Julian day
Plastichrone	8	13	30	5	9	29	Days
Leaf Length	20	26	33	390	1,203	1,222	cm
Leaf Age	20	28	49	46	60	107	Days
LAI		1.6	5.2		46	125	$\text{m}^2 \text{m}^{-2}$
Leaves		22			29		leaves $\text{y}^{-1}$
NPP Plant		294			8,142		$\text{mg C y}^{-1}$
NPP Pop.		343			8,810		$\text{g C m}^{-2} \text{y}^{-1}$
BIO Plant		124			1,913		$\text{mg C}$
BIO Pop.		149			2,062		$\text{g C m}^{-2}$

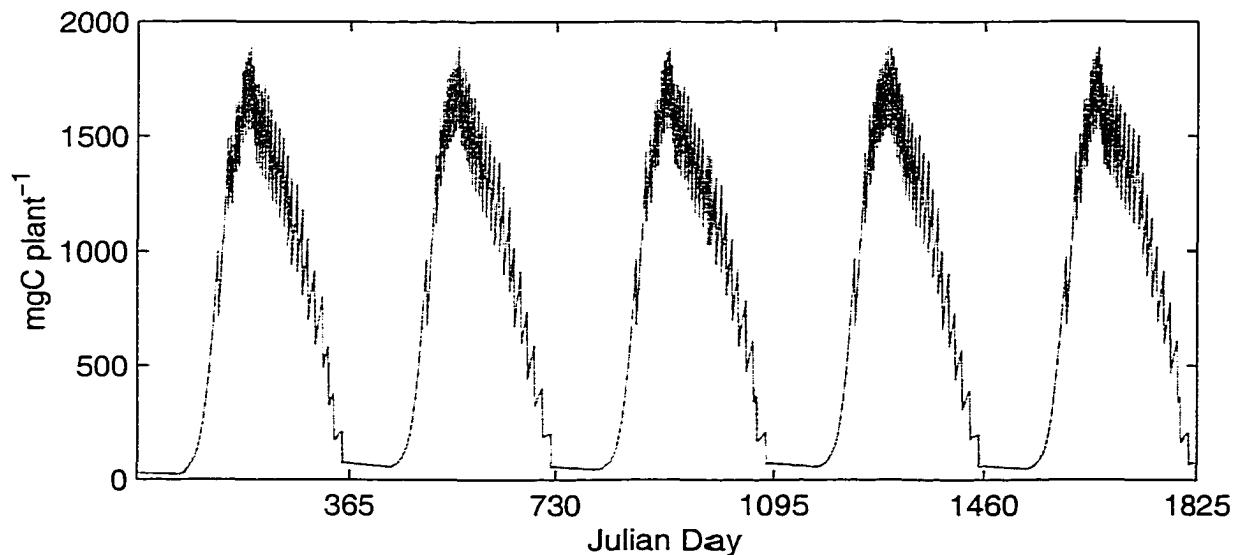


Figure 4.22: Biomass plot of the NPP-Plant configuration showing stability over 5 years (i.e. there is no evident trending).

on an areal basis is much higher than those of the nominal configuration (8,142 mg C y<sup>-1</sup> and 8,810 g C m<sup>-2</sup> y<sup>-1</sup> vs. 294 mg C y<sup>-1</sup> and 343 g C m<sup>-2</sup> y<sup>-1</sup>). Plant and areal maximum biomass are also considerably higher than the nominal configuration (1,913 mg C and 2,062 g C m<sup>-2</sup> vs. 124 mg C and 149 g C m<sup>-2</sup> ).

The strategy for NPP-Plant is to produce a plant that maximizes energy harvesting while minimizing respiration costs. This strategy is illustrated in how the controlling parameters behave (Figure 4.25). Energy collection is accomplished by several means: first, by increasing PSU density and antenna chl to the maximum values, and second, by configuring leaf width, degree-days between shoots, P:R stop, and P:R abscise values to grow a large leaf area (LAI) that is maintained for a long period of time. Along with the need for high production is the requirement for low respiration. A high Shoot:Root ratio minimizes the amount of carbon in the root system that would increase respiration costs. P:R stop and P:R abscise minimize respiration losses by abscising leaves before their respiration costs become too large.

#### 4.5.2 Strategy Six: NPP-Population

Biomass of individual plants for the NPP-Population was higher than the nominal configuration (Figures 4.26 and 4.27). On an areal basis, biomass is much higher due to the higher shoot density (Figure 4.30h). This is also reflected in the maximum biomass values in Table 4.9 (273 mg C for the plant and 3,412 g C m<sup>-2</sup> on an areal basis). Table 4.9 shows plastichrone interval was slightly longer than the nominal configuration (up to 44 days vs. 30 days). Leaf lengths were shorter (up to 18 cm vs. 33 cm) and leaf age was

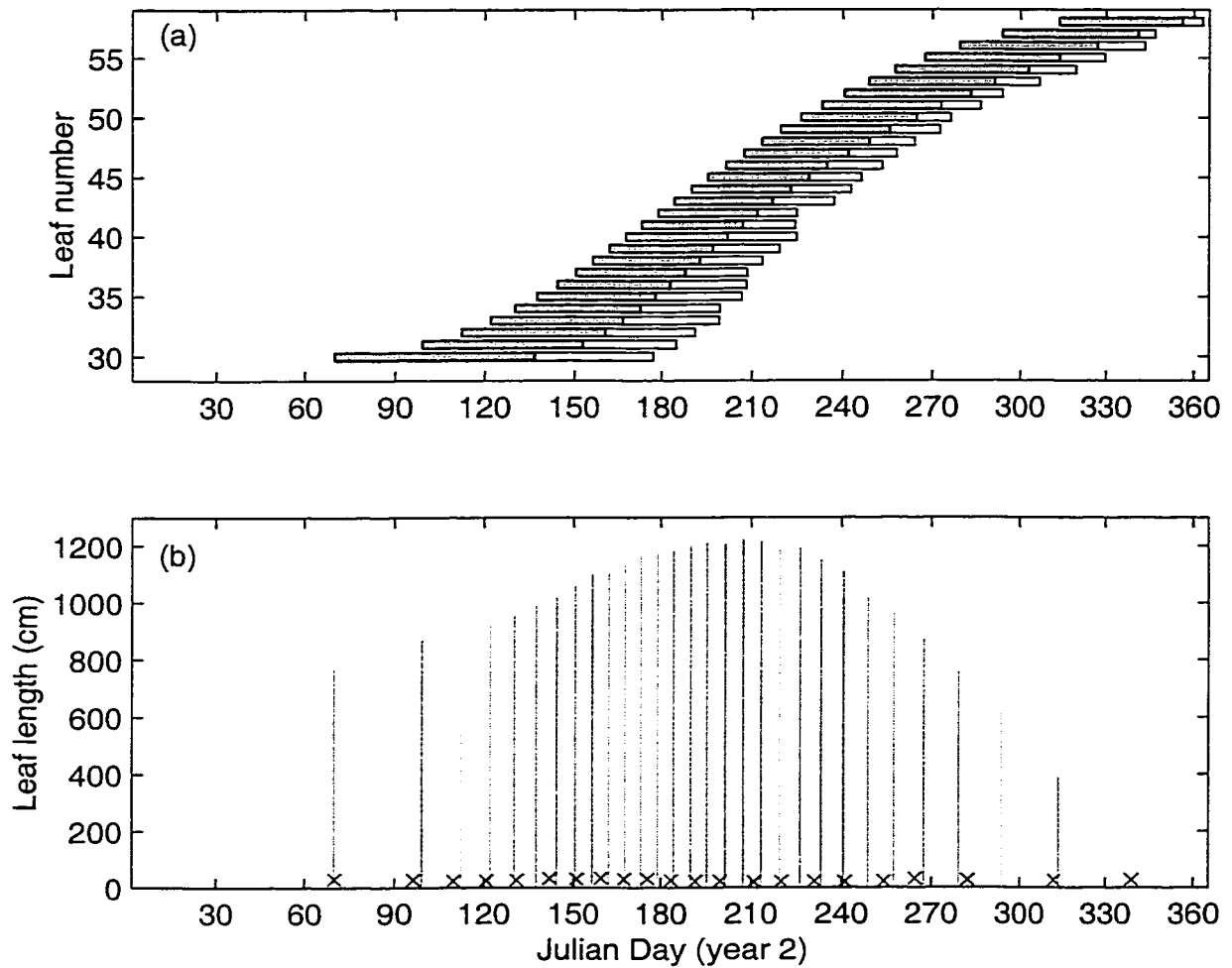


Figure 4.23: NPP-Plant configuration leaf growth. a) each bar represents the start date (left edge), growth stage (left shaded area), mature stage (right unshaded area), and abscission (right edge). b) lines indicate the start date (x axis) and the final length (y axis) of the leaf. The x's represent the lengths and timing of leaves from the nominal configuration.

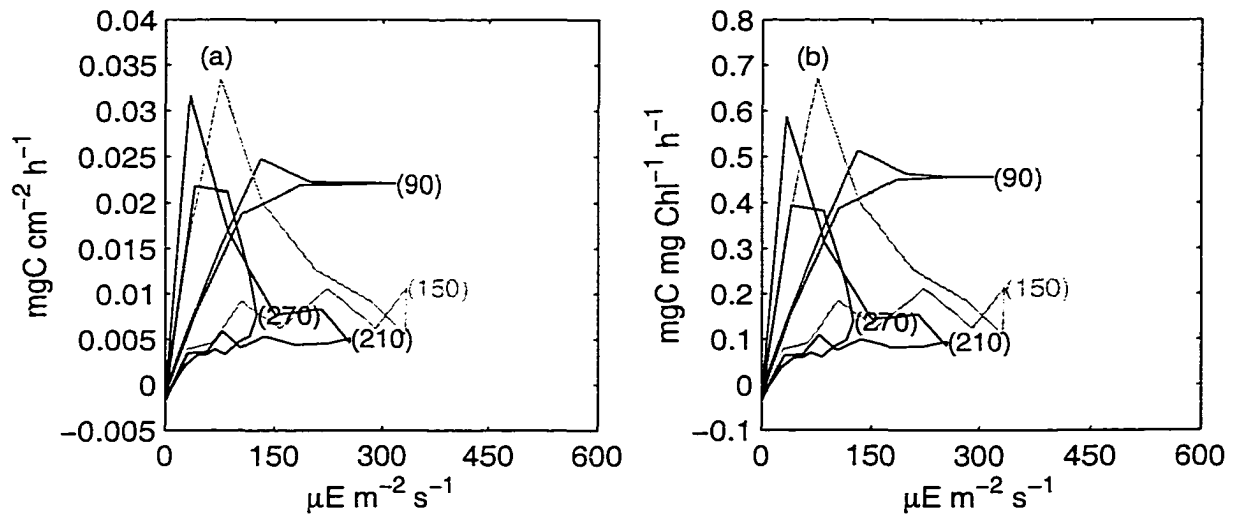


Figure 4.24: NPP-Plant configuration whole-plant production vs. irradiance plots based on leaf area (a) and chl (b). Each line represents 24 hrs of data; the hysteresis is due to production differences between morning and afternoon. The numbers at the end of each line indicate the Julian day of the second year of simulation from which the data were taken.

much longer (up to 170 days vs. 49 days). While leaf lengths were shorter, the shoot density was high and leaves were wide (Figure 4.30h and 4.30c) contributing to a large LAI (up to  $474 \text{ m}^2 \text{ m}^{-2}$  vs.  $5.2 \text{ m}^2 \text{ m}^{-2}$ ). Leaf dimension and density reduced the maximum light available to about  $150 \mu\text{E m}^{-2} \text{s}^{-1}$  (Figure 4.29). The NPP-Population configuration used  $30 \text{ leaves y}^{-1}$ , which along with the high LAI, high PSU density, and high antenna chl (Figure 4.30a and 4.30b), contributed to high NPP on both a plant and areal basis ( $2,768 \text{ mg C y}^{-1}$  and  $34,505 \text{ g C m}^{-2} \text{ y}^{-1}$  vs.  $294 \text{ mg C y}^{-1}$  and  $343 \text{ g C m}^{-2} \text{ y}^{-1}$ ).

Maximizing NPP at the level of a population of plants calls for a strategy of maximizing population production while minimizing population respiration. The plants that comprise this population take many of the controlling parameters to extreme limits (Figure 4.30) suggesting that if a larger range were available, the GA would take advantage of it. Shoot

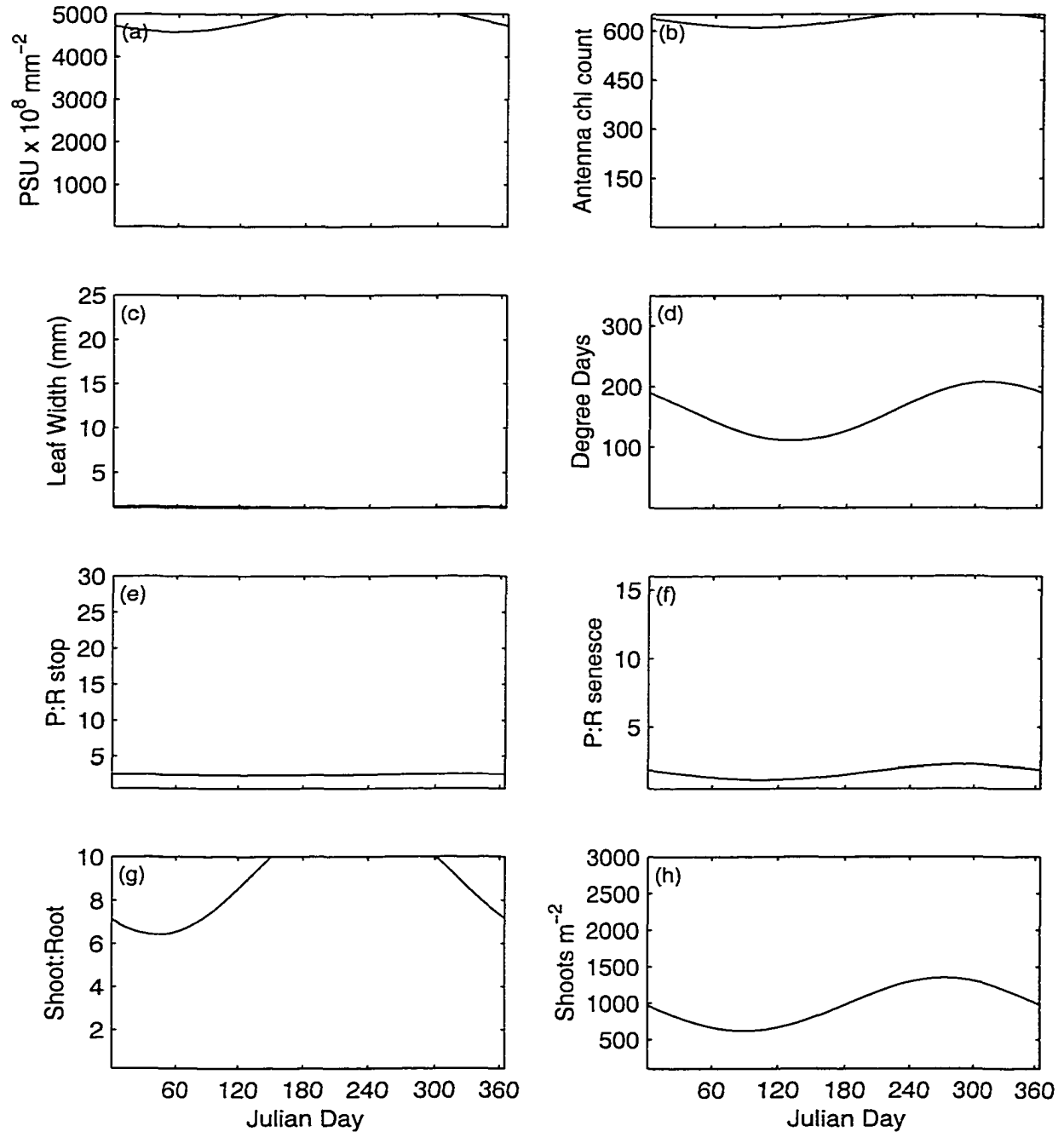


Figure 4.25: NPP-Plant configuration  $\Gamma$  variable plots. Each curve is computed from its  $\Gamma$  variable (Table 2.3) as in Figure 2.3.

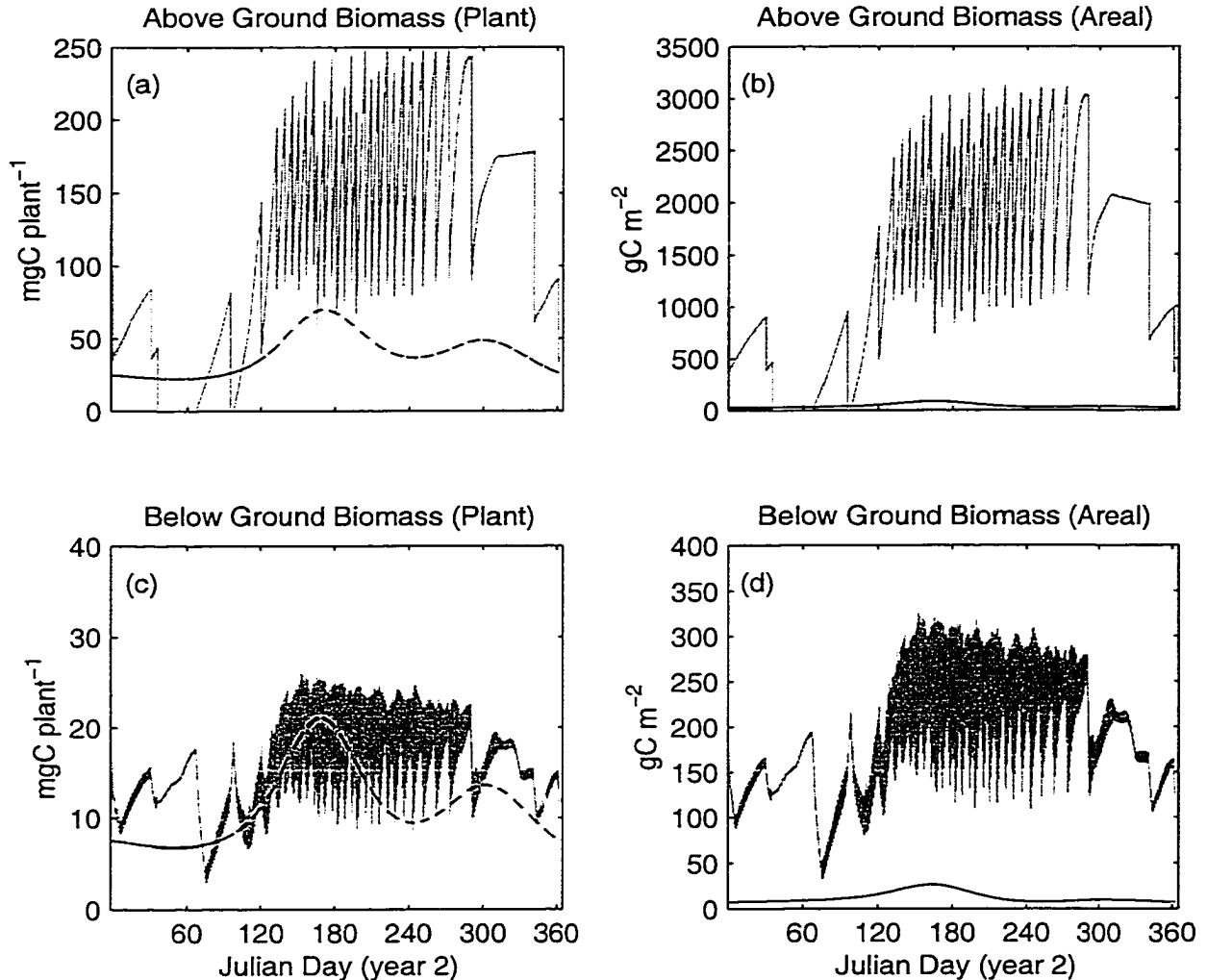


Figure 4.26: Biomass from the NPP-Population configuration compared to BWM99 model biomass. Output from the BWM99 model shown as dashed (smooth) line. Output from the NPP-Population configuration in black/gray (jagged) lines. a) Above-ground and c) below-ground biomass of an individual plant. b) Above-ground and d) below-ground biomass of a square meter of seagrass bed. The Vgrass model simulates individual leaves instead of lumping their biomass into one state variable. The growth and abscission of the individual leaves causes the biomass to fluctuate. Biomass from the single plant is multiplied by shoot density (Moore 1996), and therefore, the areal biomass is subject to the same fluctuations.



Table 4.9: NPP-Population configuration performance metrics. The first six metrics are computed from the second year of the simulation. Metrics with a range of values are reduced to minimum, average, and maximum values. NPP is Net Primary Production. BIO is the peak biomass. NPP and BIO are the average of peak values obtained during years 2 through 5 of the simulation.

Metric	Nominal Configuration			NPP-Population Config.			Units
	Min	Avg	Max	Min	Avg	Max	
First Shoot		70			67		Julian day
Plastichrone	8	13	30	5	9	44	Days
Leaf Length	20	26	33	6	15	18	cm
Leaf Age	20	28	49	36	62	170	Days
LAI		1.6	5.2		174	474	$m^2 m^{-2}$
Leaves		22			30		leaves $y^{-1}$
NPP Plant		294			2,768		$mg C y^{-1}$
NPP Pop.		343			34,505		$g C m^{-2} y^{-1}$
BIO Plant		124			273		$mg C$
BIO Pop.		149			3,412		$g C m^{-2}$

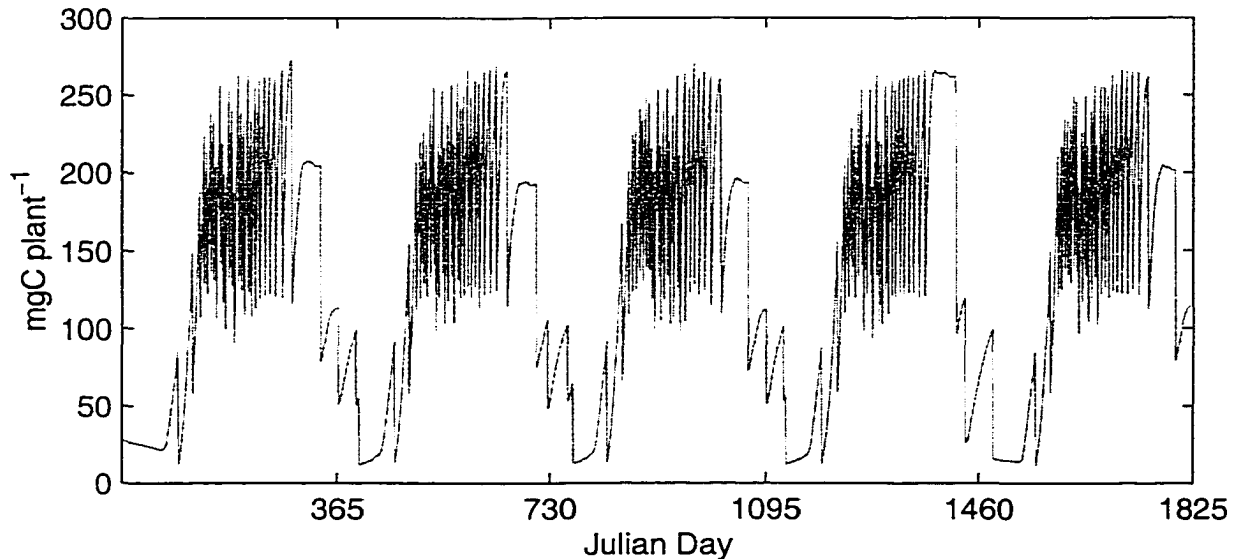


Figure 4.27: Biomass plot of the NPP-Population configuration showing stability over 5 years (i.e. there is no evident trending).

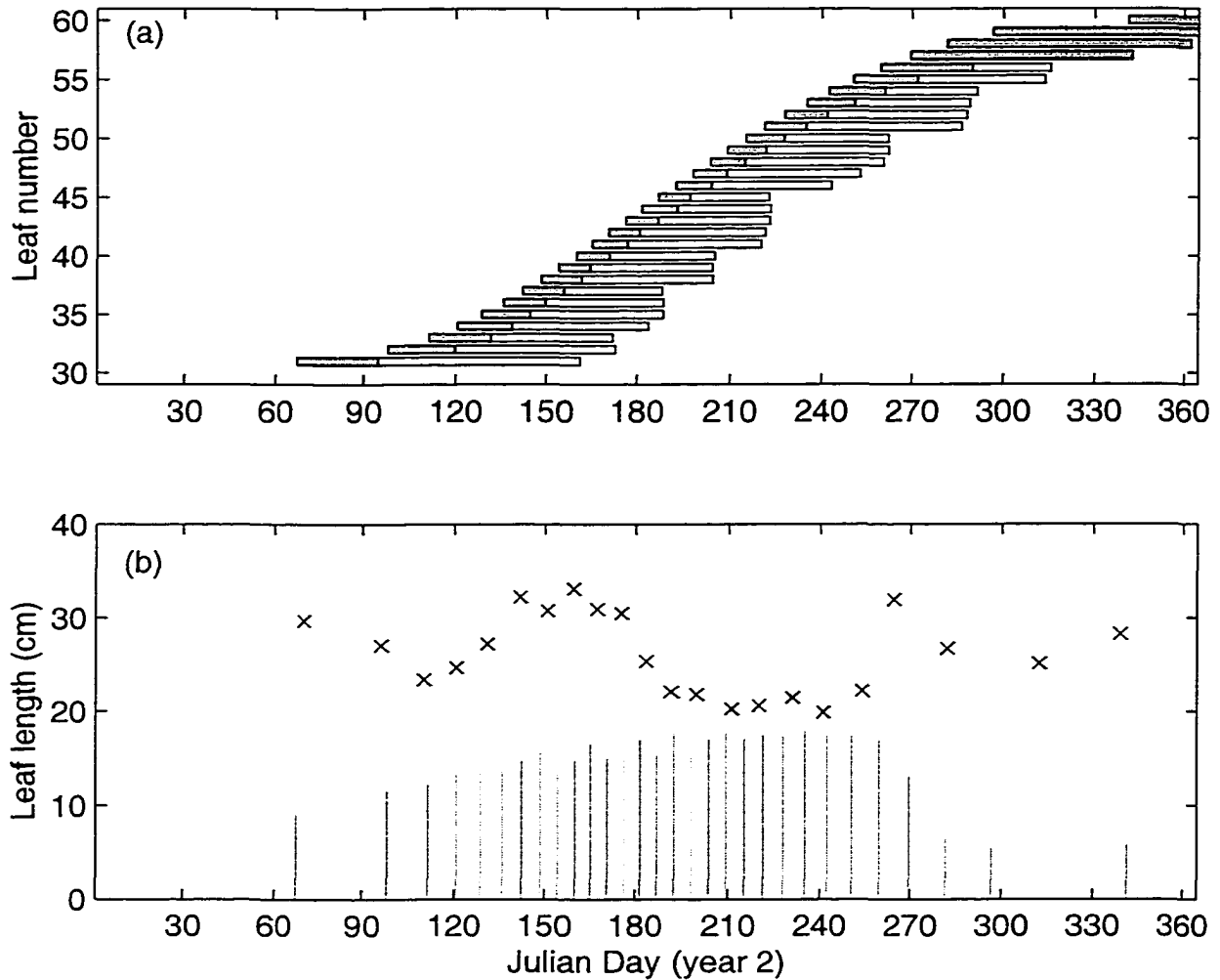


Figure 4.28: NPP-Population configuration leaf growth. a) each bar represents the start date (left edge), growth stage (left shaded area), mature stage (right unshaded area), and abscission (right edge). b) lines indicate the start date (x axis) and the final length (y axis) of the leaf. The x's represent the lengths and timing of leaves from the nominal configuration.

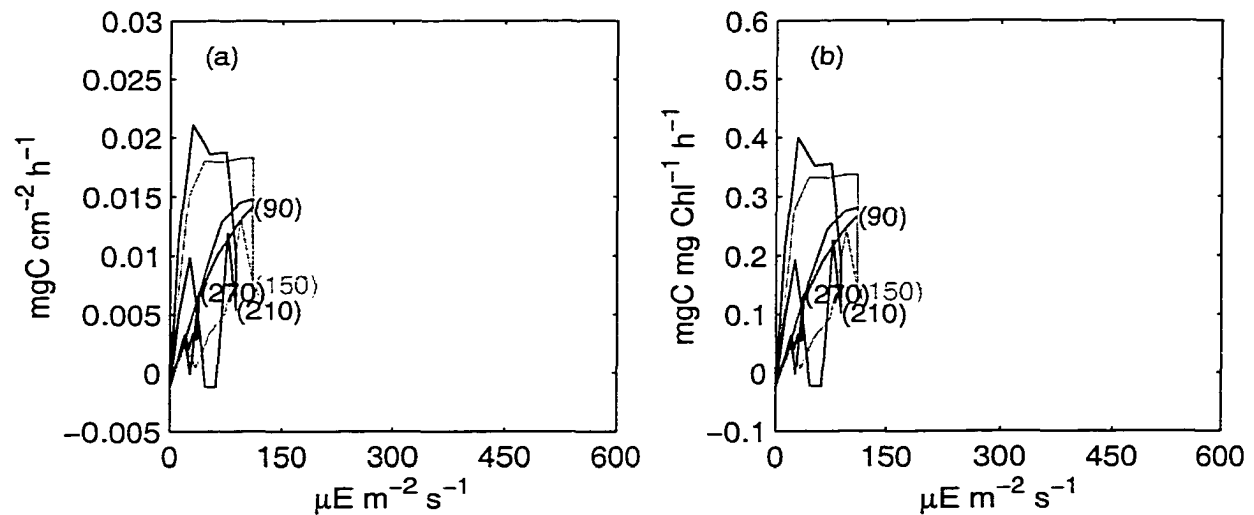


Figure 4.29: NPP-Population configuration whole-plant production vs. irradiance plots based on leaf area (a) and chl (b). Each line represents 24 hrs of data; the hysteresis is due to production differences between morning and afternoon. The numbers at the end of each line indicate the Julian day of the second year of simulation from which the data were taken.

density is in the 10,000 to 12,500 shoots  $\text{m}^{-2}$  range as compared to the nominal case with shoot densities in the 1,100 shoots  $\text{m}^{-2}$  range. Shoot density, leaf width, and degree-days between shoots function to produce many plants with wide leaves. The GA is limited to growing 150 leaves over the entire 5-year simulation run, or 30 leaves  $\text{y}^{-1}$ . This configuration used all 30 leaves suggesting that the GA might choose a configuration capable of growing more leaves if it were possible. P:R stop and P:R abscise work together so that leaves reach maturity at a short length and are abscised as late as possible. P:R abscise never goes below 1 so that leaves are abscised just before their daily respiration exceeds production. Shoot:Root is high to minimize the respiration costs of a large root system.

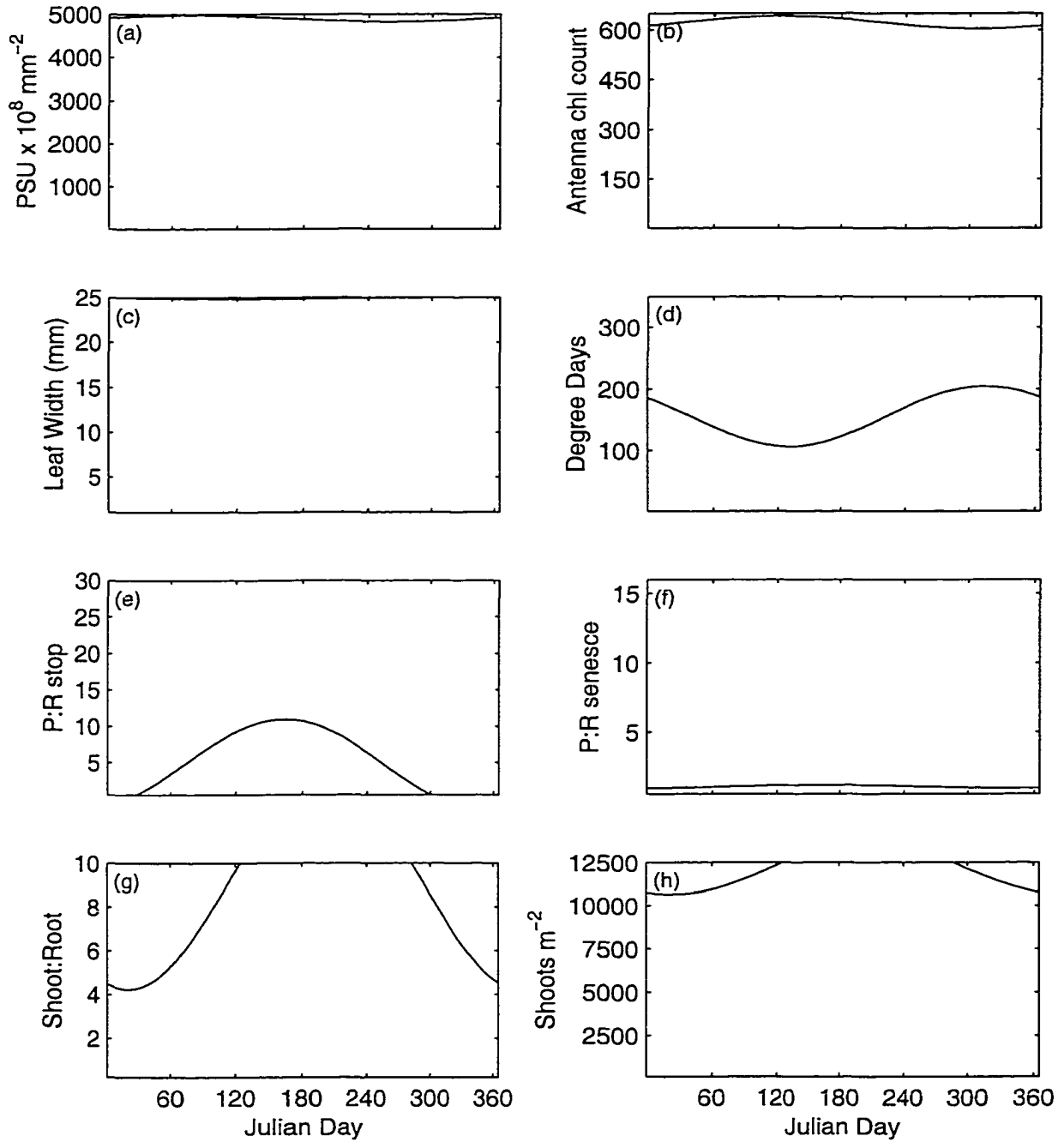


Figure 4.30: NPP-Population configuration  $\Gamma$  variable plots. Each curve is computed from its  $\Gamma$  variable (Table 2.3) as in Figure 2.3.

### 4.5.3 NPP-Plant vs. NPP-Population

In comparing the configuration for NPP-Plant to NPP-Population, there are a few similarities. Both configurations have a high Shoot:Root ratio that reduces the respiration costs of a large root system. An average of 30 leaves  $y^{-1}$  are available (150 leaves over 5 years), NPP-Plant uses 29 and NPP-Population uses 30. Both configurations also have selected high PSU densities and antenna chl counts. Each of these factors reaches the maximum allowed suggesting that larger values would be selected if possible.

Differences between the two configurations show that maximizing NPP at each scale requires a different strategy. Leaves for the NPP-Plant configuration are long (over 1.2 m vs. 15 cm) and thin (1 mm vs. 25 mm) which lowers LAI (maximum of  $125 \text{ m}^2 \text{ m}^{-2}$  vs. up to  $474 \text{ m}^2 \text{ m}^{-2}$ ) and increases the amount of light available at the leaf's surface (maximum of  $300 \mu\text{E m}^{-2} \text{ s}^{-1}$  vs.  $150 \mu\text{E m}^{-2} \text{ s}^{-1}$ ).

The NPP-Plant configuration has higher NPP on a per plant basis than does the NPP-Population configuration ( $8,142 \text{ mg C y}^{-1}$  vs.  $2,768 \text{ mg C y}^{-1}$ ). The NPP-Plant configuration has fewer but more productive plants. Meanwhile, the NPP-Population areal NPP is much higher than that of the NPP-Plant configuration ( $34,505 \text{ g C m}^{-2} \text{ y}^{-1}$  vs.  $8,810 \text{ g C m}^{-2} \text{ y}^{-1}$ ). The NPP-Population configuration has more plants but the plants are less productive. These relationships are in line with the goal of each test: NPP-Plant was to maximize NPP for the plant while NPP-Population was to maximize NPP on an areal scale. But since it has been shown in previous tests that carbon is not conserved when scaling up to the population, further comparison may not be meaningful.

## 4.6 Optimization Goal:

### Maximization of Longevity

#### 4.6.1 Strategy Seven: LONG-Population

The goal of long term survival requires that a plant survive for 20 years of simulation time. The fitness function for this goal returned the total number of days that the plant was able to survive.

As with the other searches, a population of 450 individuals was run through 200 generations. Of the 90,000 configurations, 88,479 were able to run the entire 20 years. Since so many configurations were able to reach the goal, culling one of them for analysis was difficult since there was no way to select the best one. Instead histograms were made to indicate traits that were selected by many of the configurations. Plots within Figures 4.31 to 4.38 are histograms of each of the 25 controlling parameters.

The histograms are provided to show the range of values that lead to successful configurations. What cannot be shown with the histograms are the combinatorial effects. For example, PSU density average has two relatively high peaks near  $2,500 \times 10^8$  PSU  $\text{mm}^{-2}$  and  $3,500 \times 10^8$  PSU  $\text{mm}^{-2}$  while PSU density amplitude has peaks at 250 chl PSU $^{-1}$  and 350 chl PSU $^{-1}$ . Other parameters also have peaks that are nearly equal. What cannot be shown here is which PSU density average peak works best with either of the two PSU density amplitude peaks. If it were a simple matter of two parameters, fitness testing could be used to make comparisons of the combinations. Since there are 25 parameters, testing is beyond the scope of this study.

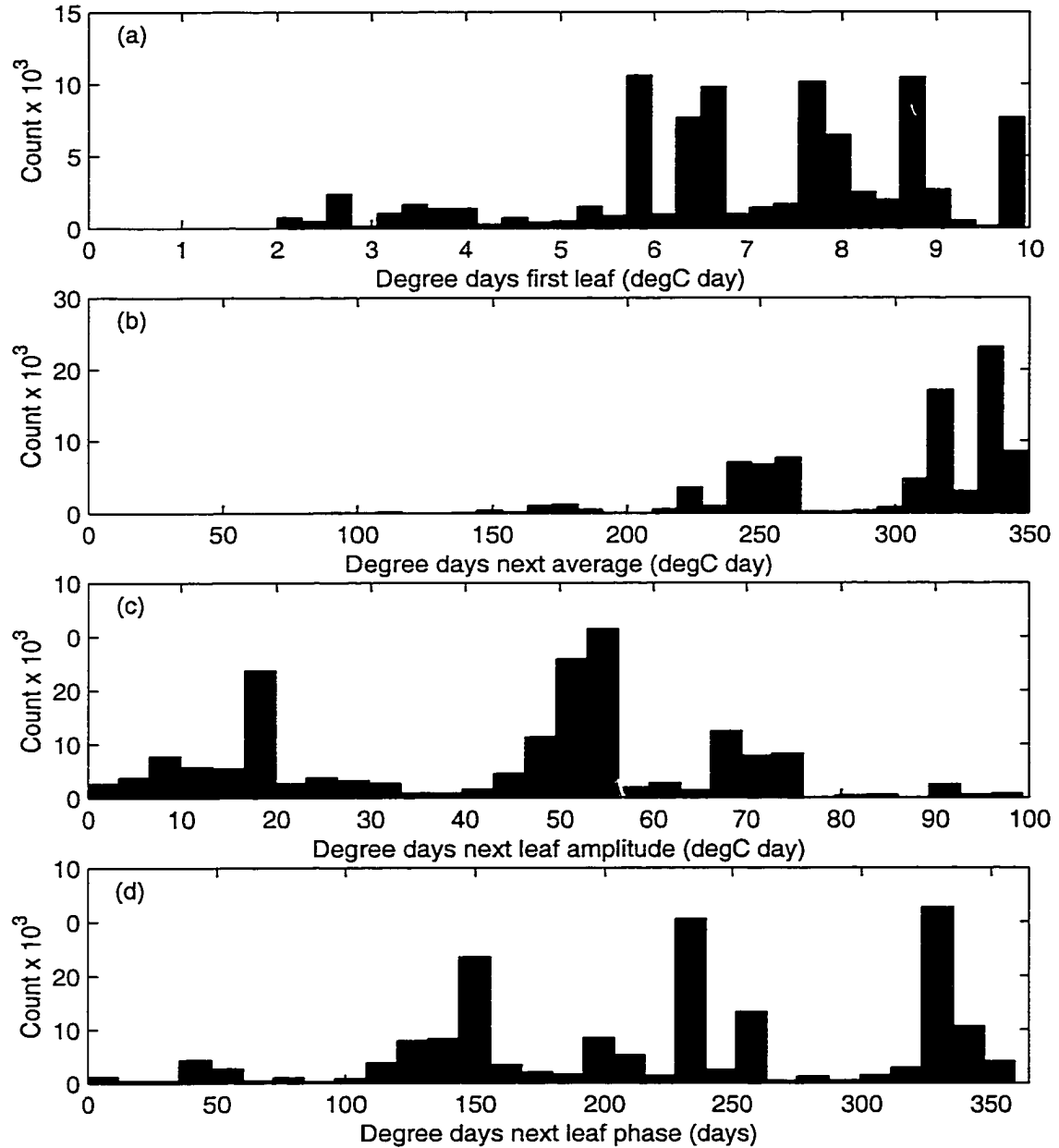


Figure 4.31: Histogram of degree days to first leaf selection counts (a), and degree days to next leaf selection counts for average (b), amplitude (c), and phase (d). The range of values along the X-axis coincide with the selection range available to the GA during the search.

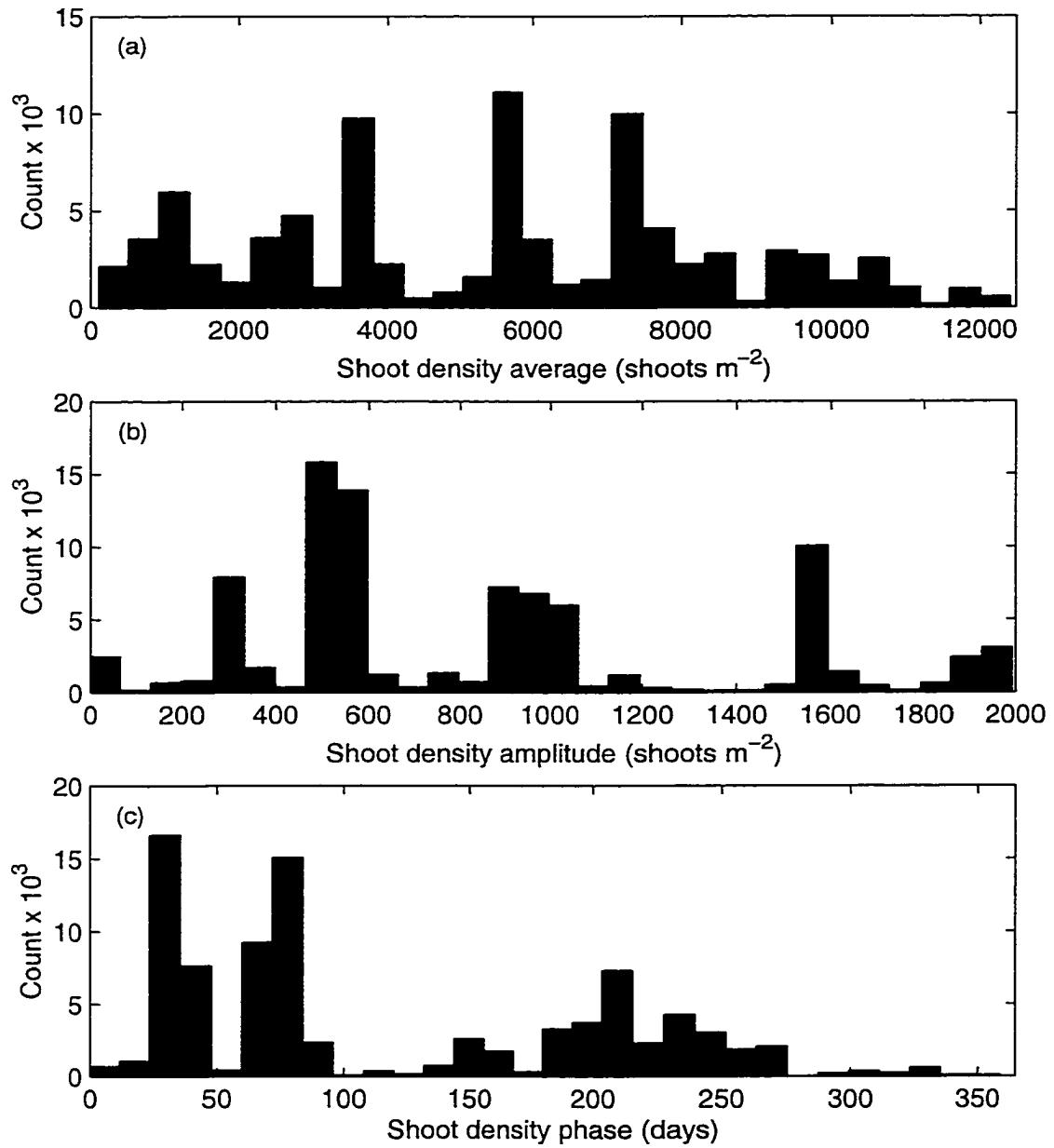


Figure 4.32: Histograms of Shoot density selection counts for average (a), amplitude (b), and phase (c). The count (y-axis) indicates the number of individuals found with the range indicated by the x-axis. The range of values along the x-axis coincide with the selection range available to the GA during the search.



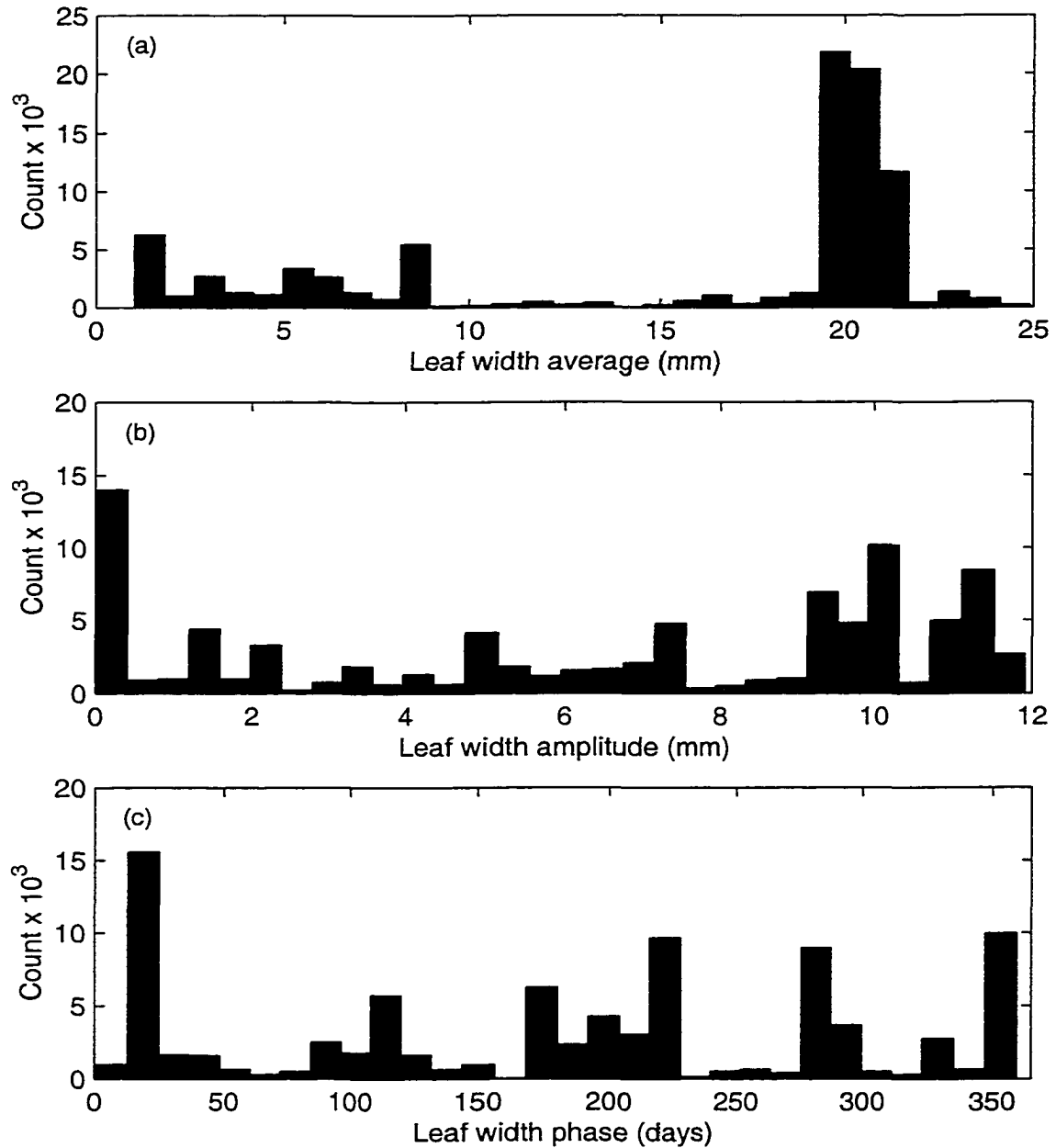


Figure 4.33: Histograms of Leaf width selection counts for average (a), amplitude (b), and phase (c). The count (y-axis) indicates the number of individuals found with the range indicated by the x-axis. The range of values along the x-axis coincide with the selection range available to the GA during the search.

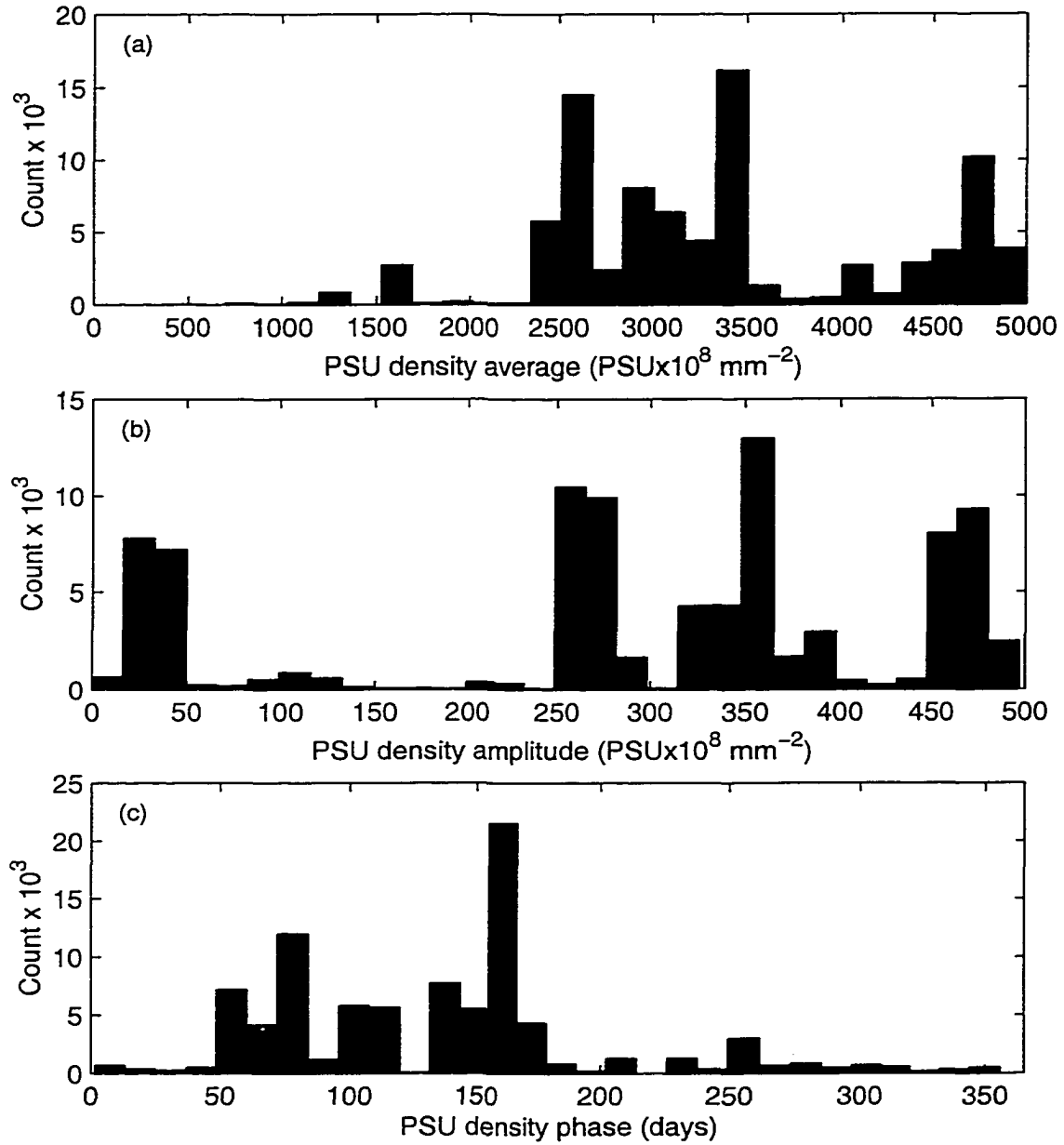


Figure 4.34: Histograms of PSU Density selection counts for average (a), amplitude (b), and phase (c). The count (y-axis) indicates the number of individuals found with the range indicated by the x-axis. The range of values along the x-axis coincide with the selection range available to the GA during the search.

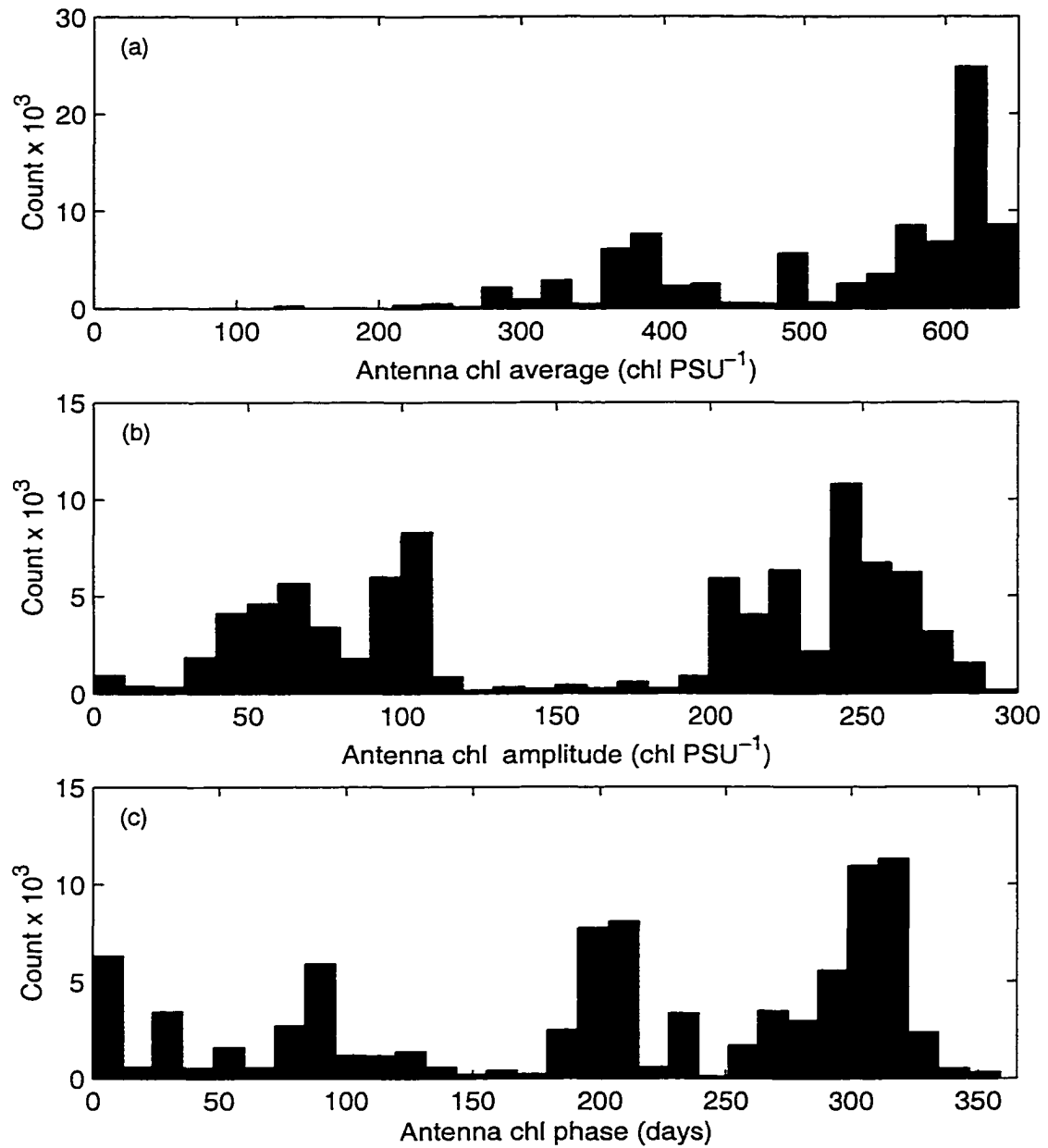


Figure 4.35: Histograms of PSU antenna chl selection counts for average (a), amplitude (b), and phase (c). The count (y-axis) indicates the number of individuals found with the range indicated by the x-axis. The range of values along the x-axis coincide with the selection range available to the GA during the search.

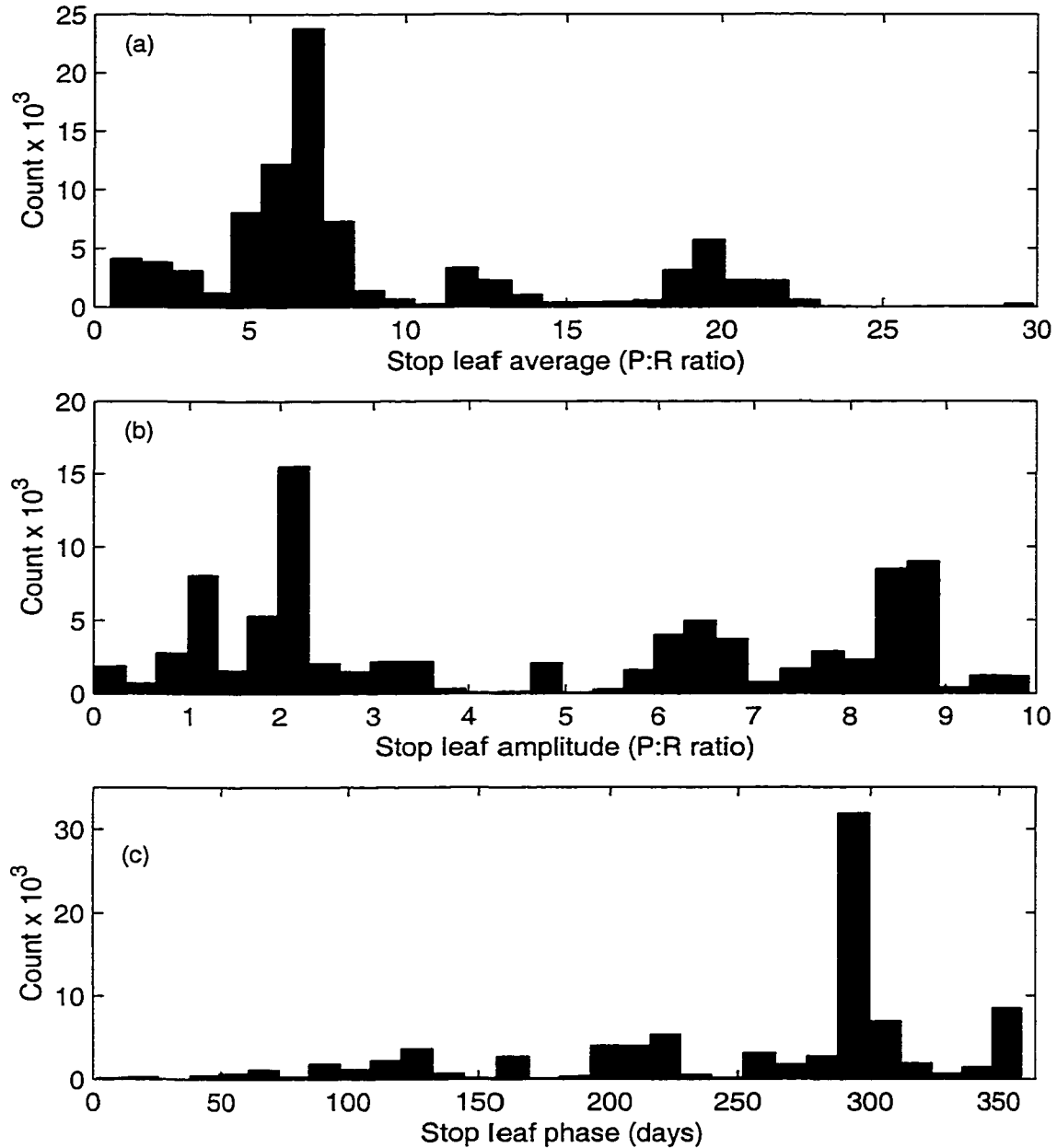


Figure 4.36: Histograms of stop leaf P:R ratio selection counts for average (a), amplitude (b), and phase (c). The count (y-axis) indicates the number of individuals found with the range indicated by the x-axis. The range of values along the x-axis coincide with the selection range available to the GA during the search.

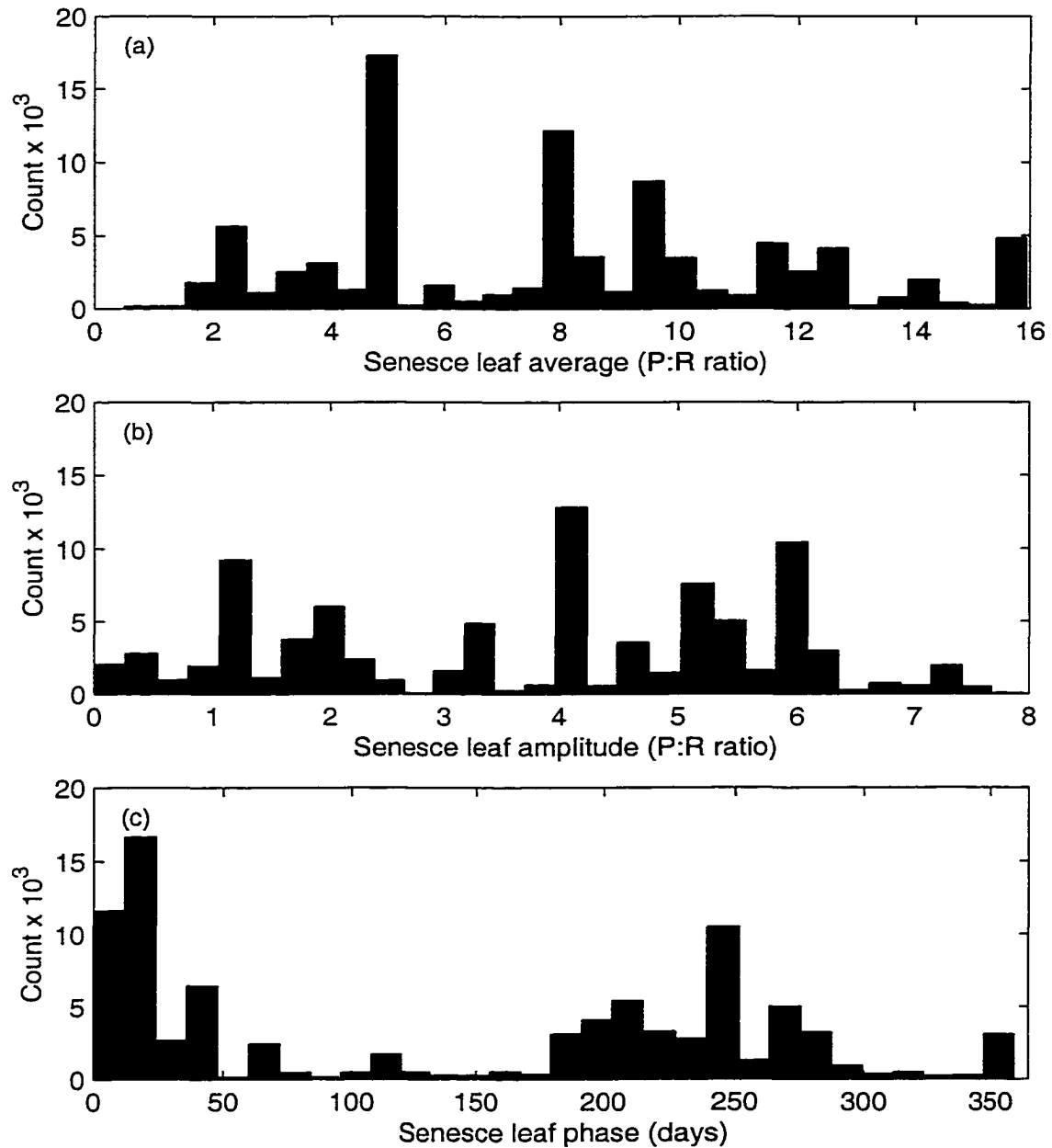


Figure 4.37: Histograms of Abscise leaf P:R ratio selection counts for average (a), amplitude (b), and phase (c). The count (y-axis) indicates the number of individuals found with the range indicated by the x-axis. The range of values along the x-axis coincide with the selection range available to the GA during the search.

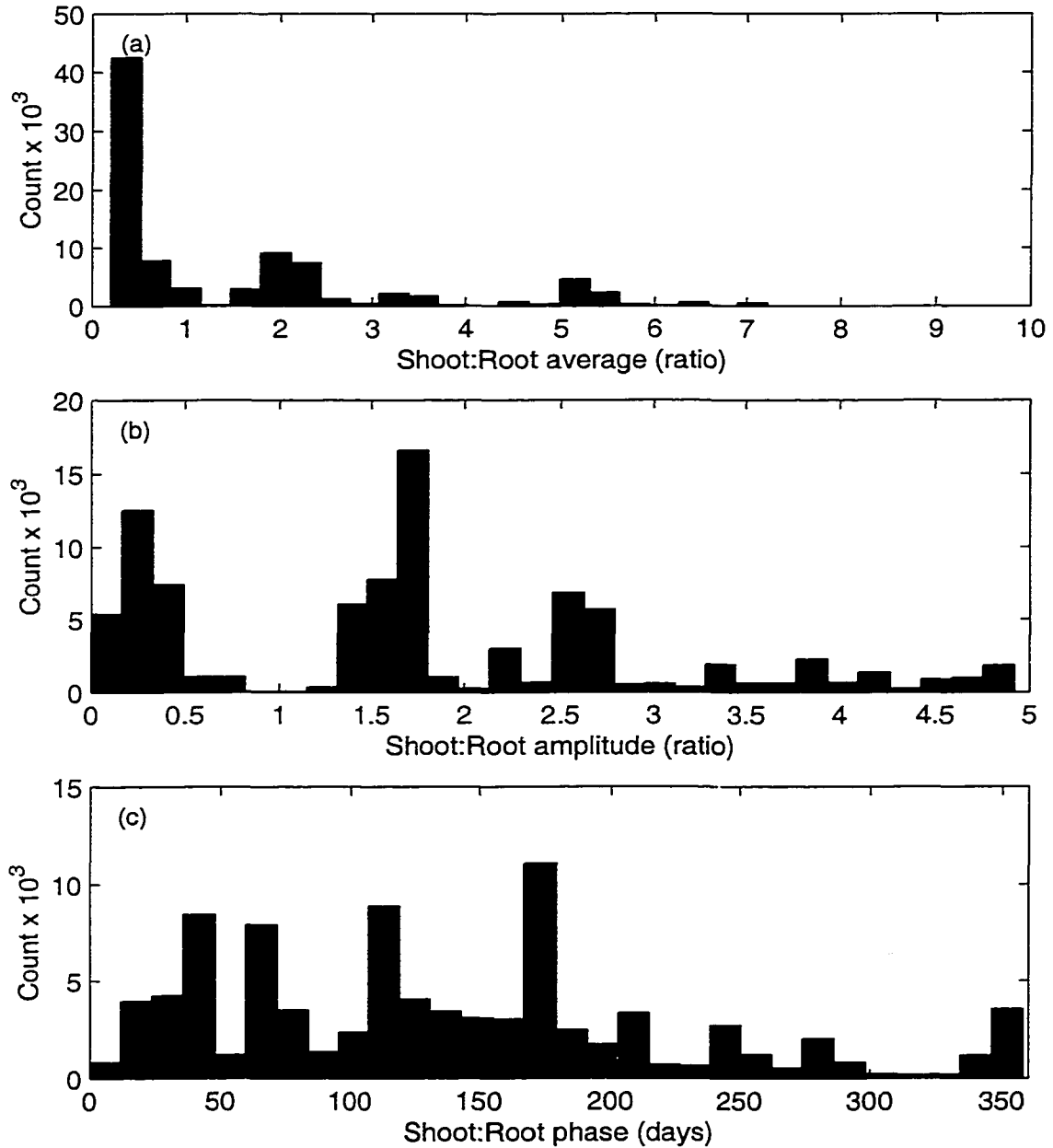


Figure 4.38: Histograms of shoot to root ratio selection counts for average (a), amplitude (b), and phase (c). The count (y-axis) indicates the number of individuals found with the range indicated by the x-axis. The range of values along the x-axis coincide with the selection range available to the GA during the search.

For analysis, the value of the abscissa at the highest peak was chosen from each of the 25 histograms Table 4.10. The 25 values were grouped into a chromosome evaluated in the same manner as the *most fit* individuals from other tests.

Long term survival was only run at the population scale. Running the test at the scale of plant was not done because each of the optimal plant configurations was able to run for 20 years. Also, since parameters were chosen from the histograms, and there are combinatorial complications, the resulting configuration may not represent the most fit individual. In fact, there is no *most fit* individual for the LONG test; it is possible that a large group of configurations could persist for an indefinite period of simulated time.

Above ground biomass (Figure 4.39a) for the LONG configuration is similar to that of the nominal configuration while below ground biomass is about twice as high (Figure 4.39c). Shoot density differences lead to much higher areal biomass for both above and below ground (Figure 4.39b and 4.39d) and the 5 year plot (Figure 4.40) shows that biomass is stable over a 5 year run.

The first leaf emerges on Julian day 70 for both the LONG and the nominal configurations but the plastichrone interval, on average, is shorter for the nominal case (20 days vs. 13 days, Table 4.11). Leaf length for the LONG configuration is shorter (up to 19 cm vs. up to 33 cm) but the leaves are wider (19.7 mm vs. 5.0 mm, Figure 4.10). Leaf area combined with higher shoot density also leads to a higher LAI (up to  $83 \text{ m}^2 \text{ m}^{-2}$  vs. up to  $5.2 \text{ m}^2 \text{ m}^{-2}$ ) even though fewer leaves are grown (14 leaves vs. 22 leaves). While LAI is much higher, light availability is similar to the nominal case (up to ca.  $400 \mu\text{E m}^{-2} \text{ s}^{-1}$  Figure 4.42).

Table 4.10: Controlling parameters for the LONG configuration. Parameter values are chosen from the highest peak of each histogram (Figures 4.31 to 4.38)

Parameter	Nominal	LONG	Units
Degree-days first leaf	6	6	°C Day
Degree-days next average	150	335	°C Day
Degree-days next amplitude	65	55	°C Day
Degree-days next phase	240	329	Days
Shoot density average	1075	5651	Shoots m <sup>-2</sup>
Shoot density amplitude	360	498	Shoots m <sup>-2</sup>
Shoot density phase	250	30	Days
Leaf width average	5.0	19.7	mm
Leaf width amplitude	0.1	0.2	mm
Leaf width phase	180	19	Days
PSU density average	750	3422	10 <sup>8</sup> PSU mm <sup>-2</sup>
PSU density amplitude	200	356	10 <sup>8</sup> PSU mm <sup>-2</sup>
PSU density phase	60	161	Days
PSU antenna average	450	617	Chl PSU <sup>-1</sup>
PSU antenna amplitude	20	244	Chl PSU <sup>-1</sup>
PSU antenna phase	360	317	Days
Stop leaf P:R average	3.0	6.9	Ratio
Stop leaf P:R amplitude	5.0	2.1	Ratio
Stop leaf P:R phase	180	294	Days
Abscise leaf P:R average	9.0	4.9	Ratio
Abscise leaf P:R amplitude	4.0	4.1	Ratio
Abscise leaf P:R phase	300	18	Days
Shoot:Root average	4.0	0.4	Ratio
Shoot:Root amplitude	0.3	1.7	Ratio
Shoot:Root phase	50	173	Days



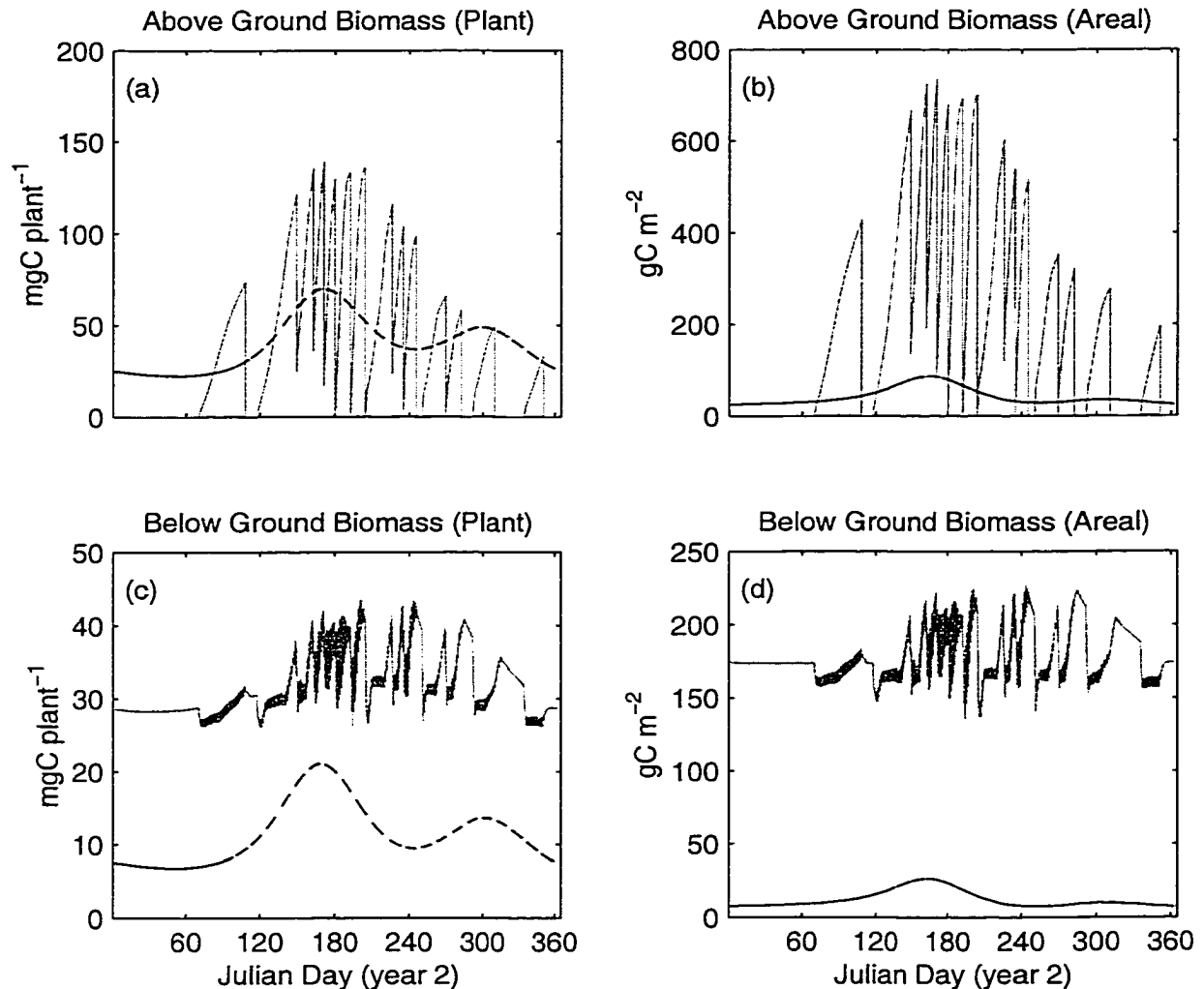


Figure 4.39: Biomass from the LONG configuration compared to BWM99 model biomass. Output from the BWM99 model shown as dashed (smooth) line. Output from the LONG configuration in black/gray (jagged) lines. a) Above-ground and c) below-ground biomass of an individual plant. b) Above-ground and d) below-ground biomass of a square meter of seagrass bed. The Vgrass model simulates individual leaves instead of lumping their biomass into one state variable. The growth and abscission of the individual leaves causes the biomass to fluctuate. Biomass from the single plant is multiplied by shoot density (Moore 1996), and therefore, the areal biomass is subject to the same fluctuations.

Table 4.11: LONG configuration performance metrics. The first six metrics are computed from the second year of the simulation. Metrics with a range of values are reduced to minimum, average, and maximum values. NPP is Net Primary Production. BIO is the peak biomass. NPP and BIO are the average of peak values obtained during years 2 through 5 of the simulation.

Metric	Nominal Configuration			LONG Configuration			Units
	Min	Avg	Max	Min	Avg	Max	
First Shoot		70			70		Julian day
Plastichrone	8	13	30	12	20	47	Days
Leaf Length	20	26	33	5	13	19	cm
Leaf Age	20	28	49	13	33	73	Days
LAI		1.6	5.2		19	83	$\text{m}^2 \text{m}^{-2}$
Leaves		22			14		leaves $\text{y}^{-1}$
NPP Plant		294			771		$\text{mg C y}^{-1}$
NPP Pop.		343			4,076		$\text{g C m}^{-2} \text{y}^{-1}$
BIO Plant		124			180		$\text{mg C}$
BIO Pop.		149			945		$\text{g C m}^{-2}$

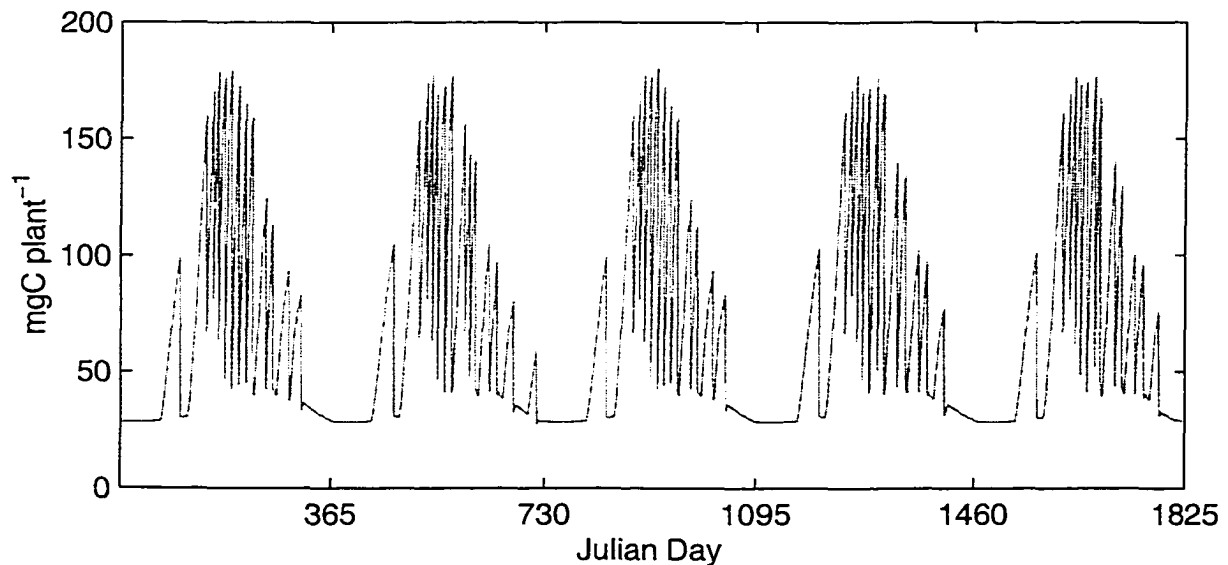


Figure 4.40: Biomass plot of the LONG configuration showing stability over 5 years (i.e. there is no evident trending).

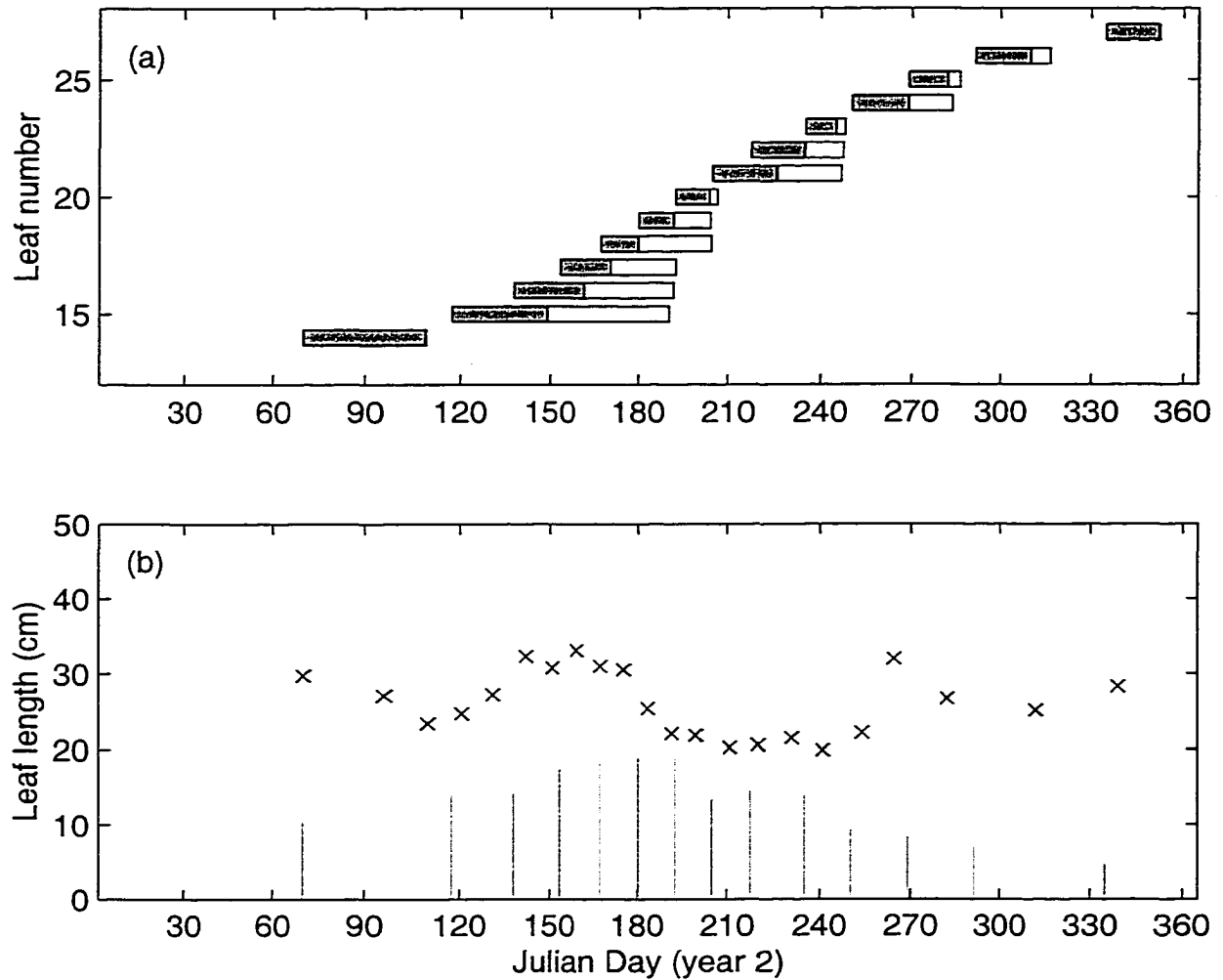


Figure 4.41: LONG configuration leaf growth. a) each bar represents the start date (left edge), growth stage (left shaded area), mature stage (right unshaded area), and abscission (right edge). b) lines indicate the start date (x axis) and the final length (y axis) of the leaf. The x's represent the lengths and timing of leaves from the nominal configuration.

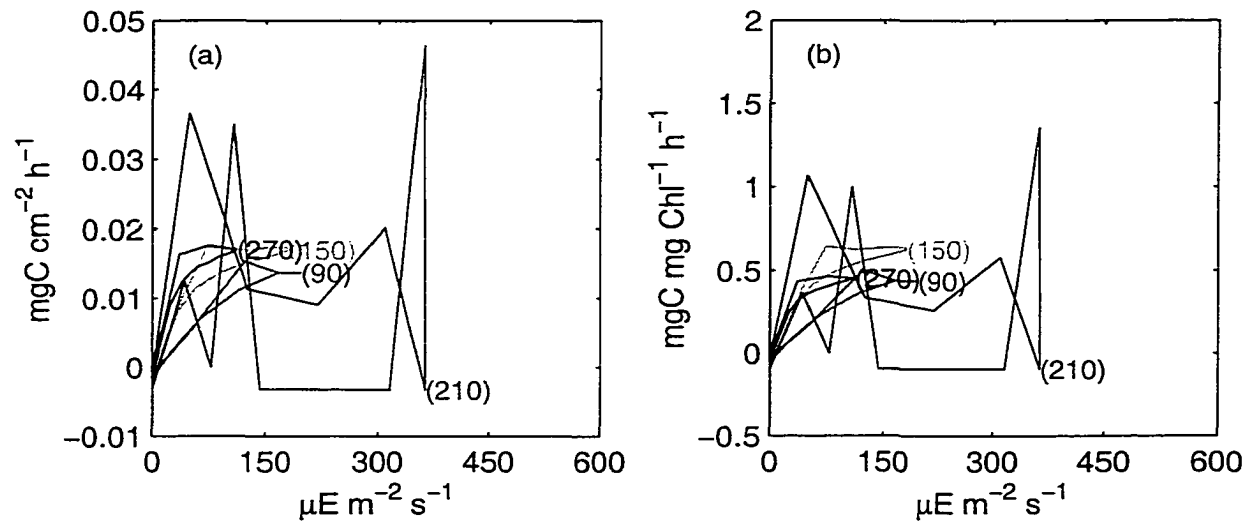


Figure 4.42: LONG configuration whole-plant production vs. irradiance plots based on leaf area (a) and chl (b). Each line represents 24 hrs of data; the hysteresis is due to production differences between morning and afternoon. The numbers at the end of each line indicate the Julian day of the second year of simulation from which the data were taken.

Higher PSU densities (over  $3,000 \times 10^8 \text{ PSU mm}^{-2}$  vs.  $1,000 \times 10^8 \text{ PSU mm}^{-2}$ ) antenna chl counts (over 600 vs. 450), and increased LAI, work together to produce much higher NPP values ( $771 \text{ mg C y}^{-1}$  vs.  $294 \text{ mg C y}^{-1}$  plant,  $4076 \text{ g C m}^{-2} \text{ y}^{-1}$  vs.  $343 \text{ g C m}^{-2} \text{ y}^{-1}$  areal) and higher peak biomass values ( $180 \text{ mg C}$  vs.  $124 \text{ mg C}$  plant,  $945 \text{ g C m}^{-2}$  vs.  $149 \text{ g C m}^{-2}$ ).

For each of the previous strategies the controlling parameter function plots (Figure 4.43) were evaluated with respect the fitness function. Since many configurations lead to a plant capable of surviving 20 years, evaluation is impossible. This indicates a stability with respect to the structure of the mathematical model and indicates that perhaps more constraints are needed within the model. More constraints within the model might limit the range of parameter selection and perhaps better reveal a long term survival strategy.

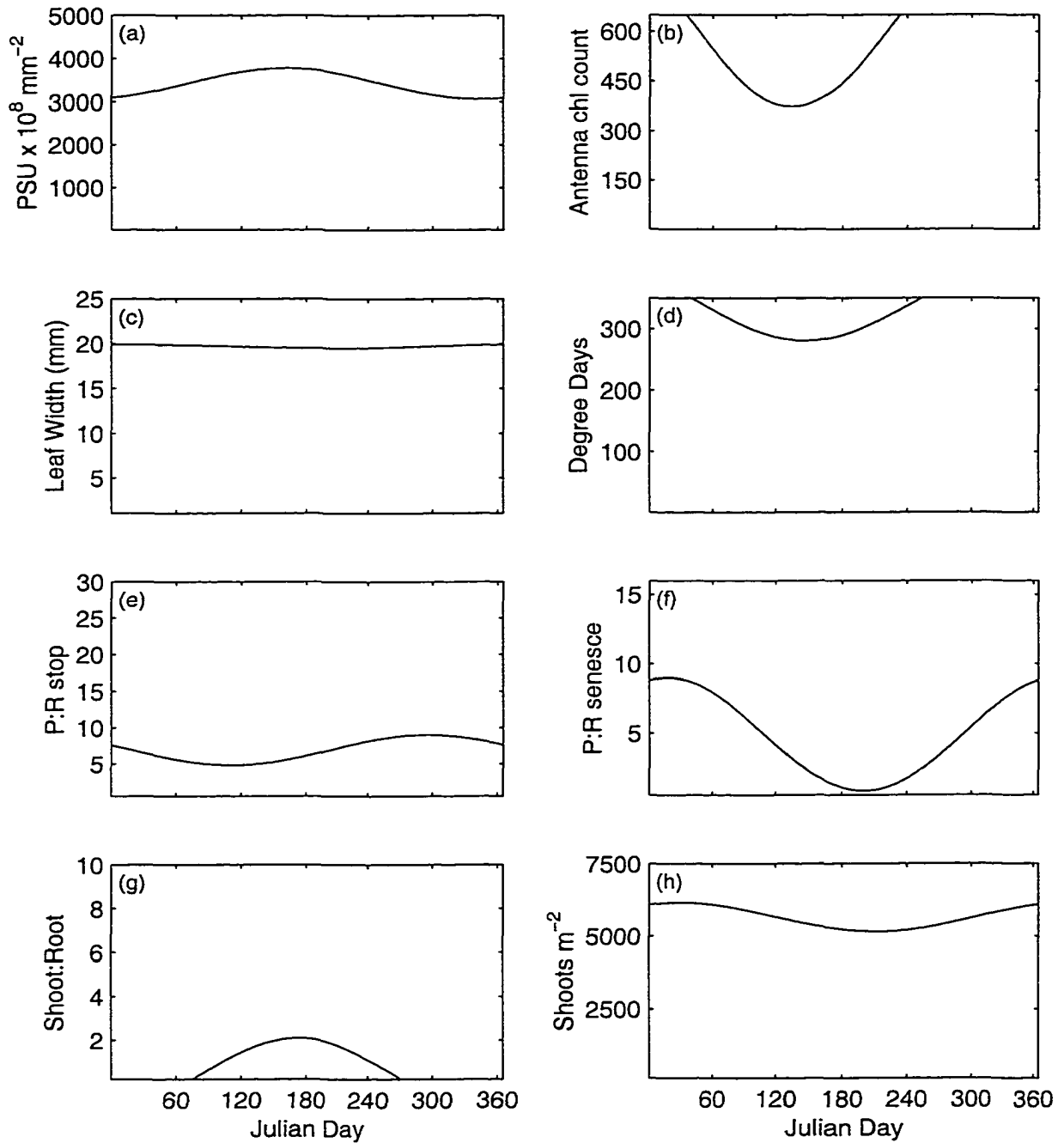


Figure 4.43: LONG configuration  $\Gamma$  variable plots. Each curve is computed from its  $\Gamma$  variable (Table 2.3) as in Figure 2.3.

## 4.7 Discussion

The objective for this study was to build and demonstrate a computational framework capable of testing plant growth strategies. The framework included a simulation model of the eelgrass (*Zostera marina*), Vgrass, combined with a GA. The GA searched for combinations of Vgrass' controlling parameters required for Vgrass to fulfill one of several growth strategies. The resulting parameter configurations lead to Vgrass biomass and leaf growth patterns that illustrated how a plant might grow if it were following one of the growth strategies. All of the results were compared to a nominal run of the Vgrass model.

This study did not have the goal of explaining the underlying mechanisms required to fulfill a growth strategy. Instead, this study searched for patterns of plant growth that should emerge if a mechanism were in place to drive the strategy.

### 4.7.1 The strategies

Three *maximizing* growth strategies were tested at the plant and population scales along with the *non-maximizing* strategy of longevity. While the goal of longevity might be considered as testing for plant persistence, it is considered differently from the maximization goals. The three maximal strategies work at optimizing plant growth over a few seasons. Longevity simply looked for parameter configurations that allowed the plant to merely persist for 20 years of simulated growth.

The three optimal strategies were maximization of relative growth rate, maximization of biomass and maximization of net primary production. All three of the optimal tests produced plants that were not biologically realistic; none of them produced plant growth

behaviors similar to the nominal run. The plant model did not consider allocation to reproduction which might change some of the allocation behaviors. That the results were not biologically realistic, suggests that plant growth is not driven by any of the growth strategies that maximize a growth function.

Givnish (1983a) suggests that experiments searching for growth strategies should all be compared to maximized biomass. Results from this study clearly show that maximizing biomass is not an appropriate benchmark. When biomass is maximized, there is no notion of *economy* in the plants growth. In pursuit of maximized biomass, leaves are grown and remain attached even though their P:R ratios are less than one. *Why would a plant grow a leaf that becomes a sink for massive amounts of carbon and then abscise it?* Maximizing biomass would have short-term benefit; quickly growing many leaves would exclude possible competitors for space and light. But once the biomass is attained, and the competitors have been excluded, there is no long-term advantage to keeping leaves that ultimately become large carbon sinks.

In the case of maximizing biomass at the population scale, seasonal change in shoot density was selected by the GA. Figure 4.20 shows that the GA selected to increase shoot density after the typical growing season. Recall that the increase in biomass is purely mathematical; existing plants did not contribute carbon to the increase in shoot density. Meanwhile the GA did not control seasonal shoot density for the BIO-Plant test. In the BIO-Plant test the GA chose a configuration of controlling parameters that quickly built many leaves, and used the highly productive part of the season to amass a large below-ground reserve (Figures 4.11 and 4.13). Later in the year the below ground reserves were

used so that total plant biomass continued to increase (Figure 4.12). This is interesting in the sense that the GA chose a strategy where total plant biomass was able to increase, while shoot density (self shading) was increasing, some early leaves were operating as carbon sinks, and light availability was decreasing (Equation 2.1). This illustrates the ability of the GA to coordinate a rather complex set of variables in order to achieve the goal. This may have application in considering forestry tables (Harper, 1977) for thinning and optimizing wood harvest. The GA has been applied in a similar study to consider space allocation in nurseries (Annevelink and Broekmeulen, 1995).

While the tests for maximizing biomass did not include respiration costs, the test for maximizing net primary production did. Maximizing NPP involved integrating NPP through each simulation year and then maximizing this number. In essence, production was maximized while respiration was minimized. But even with this trade-off in place, the resulting plant is not biologically realistic. Leaf emergence patterns in Figures 4.23 and 4.28 (ignoring leaf size) are similar to those of the nominal model in that leaf initiation is spread out over the entire year. The leaves also have a mature/non-growth period before abscission and a new leaf emerges while others are still growing or mature; there is overlap. In an ecological context, this shows that in order to achieve higher values of NPP, leaves should emerge, grow, and abscise in a continuous cycle. Given that production and respiration are both included in this emergent pattern, it suggests that an economic strategy is at play. This pattern of leaf growth for *Zostera marina* may represent a dynamic optimal allocation strategy. This strategy is consistent with Kikuzawa (1995) where the turn over of leaves is shown to be an optimizing strategy for carbon gain in a light limited environment.



Results from the test for maximizing relative growth rate are directly related to formulation of the fitness function. RGR for the plant is measured at two week intervals and then later summed for the entire year. Leaf emergence and abscission follow a 2 week cycle (Figure 4.3). Chapter 3 showed examples of the GA taking advantage of model construction; here the GA took advantage of the fitness function. This is not a flaw in the GA, it is a direct outcome of the fitness function. If a different fitness function were used to measure RGR, the solution would have been different.

In testing for longevity, 98% of the 90,000 configurations were able to complete 20 years of simulated growth. This reveals the stability of the Vgrass model but did nothing to strain the capabilities of the GA. All of the resulting configurations were combined to generate a representative configuration based on highly selected parameter values. The resulting biomass patterns (Figure 4.39) and plant growth patterns (Figure 4.41) are significant in the sense that they follow, in general ways, both modeled and observed behaviors.

#### 4.7.2 Another look at allocation

Thornley (1998) classifies allocation models into three categories, a) empirical, using a constant or variable allocation parameter; b) teleonomic, or goal oriented; c) mechanistic, showing a relationship between the source, transport, and sink. Two of these three categories generally reflect the time scale at which the study is conducted. Simulation models are typically run at the time scale of years and many use an empirical approach to allocation; allocation theory is not the main purpose for the model. As examples, the seagrass models of Wetzal and Neckles (1984), Verhagen and Nienhus (1986), and Buzzelli et al.

(1996) use an empirical relationship for allocation. If evolutionary stability for a species can be described as a teleological goal, Sakai (1993) shows that allocation to reproductive tissue is optimal. The third category of modeling, mechanistic, has been used at all of the three time scales mentioned earlier (Thornley, 1998). However, a mechanistic model model is based on processes that occur on a short time scale.

Models to explain possible mechanisms for allocation have been tested. Thornley (1976) derives several steady-state allocation models based on tomato plants. Allocation is determined by concentration differences between plant parts and is sufficient to mimic observed plant behaviors. In a summary of shoot:root allocation models, Wilson (1988) compares four models including a complex model that invokes phytohormone control. The more sophisticated models do not perform any better at explaining allocation than does Thornley's simple model. These modeling approaches suggest that, regardless of time scale, the underlying mechanism(s) for allocation are relatively simple.

Others have complicated biomass allocation theory by including nutrients and storage. While biomass can be used to determine how energy, or biomass, is allocated (Hickman and Pitelka, 1975), it probably cannot be used to represent how nutrients are allocated (Abrahamson and Caswell, 1982). Abrahamson and Caswell (1982) do suggest, however, that biomass may be a reasonable currency to measure allocation patterns because it may reflect an integration of all the individual mineral allocations. They also note that considering only biomass negates any consideration of what or if any nutrient is limiting growth. A plant will allocate resources to tissue growth to enhance uptake of a limiting nutrient or water (Chapin et al, 1987). This complicates the notion of optimal allocation since al-

locating more biomass for nutrient collection involves two optimal strategies: optimization of biomass allocation vs. optimal collection or retention of nutrients. Ryser (1996) points out that tissue structure prevents simultaneous optimization of both nutrient acquisition and nutrient conservation. Fast growing, low density tissue has the short-term advantage of rapid nutrient uptake or large surface area for light harvesting, but has a shorter life span. In low nutrient environments, slower growing, high density tissue has the long-term advantage of nutrient conservation, and longer organ life span. Therefore, a plant cannot maximize both growth rate and nutrient conservation. Maximizing growth rate would imply using all available energy resources for growth and not storing energy for periods when resource supply is diminished. Maximizing conservation would imply limiting growth during high nutrient availability so as to provide a reserve for growth during low nutrient periods. *Can these arguments be unified and simplified?*

To summarize, various studies (outlined earlier) have shown through theory and mathematical models that allocation is optimized at various scales from stomatal conductance, to canopy structure, to evolutionary stability. Meanwhile, plant allocation has also been cast in economic terms (Chapin et al. 1990; Bloom et al. 1985; Chapin et al. 1987). The complications appear to arise at the short-term time scales where it is difficult to discern the importance of seemingly competing strategies. *But these do not have to be at odds with each other.*

Weible (2000) provides an interesting study in symmorphosis, the optimal allocation of resources based on the cost and benefit of different allocation options. In this book, animal physiology is shown to follow optimal strategies from the scale of the muscle cell to

the lungs of various mammals. The author is able to show that at each scale there was a cost-benefit function in the design. For instance, increasing hematocrit (the percentage by volume of red blood cells in a given sample of blood) increases blood viscosity and likewise the amount of energy that must be expended to pump the blood. At the same time, when hematocrit increases, the rate of blood flow can decrease since the blood is carrying a richer supply of oxygen to the tissues. This would in effect lower the amount of energy required for pumping blood. There is a balance where the cost of increasing viscosity equals the cost of decreased blood flow. Mammal design is very close to this point. Dogs are shown to have a higher hematocrit percentage; they trade the cost of viscosity to attain higher performance. Goats, which are sedentary, have a lower hematocrit percentage.

The point of including mammal design in this progression is to take advantage of the design differences in dogs and goats. Their design is not quite optimal at one scale in order to have advantages at another. It seems logical that plants would share similar traits. For example, the PI curve demonstrates that plant design is not optimal at all scales. In chapter 3 it was shown that a cost differential was needed in order for the GA to select realistic photosynthetic parameters. Without the cost differential in chl allocation, plants would not have the typical PI curve. There would be no saturation. *Why build apparatus that saturates? If there is no difference in cost, it is an expense that carries no benefit.* The periods of saturation may be relatively short compared to the amount of time spent in a non-saturated state. Given the various costs of chl allocation, it may be better to tune the photosynthetic apparatus for energy capture during periods of low light availability. In similar fashion, the trade-offs regarding nutrient allocation and storage may at times be

non-optimal at one scale in order for improved performance at another. Likewise, models built around optimal allocation cannot be formulated as steady state models. As was shown with the NPP-Plant test, the phenology of leaves is a dynamic process that may be following an optimal allocation strategy.

### 4.7.3 The GA in ecological simulations

What are some of the pitfalls and benefits in applying the GA to ecological simulations? When adding a GA to a simulation there are sometimes subtle details that must be considered in the design of the model and in the formulation of the fitness functions.

In concept, the only limits on the GA search are expressed in the search limits of the controlling parameters. This is definitely not the case, the model itself may provide unforeseen limits on the GA. As an example, the array used to store leaf information was initially set to 100. For a 5 year simulation this limited the plant to an average of 20 leaves per year. The array size had to be changed to 150 before the nominal simulation would run reasonably well for the full 5 year period.

The controlling parameters can also be used in unexpected ways by the GA. In the search for maximum areal biomass the GA took advantage of the fact that it controlled shoot density. The GA configured a plant capable of quickly gaining biomass while staying within spatial biomass limits, and then used shoot density to effectively multiply that biomass into an areal maximum.

The mathematical structure of  $V_{grass}$  was considered a limiting factor in search behavior, but its importance was underestimated. In an early version of the model, there was

no limit on below ground biomass and no limit on the concentration of mobile carbon in the leaves. It was assumed that the shoot:root ratio and limits on above ground biomass, caused by shading, would also limit root growth and leaf mobile carbon. *These limits were not needed for the nominal model to run correctly.* When searching for a means to optimize a function, the GA took advantage of these mathematical features and used them to store carbon. Plant biomass reached values on order of  $10^5$  mg C while leaf width and length remained in nominal ranges. The biomass accumulated in root carbon and at very high concentrations of mobile carbon within the leaves.

In the process of searching for a solution, the GA can balance costs and benefits. Initially, all chlorophyll was considered of equal cost. As was mentioned in chapter 2, cost values had to be calibrated so that solutions matching the BWM99 model had normal PI curves. When all chl had equal cost, the GA selected PSU densities and antenna chl counts such that the PSU never reached saturation. This points to a fundamental difference in how models need to be constructed for use with a GA. A simple production vs. irradiance curve cannot be used to model light harvesting if chl dynamics are to be considered. In general, any adaptation to be modeled must consider the cost as well as the benefit of different adaptive configurations.

A model that behaves well for the nominal and validation steps may not work well when coupled with a GA. Experience gained here shows that testing the mathematical nature of the model becomes just as important as testing the sensitivity of the model's parameters.

GA results are a direct function of how the fitness of a configuration is evaluated. This was shown with the RGR test as the leaf growth patterns followed the two-week sampling

periods of the fitness function.

As a benefit, the GA has the ability to search solution spaces that may have discontinuities and optimal surfaces that might be visualized as mountain ranges. It was shown in Chapter 3 that since the GA works with a population of solutions, a secondary *sensitivity analysis* can be performed. Analyzing the selection ranges of the various parameters can reveal which parameters (and their values) are more important in the selection process.

In another role the GA forms the basis for allowing ecological simulations to become adaptive. This requires many individuals to be modeled simultaneously and implementing a reproductive feature within the population of individuals. Successful patterns persist and emulate the selection process found in the natural system. In a model where costs and benefits are accurately modelled, the persistent individuals should reveal how the cost and benefits at several scales affect each other.

#### 4.7.4 Suggestions for further research

First, the shade model should be calibrated. Also, this model is not valid in the tropics where the sun would be directly over head. Note in figure 2.2 that the leaves are perfectly vertical and would not collect light.

Second, chl dynamics in the model need further refinement. It was relatively easy to construct a set of equations that were effective at mimicking the light harvesting behavior of different chl configurations. But light harvesting is only part of the needed model. It was shown in Chapter 2 that the metabolic cost of building PSU's must be considered. The cost of adding chl as antenna is different than the cost of chl in the base reaction center.

For this study, cost parameters were calibrated based on various model runs with the GA in Chapter 2. Since most of the Production vs. Irradiance curves in Chapter 3 exhibit abnormal behavior, it is apparent that more attention should be made to the construction and tuning of chl dynamics.

Third, further reading about GA applications and Johnson (1996) indicate weakness with the binary chromosome used here. In a case where 1 or 2 bits in the chromosome are critical to search success, many generations can go by before these bits are set correctly. The binary search may not give equal weight to the entire search space and may not search the area where a maximum can be found. This may have occurred when validating the GA by searching for a configuration that could reduce RMS error below that of the nominal configuration. After several attempts with an improved model that should have performed better, the GA could not outperform, or even match the results it found on an early attempt before the model was improved.

Lastly, using sine waves to allow seasonal variation in plant attributes may not be descriptively accurate for all of the attributes. As opposed to a single number with no seasonal variation, the sine waves did allow for more variations in plant behavior. It would be interesting to develop a plant-growth-grammar to describe plant behavior. A grammar based approach has a potential to be much more descriptive of plant behavior than sine waves and may perform better with the GA. Johnson (1996) demonstrated the usefulness of a grammar based approach.



## 4.8 Literature Cited

- Abrahamson, W. G., and Caswell, H., 1982. On the competitive allocation of biomass, energy, and nutrients in plants. *Ecology*, 63, 982-991.
- Annevelink, E., and Broekmeulen, RACM, 1995. The genetic algorithm applied to space allocation planning in pot-plant nurseries.
- Bloom, A. J., Chapin, F. S. III, and Mooney, H. A., 1985. Resource limitation in plants – an economic analogy. *Ann. Rev. Ecol. Sys.*, 16, 363-392.
- Buzzelli, C. P., Wetzel, R. L., and Meyers, M. B., 1999. A linked physical and biological framework to assess biogeochemical dynamics in a shallow estuarine ecosystem. *Estuarine, Coastal and Shelf Science*, 49, 829-851.
- Chapin, F. S. I., and Bloom, A. J., Field, C. B., Waring, R. H., 1987. Plant responses to multiple environmental factors. *BioScience*, 37, 49-57.
- Chapin III, F. S., Schulze, E., Mooney, H. A., 1990. The ecology and economics of storage in plants. *Ann. Rev. Ecol. Syst.* 21, 423-427.
- Givnish, T. J., 1983a. On the economy of plant form and function. Cambridge University Press, New York, 717 pp.
- Givnish, T. J., 1983b. Optimal stomatal conductance, allocation of energy between leaves and roots, and the marginal cost of transpiration. In: Givnish, T. J. On the economy of plant form and function. Cambridge University Press, New York, 717 pp.
- Gleeson, S. K., and Tilman, D., 1992. Plant allocation and the multiple limitation hypothesis. *Am. Nat.*, 139, 1322-1343.
- Grime, J. P., 1977. Evidence for the existence of three primary strategies in plants and its relevance to ecological and evolutionary theory. *Am. Nat.*, 111, 1169-1194.
- Harper, J. L., 1977. Population biology of plants. Academic Press, New York, 892 pp.
- Hickman, J. C., Pitelka, L. F., 1975. Dry weight indicated energy allocation in ecological strategy analysis of plants *Oecologia*, 21, 117-121.
- Johnson, C. M., 1996. A grammar-based technique for genetic search and optimization. Dissertation, College of William and Mary, Williamsburg, VA.

- Kastner-Maresch, A. E., and Mooney, H. A., 1994. Modelling optimal plant biomass partitioning. *Eco. Mod.*, 75/76, 309-320.
- Kikuzawa, K., 1995. Leaf phenology as an optimal strategy for carbon gain in plants. *Can. J. Bot.*, 73, 158-163.
- Kozłowski, J., and Janczur, M., 1994. Density-dependent regulation of population number and life-history evolution: optimization of age at maturity in a simple allocation model for annuals and biennials. *Eco. Mod.*, 73, 81-96.
- Lambers, H., Chapin III, F. S., and Pons, T. L., 1998. *Plant Physiological Ecology*. Springer-Verlag New York Inc., New York, 540 pp.
- McNamara, J. M., 1994. Timing of entry into diapause: optimal allocation to growth and reproduction in a stochastic environment. *J. Theor. Bio.*, 168(2), 201-209.
- Moore, K. A., 1996. Dissertation: Relationships between seagrass growth and survival and environmental conditions in a lower Chesapeake Bay tributary. University of Maryland.
- Poorter, H., and Garnier, E., 1999. Ecological significance of inherent variation in relative growth rate and its components. In: *Handbook of functional plant ecology*. Ed. Pugnaire, F. I., and Valladares, F., Marcel Dekker Inc., New York, 901 pp.
- Ryser, 1996. The importance of tissue density for growth and life span of leaves and roots: a comparison of five ecologically contrasting grasses. *Func. Ecol.*, 10, 717-723.
- Sakai, S., 1993. Allocation to attractive structures in animal-pollinated flowers. *Evolution*, 47(6), 1711-1720.
- Sakai, S., 1995. Optimal resource allocation to vegetative and sexual reproduction of a plant growing in a spatially varying environment. *J. theor. Biol.*, 175, 271-282.
- Sakai, S. and Sakai, A., 1995. Flower size-dependent variation in seed size: theory and a test. *Am. Nat.*, 145, 918-934.
- Takada, T., and Nakajima, H., 1996. The optimal allocation for seed reproduction and vegetative reproduction in perennial plants: an application to the density-dependent transition matrix model. *J. Ther. Bio.*, 182(2), 179-191
- Thornley, J. H. M., 1976. *Mathematical models in plant physiology*. New York, Academic Press.

- Thornley, J. H. M., 1998. Modelling shoot:root relations: the only way forward? *Ann. Bot.*, 81, 165-171
- Verhagen, J. H. G., and Nienhuis, P. H. 1983. A simulation model of production, seasonal changes in biomass and distribution of eelgrass (*Zostera marina*) in Lake Grevelingen. *Mar. Ecol. Prog. Ser.*, 10(2), 195-197.
- Weibel, E. R., 2000. *Symmorphosis: on form and function in shaping life*. Harvard University Press, Cambridge MA., 263 pp.
- Wetzel, R. L., and Neckles, H. A., 1986. A model of *Zostera marina* L. photosynthesis and growth: simulated effects of selected physical-chemical variables and biological interactions. *Aquat. Bot.*, 26, 307-323.
- Wilson, J. Bastow, 1988. A review of evidence on the control of shoot:root ratio, in relation to models. *Annals of Botany*, 61, 433-449.
- Zimmerman, R. C., Kohrs, D. G., and Alberte, R. S., 1996. Top-down impact through a bottom-up mechanism: the effect of limpet grazing on growth, productivity and carbon allocation of *Zostera marina* L. (eelgrass). *Oecologia*, 170, 560-567.

## Chapter 5

# Concluding Remarks

The objective of this study was to build a computational framework within which plant growth strategies could be tested. The computational framework consisted of a simulation model (Vgrass) and a genetic algorithm (GA). Vgrass was a carbon based model of *Zostera marina* that was built from existing published models, published photosynthesis data, and general plant physiology information. In Vgrass, leaf geometry was computed and leaf size and shoot density were used to compute self shading. Self shading attenuated light available to the leaves and became a feedback mechanism limiting leaf growth. The model was run at two shoot densities and was qualitatively found to replicate biomass and leaf growth data from Orth and Moore (1986). The relationship between leaf length and shoot density was shown to be related to light availability.

Vgrass was coupled with a GA to demonstrate the use of a GA with an ecologically based simulation. The GA was used as an optimization method to find a configuration of Vgrass controlling parameters that minimized the RMS error between the biomass output of

Vgrass and the model of Buzzelli et al. (1999). The GA was also shown to be more than an optimization method. Since the GA works with populations of potential configurations there can be a number of individuals with fitness values near that of the most fit. Configurations with a fitness value within 10% of the most fit individual were compared. Among the set of individuals some Vgrass parameters were found to be constrained to narrow ranges of selection. Some parameters were found to have two ranges of selection while others were found to have wide ranges of selection. This demonstrated two features of the GA. First, it revealed parameters whose values were more critical in achieving the fitness goal. Second, it demonstrates the ability of the GA to find ranges of near optimal solutions.

Lastly, the computational framework of Vgrass and the GA were used to test plant growth strategies. The strategies were maximization of relative growth rate, maximization of biomass, and maximization of net primary production. As a non-growth strategy, longevity (the ability to survive 20 simulated years) was also tested. The results from each of the tests that maximized a growth pattern revealed plants that were not biologically realistic. Meanwhile, the longevity example showed many plant configurations able to survive 20 years. The results suggest that plant growth may not be goal driven.

*So is there a growth strategy that drives allocation?* Experimental evidence suggests that a growth strategy is not necessary for optimal allocation (Givnish, 1983). Results from this study show that allocation based on maximizing growth leads to biologically unrealistic behavior.

There is research in the area of artificial life which also suggests that growth strategies are not necessary. Artificial worlds, called artificial life or A-life, have been created in

software with the aim of isolating and replicating key features of natural systems. Resnick (1994) demonstrated how the simple actions of individuals form complex behavior without centralized control. In a simulation of termite construction behavior, 1,000 A-life termites were placed on a large grid (unspecified) on which 2,000 chips of wood were placed randomly. Rules that governed the behavior of the termites were; 1) a termite not carrying anything that bumped into a wood chip, picked up the chip; 2) a termite carrying a wood chip that bumped into another chip (or pile of chips) placed its chip on the pile. Within a few iterations of the model hundreds of piles were formed. Piles grew and diminished and after 20,000 iterations only 34 piles remained. Ant foraging, traffic jams, and other examples were used to demonstrate that individual decentralized (no command hierarchy) behavior can result in complex, apparently directed systems.

In a computational science dissertation, Johnson (1996) demonstrates a grammar based genetic algorithm method in an A-Life world that has ecological significance. The genetic algorithm is an artificial intelligence search method that is based on principles of natural selection (Goldberg, 1989). A computer model of a 200 x 200 toroidal grid (a doughnut shape so there are no edges) was set up in which each cell could contain an *animal*, a rock, or a piece of food. The goal for each animal was to move about and find food to support its metabolism. Animals were allowed to select for hearing, seeing, speed, and hunting strength (strong animals could consume weak animals). Selecting stronger features resulted in a higher metabolism rate. Animals were allowed to develop a *mind* to control how the senses, speed, hunting strength, and grid movement would develop into a behavioral pattern. At different times in the experiment three dominant *species* appeared. The *gatherer* had

strong sight and fast movement; it could see the food and get it quickly. The *hunter* had a strong sense of hearing and would move anywhere another animal was heard, sometimes going around rocks. The hunter did not need to move quickly and took advantage of animals that moved more often. Finally, a *scavenger* developed with minimal sensory and motor functions. The scavenger found animals that could not move and would wait for them to die; simple features gave it a low metabolism rate.

These examples demonstrate that complex behavior can be the result of simple interactions and that computational methods from A-Life and artificial intelligence can be used to demonstrate classical ecological principles. The next step is to substitute the A-life entities with the simulation of a real ecological entity. Examples of this have already been published. In an example to explain rat pup huddling, Schank and Alberts, (1997) show that the complex behavior can be explained by individuals behaving according to a simple set of rules which are related to sensorimotor activities. In another example (mentioned in Chapter 3), Huse et al. (1999) use a genetic algorithm and a neural network to control the spatial movement in an individual based fish simulation.

Complex behavior does not have to be the result of a goal oriented principle, and very likely is not. It may be that humans apply anthropomorphic qualities to apparently directed complex non-sentient collectives.

## 5.1 Literature Cited

- Buzzelli, C. P., Wetzel, R. L., and Meyers, M. B., 1999. A linked physical and biological framework to assess biogeochemical dynamics in a shallow estuarine ecosystem. *Estuarine, Coastal and Shelf Science*, 49, 829-851.
- Givnish, T. J., 1983. *On the economy of plant form and function*. Cambridge University Press, New York, 717 pp.
- Goldberg, D. E., 1989. *Genetic Algorithms in search, optimization, and machine learning*. Reading, Massachusetts: Addison-Wesley.
- Huse, G., Strand, E., and Giske, J., 1999. Implementing behaviour in individual-based models using neural networks and genetic algorithms. *Evol. Eco.* 13, 469-483.
- Orth, R. J., and Moore, K. A., 1986. Seasonal and year-to-year variations in the growth of *Zostera marina* L. (eelgrass) in the lower Chesapeake Bay. *Aquat. Bot.* 24, 335-341.
- Johnson, C. M., 1996. *A grammar-based technique for genetic search and optimization*. Dissertation, College of William and Mary, Williamsburg, VA.
- Resnick, M., 1994. *Turtles, termites, and traffic jams: explorations in massively parallel microworlds*. Cambridge, MIT Press.
- Schank, J. C., and Alberts, J. R., 1997. Self-organized huddles of rat pups modeled by simple rules of individual behavior. *J. Theor. Biol.*, 189, 11-25.



# VITA

William James Seufzer

Born in Stanley, Wisconsin on September 28<sup>th</sup>, 1961. Graduated from Augusta High School, Augusta, Wisconsin, in May of 1979. Attended Milwaukee School of Engineering from September of 1979 to May of 1983 and graduated with a Bachelor of Science in Electrical Engineering. Enlisted into United States Air Force College Senior Engineering Program in May of 1982. Attended Officer Training School, San Antonio, Texas in the summer of 1983 and commissioned as 2<sup>nd</sup> Lieutenant on September 8<sup>th</sup>, 1983. Assigned position as Avionics Systems Engineer at Wright-Patterson Air Force Base, Dayton, Ohio. Separated from United States Air Force as 1<sup>st</sup> Lieutenant on September 7<sup>th</sup>, 1987. Employed by General Research Corporation and Control Data Corporation (sequentially) from September 1987 to August 1990. Entered College of William and Mary, School of Marine Science in August 1990 and graduated with a Master of Science in Marine Science in December 1994. Entered Ph.D. program in January of 1995, graduated July, 2001. Married to Mary Gilliam of Chester, Virginia on May 20, 1995. First child, Olivia Grace, born on January 3, 2000. Second child due November, 2001. Employed by Science Applications International Corporation in support of the NASA Langley Atmospheric Sciences Data Center, Hampton, Virginia.